

**Use of Growth Factors and Adhesive Ligands to Promote Connective
Tissue Progenitor Colony Formation from Fresh Marrow**

by

Nicholas A. Marcantonio

**Sc.B Biomedical Engineering
Brown University, 2002**

**Submitted to the Department of Biological Engineering in Partial Fulfillment of the
Requirements for the Degree of**

**Doctor of Philosophy in Biological Engineering
at the
Massachusetts Institute of Technology**

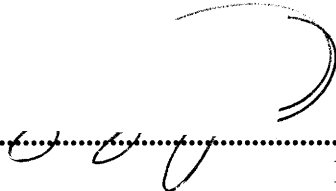
June 2008

© 2008 Massachusetts Institute of Technology. All rights reserved.

Signature of Author:.....

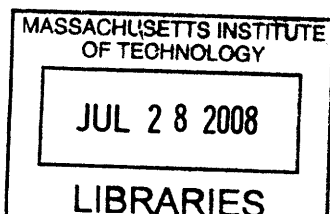
**Department of Biological Engineering
May 22, 2008**

Certified by:.....


**Linda G. Griffith
Professor of Biological Engineering
Thesis Supervisor**

Accepted by:.....


**Alan J. Grodzinsky
Professor of Biological Engineering
Chair, Graduate Program Committee**



ARCHIVES

Thesis Committee Members

Linda G. Griffith, PhD
Professor of Biological Engineering
Massachusetts Institute of Technology
Thesis Supervisor

Douglas A. Lauffenburger, PhD
Professor of Biological Engineering
Massachusetts Institute of Technology
Thesis Chair

Frank B. Gertler, PhD
Professor of Biology
Massachusetts Institute of Technology

Alan H. Wells, MD, DMS
Professor of Pathology
University of Pittsburgh

Use of Growth Factors and Adhesive Ligands to Promote Connective Tissue Progenitor Colony Formation from Fresh Marrow

by
Nicholas A. Marcantonio

Submitted to the Department of Biological Engineering on May 22, 2008
in Partial Fulfillment of the Requirement for the
Degree of Doctor of Philosophy in Biological Engineering

Abstract

The current gold standard for bone graft material is autologous bone, which provides mechanical support, possesses factors that promote bone formation, and contains connective tissue progenitors (CTPs), a heterogeneous population of connective tissue stem and progenitor cells that contribute to neotissue formation. A major limitation to autologous bone grafts is the risk of surgical complications associated with graft harvesting as well as significant donor-site morbidity. Available bone graft substitutes are not as efficacious as autologous bone, resulting in a prescient need for improved bone grafting materials. A promising tissue engineering approach involves the use of bioactive biomaterials that can promote the selective retention of CTPs from pre-seeded autologous bone marrow. When presented in a tethered form, EGF has been shown to promote the survival and enhance the adhesion of culture expanded CTPs. Therefore, the hypothesis of this work was that tethered EGF could be used to enhance the retention of osteogenic CTPs from *freshly aspirated* bone marrow.

Numerous adhesion ligands and growth factors have been investigated for use as candidates for the functionalization of bioactive materials. In this work, we showed that synergy-RGD peptides, which incorporate the putative synergy site on fibronectin, can promote cell adhesion through both $\alpha 5\beta 1$ and $\alpha v\beta 3$ integrins. We then investigated the effects of tethered EGF on CTP colony formation in the context of defined adhesion environments using a functionalizable comb copolymer. We found that tethered EGF increased the colony forming efficiency of CTPs from fresh human marrow when cell attachment was promoted by either non-specific protein adsorption, fibronectin preadsorption, or through the synergy-RGD ligand. In contrast, soluble EGF did not increase colony formation, demonstrating the importance of the modality of ligand presentation. Quantitative image analysis also suggested that while tethered EGF did not promote increased osteogenesis at early times after cell seeding tethered EGF may induce the proliferation and migration of cells within osteogenic colonies.

These results provide important insight into both the study of the effect of EGF on CTP behavior, as well as the use of tethered EGF as a potential ligand for use in biomaterials that promote the selective retention of CTPs.

Thesis Supervisor: Linda G. Griffith
Title: Professor of Biological Engineering

Acknowledgements

First, I would like to thank my thesis advisor, Professor Linda Griffith, for her guidance and support throughout my graduate studies. As a teenager, when I first saw the iconic photo of a tissue-engineered ear on a mouse in my yearbook's year-in-news section, I could have never guessed that I would eventually have the chance to learn from one of the scientists behind it. My growth as a researcher from when I joined the lab is truly night and day, and I have been fortunate to learn from such an accomplished scientist. Just as importantly, her creativity and her passion for developing ideas that can truly help people is always evident, and is something to which I can only hope to aspire.

I would also like to thank my thesis committee members, Professor Frank Gertler and Professor Alan Wells, who have provided me with a great deal of invaluable advice and guidance, both at my committee meetings as well as in many external discussions. I would like to offer a special thanks to my thesis committee chair Professor Douglas Lauffenburger who has played a very significant role in guiding my progress. In addition, I am indebted to him for his leadership in making the Biological Engineering Department an academic community that has no peer. I have had the chance to learn from brilliant minds and have made the best friends anyone could ask for.

I am also particularly indebted to my amazing collaborators at the Cleveland Clinic, Dr. George Muschler, Cynthia Boehm, and Richard Rozic, who provided me with an opportunity to work on a project with a clear clinical impact. I have been extremely lucky to have had the chance to work with such talented, hard-working, and friendly individuals.

There are many other people without whom this thesis would not have been possible. Mohan Nair, Professor Jean E. Schwarzbauer, and Professor Siobhan Corbett kindly provided the cells used in a portion of this work, as well as expertise in working with them. I must also thank John Wright, Daniel Pregibon, and Hyung-Il Lee who provided polymers used in this work.

There are many people in the Griffith and Lauffenburger labs, both past and present, to whom I owe a debt of gratitude. I would like to thank Christina Lewis and Stacey Pawson who as lab managers have ensured the lab has always run like clockwork, Michelle Berry, Cathy Greene, Dan Darling, and Aran Parillo for all of their help regarding all things outside the laboratory, and all of my officemates, particularly Ale Wolf-Yadlin, Ben Cosgove, HD Kim, and Neil Kumar for many helpful discussions on all things science and otherwise.

I would also like to thank my labmates, Lily Koo, Ley Richardson, Vivian Fan, Eileen Dimalanta, Shan Wu, Lu Alvarez, Maria Ufret, and David Yin from whom I learned so much and who made 56-286 a great place to work. I am especially indebted to several people in the lab, including Ada Au, whose research provided much of the inspiration for the thesis work I embarked upon, as well as Shelly Peyton and Manu Platt with whom I have had so many wonderful discussions, both scientific and distinctly unscientific. Finally, I must extend a huge thank you to both William Kuhlman and Ikuo Taniguchi who were instrumental in providing many of the polymers and characterizations used in this work. However, I must also thank Ikuo for his endless chemistry experience, and more importantly, for the time talking about our shared hobbies, baseball and the WRX. More than anyone else, I am indebted to Will, who

provided me with so much guidance as a new graduate student, and continued to share his seemingly endless knowledge with me over the years.

I'd like to thank all of my friends in BE, who made the last 5+ years the best of my life. It's been wonderful to see everyone become so successful both in their careers and in life. I have to especially thank Eric Krauland and Ty Thomson who have listened to more of my inane ramblings than anyone on the earth should have to.

I am, of course, forever thankful for my wonderful family. My brother Chris has always been there for me (at least a year or two... or perhaps a couple more than that), and understands me better than anyone else. And of course, I can never thank my parents enough, for all of the support they have given me. Finally, I want to thank my beautiful and amazing girlfriend, Diana Chai, who somehow manages to keep me sane, and for some reason, continues to put up with me. I couldn't do it without her.

Table of Contents

Acknowledgements	4
List of Tables and Figures.....	8
Chapter 1. Introduction.....	9
1.1 Strategies for tissue engineering	9
1.2 PEO as an inert surface for tissue engineering	11
1.3 Ligands for biomaterial modification	12
1.4 Bone grafting	14
1.5 Tissue engineering approaches for bone grafting	15
1.6 Thesis overview	17
1.7 Thesis outline.....	19
1.8 References.....	20
1.9 Figures.....	26
Chapter 2. Investigating the integrin specificity of a novel RGD peptide containing the fibronectin synergy motif.....	29
2.1 Introduction.....	29
2.1.1 Biomaterials-mediated cell behavior	29
2.1.2 Integrins, ECM, and RGD-mediated cell adhesion	29
2.1.3 The PHSRN synergy-motif.....	31
2.1.4 Presenting synergy-RGD peptides on an inert background.....	32
2.2 Materials and methods	36
2.2.1 Comb copolymer synthesis and functionalization	36
2.2.2 Surface preparation	37
2.2.3 Synergy-RGD peptide.....	38
2.2.4 Ligand coupling	38
2.2.5 Cell culture.....	39
2.2.6 FACS analysis.....	40
2.2.7 CHO-B2 $\alpha\beta3$ adhesion experiments	42
2.2.8 CHO-B2 $\alpha5\beta1$ adhesion experiments	43
2.3 Results.....	45
2.3.1 FACS confirms CHO-B2 $\alpha5\beta1$ and CHO-B2 $\alpha\beta3$ integrin expression.....	45
2.3.2 Synergy-RGD peptide promotes rapid $\alpha\beta3$ -mediated CHO attachment and spreading.....	45
2.3.3 $\alpha\beta3$ -mediated CHO attachment to synergy-RGD peptides are PHSRN- independent.....	46
2.3.4 Synergy-RGD peptide does not promote $\alpha5\beta1$ -mediated CHO attachment at short times.....	47
2.3.5 Synergy-RGD peptide promotes $\alpha5\beta1$ -mediated CHO attachment and spreading.....	48
2.3.6 Synergy-RGD peptide promotes $\alpha5\beta1$ -mediated CHO stress-fiber formation	49

2.3.7 The PHSRN sequence in synergy-RGD does not enhance CHO-B2 $\alpha 5\beta 1$ focal adhesion or stress fiber formation.....	50
2.4 Discussion.....	52
2.5 Conclusions.....	57
2.6 References.....	57
2.7 Figures.....	63

Chapter 3. Tethered EGF enhances connective tissue progenitor osteogenic colony formation81

3.1 Introduction.....	81
3.2 Materials and Methods.....	84
3.2.1 Ligand-modified culture substrates.....	84
3.2.2 Bone marrow aspiration.....	86
3.2.3 CTP/CFU assay.....	86
3.2.4 Surface conditions.....	87
3.2.5 Statistical analysis.....	88
3.2.6 Image analysis.....	89
3.3 Results.....	90
3.3.1 Tethered EGF enhances osteogenic colony formation on minimally adhesive peptides	90
3.3.2 Tethered EGF enhances osteogenic colony formation on adsorbed serum and Fn.....	91
3.3.3 Soluble EGF is less effective than tethered EGF in fostering colony formation.....	93
3.3.4 Tethered EGF enhances CFE in multiple donor populations	94
3.3.5 Tethered EGF increases colony size on serum	95
3.3.6 Tethered EGF does not affect the number of cells expressing alkaline phosphatase within a colony	96
3.4 Discussion.....	98
3.5 Conclusion	104
3.6 References.....	104
3.7 Figures.....	112

Chapter 4. Conclusions and Future Directions.....130

4.1 References.....	134
---------------------	-----

List of Tables and Figures

Figure 1.1 EGFR signaling by soluble and tethered EGF.....	26
Figure 1.2 Stages of the stem cell life cycle	27
Figure 1.3 Differentiation pathways for connective tissue progenitors	28
Table 2.1 Cell spreading of CHO-B2 $\alpha\beta 3$ cells	47
Figure 2.1 Known family of integrin receptors.....	63
Figure 2.2 Structure of synergy-RGD and scrambled synergy-RGD peptides.....	64
Figure 2.3 Schematic of polymerization, activation, and coupling	65
Figure 2.4 Schematic of surface preparation	66
Figure 2.5 FACS profiles of $\alpha 5\beta 1$ and $\alpha\beta 3$ expression in CHO-B2 variants	67
Figure 2.6 20X images of CHO-B2 $\alpha\beta 3$ cells.....	68
Figure 2.7 20X images of CHO-B2 pcDNA control cells	69
Figure 2.8.1 20X images of CHO-B2 $\alpha 5\beta 1$ cells.....	70
Figure 2.8.2 20X images of CHO-B2 $\alpha 5\beta 1$ cells.....	71
Figure 2.9.1 60X images of CHO-B2 $\alpha 5\beta 1$ cells.....	72
Figure 2.9.2 60X images of CHO-B2 $\alpha 5\beta 1$ cells.....	73
Figure 2.10 60X images of CHO-B2 pcDNA cells	74
Figure 2.11 10X images of CHO-B2 $\alpha 5\beta 1$ cells.....	75
Figure 2.12.1 20X images of CHO-B2 $\alpha 5\beta 1$ cells.....	76
Figure 2.12.2 20X images of CHO-B2 $\alpha 5\beta 1$ cells.....	77
Figure 2.13.1 60X images of CHO-B2 $\alpha 5\beta 1$ cells.....	78
Figure 2.13.2 60X images of CHO-B2 $\alpha 5\beta 1$ cells.....	79
Figure 2.13.3 60X images of CHO-B2 $\alpha 5\beta 1$ cells.....	80
Table 3.1 Polymer blends used for colony-forming unit assay.....	85
Figure 3.1 Image of alkaline phosphatase positive CTP colony.....	112
Figure 3.2 Schematic of CFU assay protocol	113
Figure 3.3 Schematic of surface conditions used for colony-forming unit assay	114
Figure 3.4 Quantitative image analysis of CTP colonies.....	115
Figure 3.5 CTP CFE in the presence of tethered EGF.....	116
Figure 3.6 Late adherent colony formation.....	117
Figure 3.7 CTP CFE vs. total colony prevalence.....	118
Figure 3.8 CTP CFE on fibronectin in the presence of tethered EGF	119
Figure 3.9 CTP CFE in the presence of tethered or soluble EGF	120
Figure 3.10 CTP CFE in the presence of tethered EGF for healthy volunteers.....	121
Figure 3.11 CTP CFE in the presence of tethered EGF for osteoarthritic donors	122
Figure 3.12 CTP CFE in the presence of tethered EGF for all donors	123
Figure 3.13 CTP CFE as measured by quantitative image analysis	124
Figure 3.14 Colony area as measured by quantitative image analysis.....	125
Figure 3.15 Cell number per colony area as measured by quantitative image analysis	126
Figure 3.16 AP expression as measured by quantitative image analysis.....	127
Figure 3.17 Schematic of tethered EGF induced CTP activation	128
Figure 3.18 Schematic of tethered EGF induced CTP adhesion and survival.....	129

Chapter 1. Introduction

1.1 Strategies for tissue engineering

In 1993, Langer and Vacanti defined the field of tissue engineering as “an interdisciplinary field that applies the principles of engineering and life sciences toward the development of biological substitutes that may restore, maintain, or improve tissue function” and identified three general strategies that could be utilized for the development of new tissue [1] :

1. The use of cells or cell substitutes to replace defective cells or tissue
2. The use of substances that can replace tissue
3. The use of cells placed on or within matrices

Biomaterials play a crucial component in the latter two strategies. As the discipline of tissue engineering has expanded in academia, medicine and the private sector [2, 3], so has the development of new generations of biomaterials. While earlier generations of biomaterials were designed principally to promote biocompatibility, biomaterials are now being designed and developed to not only be biocompatible, but also to promote tissue-specific cell behaviors that are required for the regeneration of a functional target tissue [4]. These materials can be broadly categorized as *bioactive biomaterials* [5]. A set of key design principles for the development of biomaterials for tissue engineering applications has emerged, as a means to address the challenges involved in regenerating tissue [6, 7]. These principles can be broadly characterized as pertaining to either the bulk properties or surface properties of a biomaterial.

Because permanent materials elicit a chronic inflammatory response [8], it is highly desirable for a material to degrade or resorb over time [9]. While the surface

properties of a material are also important, resorption is largely dictated by the bulk properties of a material, including hydrophobicity, crystallinity, and the susceptibility to hydrolysis (or enzymatic degradation) of the material [9-11]. The major challenges involved with designing resorbable materials include consideration of the immunogenicity and toxicity of degradation products, as well as the maintenance of adequate mechanical strength as the material degrades. The bulk properties of a material also influence the way in which it can be processed and formed into a specific shape or geometry [6]. Therefore, it is often necessary to design a material to achieve a balance between resorption over a given timescale and the mechanical requirements for a given application.

In contrast, the surface properties of a biomaterial are primarily responsible for dictating cellular behavior in response to and interactions with the biomaterial. As noted previously, while the first generation of biomaterials was selected for inertness upon implantation, the second generation included bioactive biomaterials that would promote tissue regeneration through controlled biological interactions [4]. A prominent example of a second generation material is bioactive glass, of which many variations have been used to promote bone growth through an inorganic chemical process [12]. With the newest generation of materials, however, there is a focus on promoting behavior on the cellular and molecular level. According to Griffith and Naughton, the ideal biomaterial “would selectively interact with the specific adhesion and growth factor receptors expressed by target cells in surrounding tissues required for repair of damaged tissue [7].” To accomplish this, the general approach involves the use of a material that is by itself, biologically inert, but can be modified with ligands (i.e. adhesion peptides, growth

factors) that promote a desired response. These cell behaviors first involve cell adhesion, and may also include cell migration, proliferation, and/or differentiation [5].

1.2 PEO as an inert surface for tissue engineering

When a traditional biomaterial is placed in contact with a biological fluid, plasma proteins are thermodynamically driven to adsorb to the surface [13, 14]. These proteins include adhesive extracellular matrix (ECM) proteins, which mediate cell attachment. The process of protein adsorption is complex and differs dramatically across materials, making it difficult to predict which ECM proteins will be responsible for promoting cell adhesion upon implantation. To promote the regeneration of a specific tissue, it is desirable to have an enhanced degree of control over the cell adhesion process. For tissue engineering applications, it may be desirable to target the adhesion of one particular cell type, or even one specific adhesion receptor. As a result, it is preferable to design biomaterials that can promote adhesion through a defined set of interactions. One way in which biomaterials have been modified is through the selective pre-adsorption of a particular ECM molecule [15, 16]. This approach is useful, but is somewhat limited because of the exchange of adsorbed proteins that may occur over time [17]. Therefore, another approach that may promote a higher degree of cell specificity is through the functionalization of materials that are inherently cell resistant.

One material that has been used extensively in the development of bioactive polymeric biomaterials is polyethylene oxide (PEO) [18, 19]. This material has proven to be both biocompatible, and is highly resistant to cell adhesion without further molecular modification. Unlike most traditional polymeric biomaterials such as polyethylene, or

silicone rubbers, PEO is resistant to the process of nonspecific protein adsorption [20]. In addition, PEO-based materials can be *covalently* modified with ligands that promote cell adhesion or signaling through specific receptor-surface interactions.

1.3 Ligands for biomaterial modification

Ligands used for modifying biomaterial surfaces include cell-adhesive ligands and growth factors that promote cell proliferation, differentiation, and tissue growth. The largest volume of research to date has involved the use of small RGD peptides [21], which promote adhesion through integrins, the primary cell receptors [22]. An advantage of using small peptides is that they can be designed to target a specific binding event, unlike native ECM proteins which typically have multiple binding sites and may promote additional non-specific interactions. Modification with adhesive ligands can add a significant amount of bioactivity to a biomaterial. The adhesion state of a cell has a significant effect on other cellular activities, such as migration [23] and survival [24]. In addition to promoting the mechanical attachment of a cell to a surface, integrins can also promote intracellular signaling that further affects cell behavior [22, 25, 26].

While adhesive ligands can have a large effect on cell behavior, these effects are promoted within the context of other factors in the surrounding cellular environment [27-31]. In particular, growth factors such as epidermal growth factor (EGF) [32], platelet-derived growth factor (PDGF) [33], and fibroblast growth factor (FGF) [34] play a major role in influencing multiple aspects of cell behavior. Like adhesive ligands, the specific effect that a growth factor exerts upon a cell often depends on a number of factors including cell type, receptor expression, and concentration. Furthermore, growth factor-

induced behavior is often highly dependent upon the presence of other growth factors, or even the adhesion molecules that are promoting cellular attachment. As a result, a major area of research involves understanding how growth factors presented from a material may differentially affect a cell compared to growth factors that are presented in soluble form [35]. In some cases, the presentation of matrix-associated growth factors may better approximate the scenario that exists during tissue regeneration in nature, as many growth factors are associated with ECM proteins [36]. In fact, ECM molecules themselves have repeats that can act as ligands for growth factor receptors [37]. A clear difference between soluble and tethered growth factors is that tethered growth factors are not susceptible to depletion. However, growth factor tethering (Figure 1.1) can also prevent receptor internalization [35], which has been shown to play a major role in attenuating receptor-mediated signaling and resulting cell behaviors, such as proliferation [38].

Our group has studied the effect of tethered EGF on the behavior of a number of different cell types, and has found that the resulting behavior in many cases differs from that induced by soluble EGF [35, 39, 40]. It has been clear that an important facet of designing bioactive biomaterials that have been functionalized with growth factors involves not only the engineering challenges associated with developing the material, but also an understanding of the cellular biology that results from these unique presentation modalities. Therefore, while the use of adhesion ligands and growth factors in biomaterials has become widespread as a general tissue engineering strategy, individual approaches must be investigated and refined for specific applications. One area in particular where tissue engineering can have a clear immediate therapeutic impact is in orthopedics, specifically for bone grafting applications.

1.4 Bone grafting

It is estimated that 500,000 to 600,000 bone grafting procedures are performed each year in the U.S. alone [41]. These procedures are warranted when the body cannot promote the healing of a fracture on its own, with the most common causes including traumatic injury and fracture nonunion [42]. A bone graft material may refer to any material that can promote a bone healing response through one or more of three processes: osteogenesis, osteoconduction, or osteoinduction [43]. According to Bauer and Muschler:

An osteogenic material can be defined as one which contains living cells that are capable of differentiation into bone. An osteoconductive material promotes bone apposition to its surface, functioning in part as a receptive scaffold to facilitate enhanced bone formation. An osteoinductive material provides a biologic stimulus that induces local or transplanted cells to enter a pathway of differentiation leading to mature osteoblasts [43].

The current gold standard for bone grafting procedures is the vascularized autograft, which possesses all three of these properties [44, 45]. Autografts provide osteogenic potential as they contain bone cells and bone marrow cells which give rise to the daughter cells which can differentiate into bone. Additionally, they offer osteoconductivity by providing a collagen matrix that facilitates cell attachment, as well as osteoinductive factors including bone morphogenic proteins (BMPs) that promote osteogenesis [42, 43, 45, 46]. Furthermore, autologous grafts do not promote an immunologic reaction upon implantation, because they are derived from the graft recipient. However, the major drawback associated with autologous grafts is the morbidity associated with a second surgical procedure needed to harvest the graft, typically from the iliac crest [44]. Clearly, there is also a limited supply of bone that may be harvested as autograft material. As a result of these drawbacks, a number of bone graft substitutes have become increasingly

utilized, within the clinic. The most prominent substitute is allograft material [47], which is tissue taken from another individual of the same species [43]. Currently, allografts are estimated to be used in one-third of bone grafting procedures in North America [48]. However, allografts have several major disadvantages associated with their use. The most prominent is the small, but legitimate risk of disease transmission that may occur [49]. Because of this risk, fresh allografts are used infrequently, due to the time required to screen for disease [46]. Subsequently, most allografts are processed by being frozen or freeze-dried to reduce the host immune response, though this comes at the expense of reduced and/or eliminated osteogenic and osteoinductive potential [45, 46]. Due to these deficiencies, a number of other bone graft substitutes have begun to be utilized in the clinic or developed for use in the near future [45-47]. As part of the search for new bone graft substitutes the tissue engineering approaches described above are being applied to address this need [50].

1.5 Tissue engineering approaches for bone grafting

A number of bone graft substitutes which fit within the discipline of tissue engineering are currently available within the clinic. These include bioglass and calcium phosphate based ceramics and cements such as hydroxyapatite and tricalcium phosphate, some of which may be used in composites containing bone morphogenic proteins (BMPs), that possess some combination of osteoinductive and osteoconductive properties [41, 43-46, 51]. These technologies, however, do not offer all of the benefits that an autograft does. In particular, calcium phosphate based matrix materials do not offer sufficient mechanical support [52] and are not intrinsically osteogenic [45]. As such, a

new generation of bioactive biomaterials that can promote an improved combination of desirable properties is currently under development. These materials may be natural or synthetic, and include ceramics, polymers and composites [42].

Cell-based strategies represent another tissue engineering approach that shows a great deal of promise and have become increasingly utilized to promote bone healing [50, 53]. In general, these strategies include the transplantation of autologous or culture expanded cells into a wound site. In particular, multipotent stem and/or progenitor cells have become an attractive cell type for these applications. Stem cells, which are the source of all new tissue, have the potential to self-renew, and to give rise to daughter progenitor cells that differentiate into more committed cell types (Figure 1.2). Unlike stem cells, progenitor cells have limited capacity for self-renewal and are committed to a differentiated phenotype [50]. For orthopedic applications, the term *connective tissue progenitor* (CTP) has been used to denote the combined heterogeneous population of musculoskeletal stem and progenitor cells that are capable of both proliferation, and differentiation (Figure 1.3) [54]. CTPs can be derived from multiple sources, including cancellous bone, periosteum, muscle, and fat [53]. However the most prominent source of these cells is bone marrow.

In the late 1970s, Freidenstein was the first to show that formation of new bone could be traced to CTPs within the bone marrow [55]. Since this initial work, autologous bone marrow has been investigated as a bone graft material and been shown to promote increased healing of the wound site [56-58]. A current approach that combines the benefits of bioactive matrix materials as well as the osteogenic properties afforded by autologous bone marrow derived CTPs involves the use of materials that can support the

selective retention of these CTPs. This approach, which involves the enrichment of bone marrow cells at a graft site by pre-seeding materials that promote the attachment and retention of CTPs, has been shown to improve the efficacy of graft materials [59].

To date, this approach has been investigated with more traditional biomaterials, such as demineralized bone powder. The next step in this approach involves the development of bioactive biomaterials that have been functionalized with ligands that can enhance the attachment and retention of CTPs for use in bone grafting procedures [53, 59]. The current work is devoted to examining specific molecules that can be used in this capacity.

1.6 Thesis overview

The goal of this thesis is to contribute to the development of design principles for bone tissue engineering approaches that combine the use of bioactive biomaterials and autologous human CTPs. The specific focus is to identify molecules that can be used to design bioactive biomaterial surfaces that promote the attachment and retention of CTPs from freshly aspirated autologous bone marrow. To achieve this, we have employed a poly(methyl methacrylate)-graft-poly(ethylene oxide) (PMMA-g-PEO) amphiphilic comb copolymer that allows us to investigate specific ligands that may be used to functionalize the surface of biomaterials. The PEO-based material used in this work would not necessarily be suitable as a bulk material, but allows us to investigate principles can be applied to other biomaterials systems for surface modification. In particular, our work has focused the use of tethered EGF as a means to promote CTP retention and osteogenesis for future use in bone graft materials.

The effect of EGF on mesenchymal stem cell (MSC) and CTP behavior has been unclear. EGF has been shown to exert multiple effects on MSC and CTP proliferation, osteogenesis, or even chondrogenesis depending on the specific cell studied, and the experimental conditions used in the experiment [60-64]. However, our lab recently demonstrated that tethered EGF promoted increased spreading and survival in culture expanded CTPs, whereas soluble EGF did not [39]. Therefore, we hypothesized that tethered EGF might also be able to promote the adhesion and survival, and thus increase the retention, of CTPs from *freshly aspirated* bone marrow. To test this hypothesis, we collaborated with Dr. George Muschler, an orthopedic surgeon at the Cleveland Clinic Foundation, and members of his laboratory, principally Cynthia A. Boehm and Richard Rozic.

Because the effect that a growth factor exerts on cell behavior is often affected by other factors such as the molecules mediating cell adhesion we wanted to examine the effect of tethered EGF on CTPs in the context of multiple adhesion environments that could be considered for use in tissue engineering applications. Two of these adhesive environments are based upon the adsorption of adhesive ECM proteins. However, we also wanted to examine the effect of tethered EGF in the scenario where adhesion was mediated by a small RGD adhesion peptide. The use of multiple adhesive environments would facilitate the ability to parse effects of tethered EGF on cell adhesion, as well as to inform the use of a small RGD peptide in a clinical application.

As noted previously, the use of small adhesion peptides in bioactive biomaterials is desirable for a number of reasons. However, it has been shown that small RGD peptides do not necessarily promote binding with the same affinity and/or specificity as

the ECM molecule from which they are derived [65, 66]. As a result, previous work in our group has led to the design of a novel RGD peptide (Maria Ufret, unpublished data) and results have suggested that this peptide can promote enhanced adhesion for a number of cell types compared to traditional RGD peptides [40, 67]. Therefore, we chose to employ this peptide in our study of the effect of tethered EGF on CTP behavior. However, while this peptide showed enhanced adhesion in a number of studies, it was unclear as to which integrins were involved in mediating adhesion to this peptide. Therefore, a goal of this thesis was also to examine the ability of this peptide to promote adhesion through two different RGD-binding integrins, using a well-defined cellular system. These results could then be used to better understand the effect of tethered EGF on CTP attachment and retention in the context of well-characterized adhesive conditions.

1.7 Thesis outline

Chapter 2 of this thesis consists of an examination of cell adhesion to our novel RGD peptide through the use of immunostaining and microscopy. Context for this work and the use of RGD peptides in biomaterials is provided in the introduction to this section. Also, a discussion of the PEO biomaterial system used in this work is provided. The results of these immunostaining experiments are provided and discussed.

Chapter 3 consists of a detailed study of the effect of tethered EGF on the CTP behavior, using a well-defined colony forming unit (CFU) assay. A description of this assay, as well as the historical context for research involving CTPs and mesenchymal stem cells (MSC) are provided in this section. This work, as noted above, was a direct

collaboration with Dr. George F. Muschler and his laboratory (principally Cynthia A. Boehm, and Richard Rozic) and facilitated the use of freshly aspirated bone marrow provided from 39 individual human donors. The effect of tethered EGF was studied across multiple adhesive conditions, and compared to the effect of soluble EGF on these cells. Furthermore, data was analyzed in the context of healthy volunteers, or donors who had osteoarthritis. Finally, quantitative image analysis was performed on a subset of data to study additional parameters not available for examination in the conventional CFU assay.

Conclusions and future directions of this work are discussion in Chapter 4.

1.8 References

1. Langer, R. and J.P. Vacanti, *Tissue engineering*. Science, 1993. **260**(5110): p. 920-6.
2. Lysaght, M.J., A. Jaklenec, and E. Deweerd, *Great expectations: private sector activity in tissue engineering, regenerative medicine, and stem cell therapeutics*. Tissue Eng Part A, 2008. **14**(2): p. 305-15.
3. Nerem, R.M., *Tissue engineering: the hope, the hype, and the future*. Tissue Eng, 2006. **12**(5): p. 1143-50.
4. Hench, L.L. and J.M. Polak, *Third-generation biomedical materials*. Science, 2002. **295**(5557): p. 1014-7.
5. Hubbell, J.A., *Bioactive biomaterials*. Curr Opin Biotechnol, 1999. **10**(2): p. 123-9.
6. Griffith, L.G., *Emerging design principles in biomaterials and scaffolds for tissue engineering*. Ann N Y Acad Sci, 2002. **961**: p. 83-95.
7. Griffith, L.G. and G. Naughton, *Tissue engineering--current challenges and expanding opportunities*. Science, 2002. **295**(5557): p. 1009-14.
8. Anderson, J.M., A. Rodriguez, and D.T. Chang, *Foreign body reaction to biomaterials*. Semin Immunol, 2008. **20**(2): p. 86-100.
9. Griffith, L.G., *Polymeric biomaterials*. Acta Materialia, 2000. **48**(1): p. 263-277.

10. Gopferich, A., *Mechanisms of polymer degradation and erosion*. Biomaterials, 1996. **17**(2): p. 103-14.
11. Gunatillake, P.A. and R. Adhikari, *Biodegradable synthetic polymers for tissue engineering*. Eur Cell Mater, 2003. **5**: p. 1-16; discussion 16.
12. Hench, L.L., *Bioceramics*. Journal of the American Ceramic Society, 1998. **81**(7): p. 1705-1728.
13. Claesson, P.M., et al., *Protein Interactions at Solid-Surfaces*. Advances in Colloid and Interface Science, 1995. **57**: p. 161-227.
14. Latour, R.A., *Thermodynamic perspectives on the molecular mechanisms providing protein adsorption resistance that include protein-surface interactions*. J Biomed Mater Res A, 2006. **78**(4): p. 843-54.
15. Knoner, G., et al., *Mechanics of cellular adhesion to artificial artery templates*. Biophys J, 2006. **91**(8): p. 3085-96.
16. Otto, M., et al., *Modification of human platelet adhesion on biomaterial surfaces by protein preadsorption under static and flow conditions*. J Mater Sci Mater Med, 2004. **15**(1): p. 35-42.
17. Vroman, L. and A.L. Adams, *Findings with the recording ellipsometer suggesting rapid exchange of specific plasma proteins at liquid/solid interfaces*. Surface Science, 1969. **16**: p. 438-446.
18. Cima, L.G., *Polymer substrates for controlled biological interactions*. J Cell Biochem, 1994. **56**(2): p. 155-61.
19. Tessmar, J.K. and A.M. Gopferich, *Customized PEG-derived copolymers for tissue-engineering applications*. Macromol Biosci, 2007. **7**(1): p. 23-39.
20. Leckband, D., S. Sheth, and A. Halperin, *Grafted poly(ethylene oxide) brushes as nonfouling surface coatings*. J Biomater Sci Polym Ed, 1999. **10**(10): p. 1125-47.
21. Hersel, U., C. Dahmen, and H. Kessler, *RGD modified polymers: biomaterials for stimulated cell adhesion and beyond*. Biomaterials, 2003. **24**(24): p. 4385-415.
22. Hynes, R.O., *Integrins: bidirectional, allosteric signaling machines*. Cell, 2002. **110**(6): p. 673-87.
23. Lock, J.G., B. Wehrle-Haller, and S. Stromblad, *Cell-matrix adhesion complexes: master control machinery of cell migration*. Semin Cancer Biol, 2008. **18**(1): p. 65-76.

24. Moro, L., et al., *Integrins induce activation of EGF receptor: role in MAP kinase induction and adhesion-dependent cell survival*. EMBO J, 1998. **17**(22): p. 6622-32.
25. Giancotti, F.G. and E. Ruoslahti, *Integrin signaling*. Science, 1999. **285**(5430): p. 1028-32.
26. Schwartz, M.A., *Integrin signaling revisited*. Trends Cell Biol, 2001. **11**(12): p. 466-70.
27. Cabodi, S., et al., *Integrin regulation of epidermal growth factor (EGF) receptor and of EGF-dependent responses*. Biochem Soc Trans, 2004. **32**(Pt3): p. 438-42.
28. Giancotti, F.G. and G. Tarone, *Positional control of cell fate through joint integrin/receptor protein kinase signaling*. Annu Rev Cell Dev Biol, 2003. **19**: p. 173-206.
29. Miranti, C.K. and J.S. Brugge, *Sensing the environment: a historical perspective on integrin signal transduction*. Nature Cell Biology, 2002. **4**(4): p. E83-E90.
30. Schwartz, M.A. and M.H. Ginsberg, *Networks and crosstalk: integrin signalling spreads*. Nat Cell Biol, 2002. **4**(4): p. E65-8.
31. Yamada, K.M. and S. Even-Ram, *Integrin regulation of growth factor receptors*. Nat Cell Biol, 2002. **4**(4): p. E75-6.
32. Wells, A., *EGF receptor*. Int J Biochem Cell Biol, 1999. **31**(6): p. 637-43.
33. Alvarez, R.H., H.M. Kantarjian, and J.E. Cortes, *Biology of platelet-derived growth factor and its involvement in disease*. Mayo Clinic Proceedings, 2006. **81**(9): p. 1241-1257.
34. Eswarakumar, V.P., I. Lax, and J. Schlessinger, *Cellular signaling by fibroblast growth factor receptors*. Cytokine & Growth Factor Reviews, 2005. **16**(2): p. 139-149.
35. Kuhl, P.R. and L.G. Griffith-Cima, *Tethered epidermal growth factor as a paradigm for growth factor-induced stimulation from the solid phase*. Nat Med, 1996. **2**(9): p. 1022-7.
36. Hynes, R.O., *Cell adhesion: old and new questions*. Trends Cell Biol, 1999. **9**(12): p. M33-7.
37. Swindle, C.S., et al., *Epidermal growth factor (EGF)-like repeats of human tenascin-C as ligands for EGF receptor*. Journal of Cell Biology, 2001. **154**(2): p. 459-468.

38. Wells, A., et al., *Ligand-induced transformation by a noninternalizing epidermal growth factor receptor*. Science, 1990. **247**(4945): p. 962-4.
39. Fan, V.H., et al., *Tethered epidermal growth factor provides a survival advantage to mesenchymal stem cells*. Stem Cells, 2007. **25**(5): p. 1241-51.
40. Richardson, L.B. "EGF receptor-mediated fibroblast signaling and motility : role of nanoscale spatial ligand organization." Ph.D. Thesis. Massachusetts Institute of Technology, 2005.
41. Bucholz, R.W., *Nonallograft osteoconductive bone graft substitutes*. Clin Orthop Relat Res, 2002(395): p. 44-52.
42. Khan, Y., et al., *Tissue engineering of bone: material and matrix considerations*. J Bone Joint Surg Am, 2008. **90 Suppl 1**: p. 36-42.
43. Bauer, T.W. and G.F. Muschler, *Bone graft materials. An overview of the basic science*. Clin Orthop Relat Res, 2000(371): p. 10-27.
44. Fleming, J.E., Jr., C.N. Cornell, and G.F. Muschler, *Bone cells and matrices in orthopedic tissue engineering*. Orthop Clin North Am, 2000. **31**(3): p. 357-74.
45. Kao, S.T. and D.D. Scott, *A review of bone substitutes*. Oral Maxillofac Surg Clin North Am, 2007. **19**(4): p. 513-21, vi.
46. De Long, W.G., Jr., et al., *Bone grafts and bone graft substitutes in orthopaedic trauma surgery. A critical analysis*. J Bone Joint Surg Am, 2007. **89**(3): p. 649-58.
47. Bostrom, M.P.G. and D.A. Siegerman, *The clinical use of allografts, demineralized bone matrices, synthetic bone graft substitutes and osteoinductive growth factors: a survey study*. HSSJ, 2005. **1**(1): p. 9-18.
48. Boyce, T., J. Edwards, and N. Scarborough, *Allograft bone. The influence of processing on safety and performance*. Orthop Clin North Am, 1999. **30**(4): p. 571-81.
49. CDC, *Update: allograft-associated bacterial infections--United States, 2002*, in *MMWR Morb Mortal Wkly Rep*. 2002, Centers for Disease Control and Prevention. p. 207-10.
50. Muschler, G.F., C. Nakamoto, and L.G. Griffith, *Engineering principles of clinical cell-based tissue engineering*. J Bone Joint Surg Am, 2004. **86-A**(7): p. 1541-58.
51. Carson, J.S. and M.P. Bostrom, *Synthetic bone scaffolds and fracture repair*. Injury, 2007. **38 Suppl 1**: p. S33-7.

52. Larson, S. *Injectable phosphate cements: a review*. 2006 [cited 2008 April 18]; Available from: http://www.osteosynthesis.stryker.com/medias/pdf/wp_hydroset_technical_review_larsson.pdf.
53. Patterson, T.E., et al., *Cellular strategies for enhancement of fracture repair*. J Bone Joint Surg Am, 2008. **90 Suppl 1**: p. 111-9.
54. Muschler, G.F. and R.J. Midura, *Connective tissue progenitors: practical concepts for clinical applications*. Clin Orthop Relat Res, 2002(395): p. 66-80.
55. Friedenstein, A.J., *Precursor cells of mechanocytes*. Int Rev Cytol, 1976. **47**: p. 327-59.
56. Connolly, J.F., et al., *Autologous marrow injection as a substitute for operative grafting of tibial nonunions*. Clin Orthop Relat Res, 1991(266): p. 259-70.
57. Garg, N.K. and S. Gaur, *Percutaneous autogenous bone-marrow grafting in congenital tibial pseudarthrosis*. J Bone Joint Surg Br, 1995. **77(5)**: p. 830-1.
58. Healey, J.H., et al., *Percutaneous bone marrow grafting of delayed union and nonunion in cancer patients*. Clin Orthop Relat Res, 1990(256): p. 280-5.
59. Muschler, G.F., et al., *Selective retention of bone marrow-derived cells to enhance spinal fusion*. Clin Orthop Relat Res, 2005(432): p. 242-51.
60. Kimura, A., O. Katoh, and A. Kuramoto, *Effects of platelet derived growth factor, epidermal growth factor and transforming growth factor-beta on the growth of human marrow fibroblasts*. Br J Haematol, 1988. **69(1)**: p. 9-12.
61. Tamama, K., et al., *Epidermal growth factor as a candidate for ex vivo expansion of bone marrow-derived mesenchymal stem cells*. Stem Cells, 2006. **24(3)**: p. 686-95.
62. Owen, M.E., J. Cave, and C.J. Joyner, *Clonal analysis in vitro of osteogenic differentiation of marrow CFU-F*. J Cell Sci, 1987. **87 (Pt 5)**: p. 731-8.
63. Gronthos, S. and P.J. Simmons, *The growth factor requirements of STRO-1-positive human bone marrow stromal precursors under serum-deprived conditions in vitro*. Blood, 1995. **85(4)**: p. 929-40.
64. Kuznetsov, S.A., A.J. Friedenstein, and P.G. Robey, *Factors required for bone marrow stromal fibroblast colony formation in vitro*. Br J Haematol, 1997. **97(3)**: p. 561-70.
65. Hautanen, A., et al., *Effects of modifications of the RGD sequence and its context on recognition by the fibronectin receptor*. J Biol Chem, 1989. **264(3)**: p. 1437-42.

66. Yang, X.B., et al., *Human osteoprogenitor growth and differentiation on synthetic biodegradable structures after surface modification*. *Bone*, 2001. **29**(6): p. 523-31.
67. Yin, D. "The applications of comb polymer to the study of liver cell adhesion and signaling." M. Eng. Thesis. Massachusetts Institute of Technology, 2004.

1.9 Figures

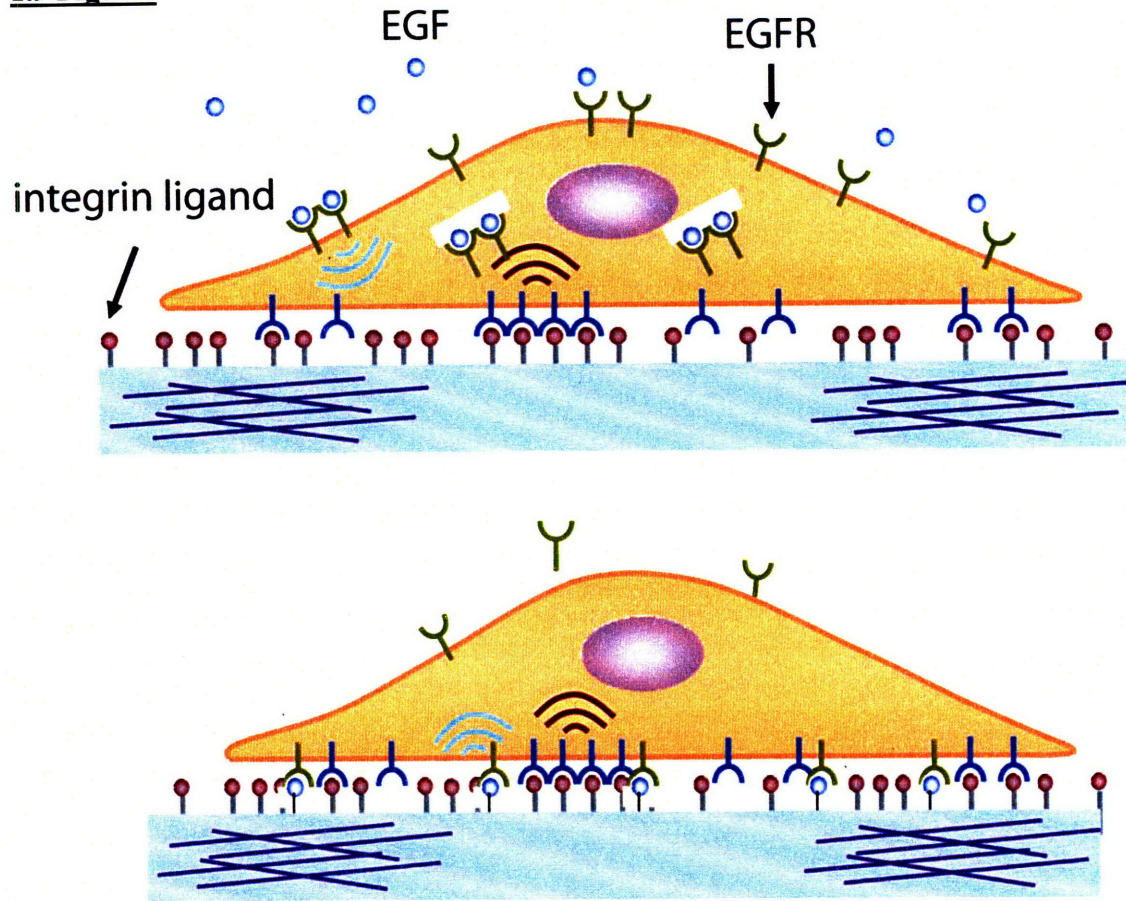


Figure 1.1 Top: soluble EGF receptor (EGFR) can signal from surface and cytosol. Bottom: EGFR is restricted to the surface, and is prevented from being internalized.

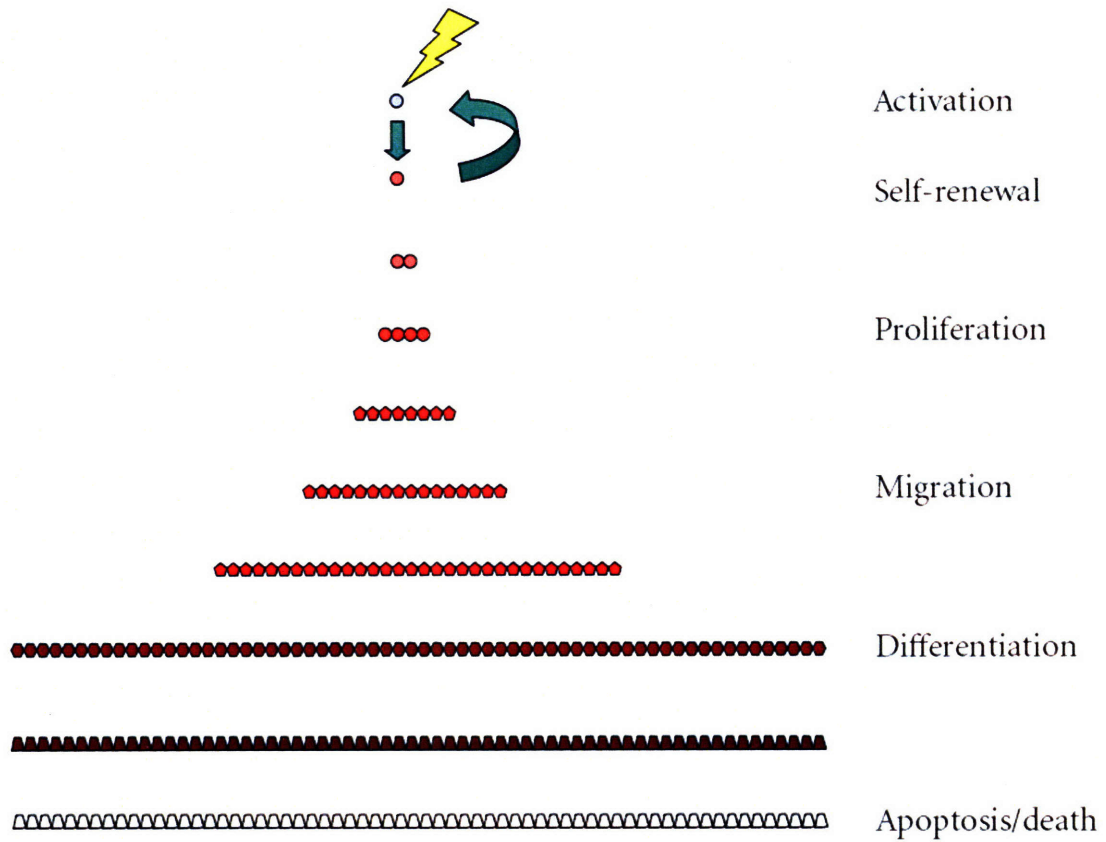


Figure 1.2 Stages of the stem cell life cycle. From the Journal of Biomedicine and Biotechnology, 3, Muschler GF, Midura RJ, Nakamoto C, Practical Modeling Concepts for Connective Tissue Stem Cell and Progenitor Compartment Kinetics, p. 170-193, 2003 (open access journal).

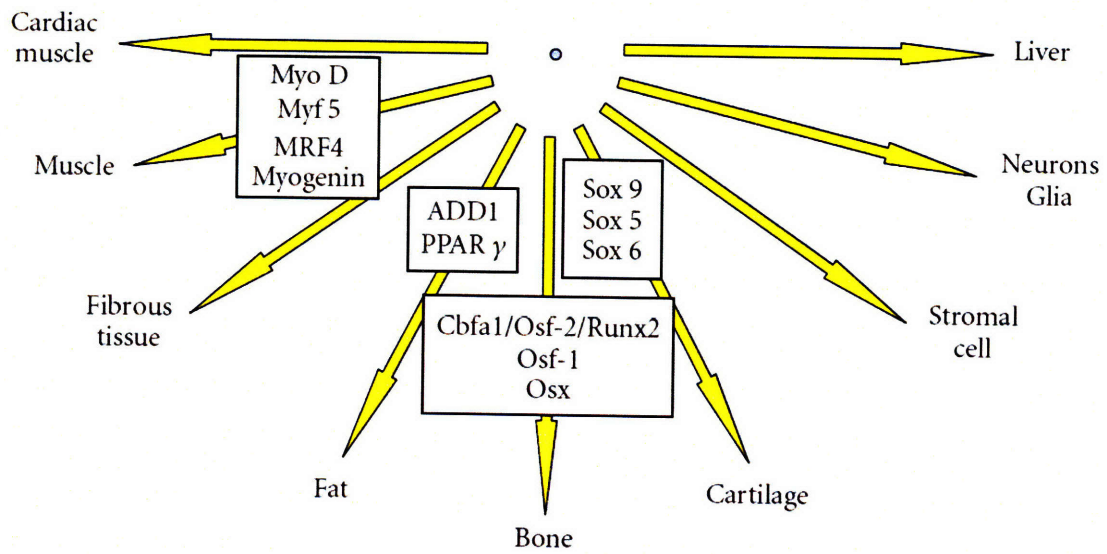


Figure 1.3 Potential differentiation pathways for connective tissue progenitors. From the Journal of Biomedicine and Biotechnology, 3, Muschler GF, Midura RJ, Nakamoto C, Practical Modeling Concepts for Connective Tissue Stem Cell and Progenitor Compartment Kinetics, p. 170-193, 2003 (open access journal).

Chapter 2. Investigating the integrin specificity of a novel RGD peptide containing the fibronectin synergy motif

2.1 Introduction

2.1.1 Biomaterials-mediated cell behavior

Promoting specific interactions between biomaterials and cells is crucial to the success of implantable biomaterials and tissue engineering. Upon implantation, protein adsorption to a biomaterial surface occurs immediately. Protein adsorption to biomaterials is a complex thermodynamically driven process that can potentially involve thousands of plasma proteins [1, 2], the most prominent of which include albumin, fibrinogen, fibronectin, and vitronectin. The major result of this adsorption process is that cell attachment to a biomaterials surface is mediated by the adsorbed proteins, and not by the material itself. The adsorption process is unique to each biomaterial and can lead to altered protein function and non-specific cell adhesion. As a result, a common approach is to utilize materials that resist non-specific protein adsorption which can then be functionalized to promote cell attachment via specific integrin-mediated binding events [3, 4]. The effects of specific cell-material interactions can enhance biocompatibility and tissue integration.

2.1.2 Integrins, ECM, and RGD-mediated cell adhesion

Integrins are the major class of cell-surface receptors responsible for mediating adhesion to extracellular matrix (ECM) proteins including fibronectin, vitronectin, laminin, and collagen [5] and play a role in cell survival, differentiation, and proliferation [6, 7]. Eight β and 18 α subunits are known to assemble into 24 distinct heterodimeric

receptors, each consisting of one α and one β subunit (Figure 2.1) [5]. In 1984, Pierschbacher and Ruoslahti showed that cellular adhesion to fibronectin was primarily mediated by the RGD amino acid sequence [8]. This motif has since been discovered to be present in vitronectin [9] and numerous other ECM proteins including laminin, fibrinogen, and tenascin [10]. Similarly, multiple integrins have been shown to bind to some form of the RGD motif, either in native ECM or as small linear or cyclic peptides [4, 5, 10]. The two most widely studied RGD-binding integrins include the fibronectin receptor $\alpha 5\beta 1$ [11] and the vitronectin receptor $\alpha \beta 3$ [12]. However, while many integrins can bind to ECM proteins containing the RGD motif, the structure of the protein and the amino acids surrounding the RGD motif have a large effect on the affinity and specificity of an integrin for a specific ECM molecule. This was demonstrated by the discovery that $\alpha \beta 3$ can bind to fibronectin as well as to vitronectin [13], whereas $\alpha 5\beta 1$ can bind only to fibronectin [14].

Given the signaling importance of integrins in adhesion and signaling, synthetic RGD-containing peptides have been widely used in many aspects of biological and pharmaceutical research [10]. As discussed in Chapter 1, RGD peptides have been utilized extensively in the development of biomaterials for tissue engineering where they have been used in place of native ECM molecules to promote cell attachment to biomaterials surfaces [4, 15, 16].

To date, a number of different RGD peptides have been investigated for their ability to selectively target specific integrins [4]. Two commonly used peptides include GRGDS, and GRGDSP which have been shown in *in vitro* studies to bind to both $\alpha \beta 3$ and $\alpha 5\beta 1$ [4]. However, linear GRGDSP was shown to inhibit cell adhesion on

vitronectin to a greater degree than on fibronectin, suggesting that GRGDSP peptides had a higher specificity for $\alpha v\beta 3$ than for $\alpha 5\beta 1$ [17]. Many cyclic-RGD peptides have also been studied [18-20] and it was observed that the specificity and affinity of these peptides depends greatly upon the exact sequence and ring structure synthesized.

2.1.3 The PHSRN synergy motif

A major limitation of small RGD peptides is that they have been found to have reduced activity compared to native ECM ligands due to the lack of complementary domains [14, 21-24]. In particular, the high affinity binding of $\alpha 5\beta 1$ to fibronectin has been traced to the existence of an additional synergy region present on fibronectin [25-27]. Within this synergy region, the PHSRN sequence has been identified to be the key motif, and is known as the synergy site [21, 28]. While the RGD motif in fibronectin is present in the 10th type-III domain, the synergy site is present in the adjacent 9th type-III domain. Currently, the exact function of the synergy-site is unclear; studies suggest that the synergy-site enhances the structural stability of the RGD-binding interaction, but is not an adhesive site in-and-of itself [29, 30]. One recent report suggested that peptides containing the PHSRN sequence may promote cell-adhesion in the absence of the RGD adhesion site [31]. A consistent picture of the role of the synergy site has not yet emerged from the many studies employing RGD peptides containing the PHSRN site, or RGD peptides mixed with PHSRN peptides, as a means to functionalize biomaterials. Several studies have shown surfaces presenting both PHSRN peptides and RGD peptides increased $\alpha 5\beta 1$ binding and cell spreading compared to RGD peptides alone [18, 32]. Additional studies have shown that peptides containing both the RGD and the PHSRN

sequences may increase cell adhesion compared to RGD alone. Benoit et al. showed that PEG hydrogels containing RGDG₁₃PHSRN increased the attachment, spreading, focal adhesion formation, proliferation, and differentiation of cultured osteoblasts compared to gels with RGD or RDGG₁₃HPRNS [33]. Mardilovich et al. observed similar results with human umbilical vein endothelial cells seeded on substrates functionalized with KSSPHSRNSGSGSGSGSGRGDSP, compared to surfaces with GRGDSP or GRGDSP+PHSRN (individual peptides) [34]. Antibody blocking experiments also suggested that $\alpha 5\beta 1$ -mediated adhesion was enhanced on KSSPHSRNSGSGSGSGSGRGDSP, compared to controls. In contrast, Petrie et al. found that RGDG₁₃PHSRN did not promote enhanced MC3T3-E1 cell adhesion strength compared to GRGDSPC alone, and presented evidence that cell adhesion to these peptides was primarily mediated by $\alpha v\beta 3$ [22]. Taken together, these results illustrate the complexity of relationship between integrin expression profiles, integrin affinity and specificity, and cell adhesion. Evidence suggests that the PHSRN sequence may be useful in biomaterials applications, although the conflicting results in the literature show that additional research is necessary to elucidate clear ways in which the PHSRN motif may be employed to enhance cell behavior.

2.1.4 Presenting synergy-RGD peptides on an inert background

To further examine the effects of the RGD and PHSRN motifs on cell behavior for use in tissue engineering applications, Maria Ufret, a post-doctoral research associate in our laboratory, designed a synergy-RGD peptide that contained both the RGD adhesion motif as well as the PHSRN synergy motif in a flexible branched configuration

based upon the structure of native fibronectin (Figure 2.2a). Because it is necessary to study the effects of this peptide on an inert adhesion background, our lab has employed a comb polymer system that can be functionalized with the synergy-RGD peptide. The system is an amphiphilic copolymer that consists of a hydrophobic poly(methyl methacrylate) (PMMA) backbone and hydrophilic poly(ethylene oxide) side chains [35]. PEO, also known as polyethylene glycol (PEG), has been shown to be both non-toxic and resistant to non-specific protein adsorption [3, 36, 37]. Because of the amphiphilic nature of the comb copolymer, when spin-coated onto glass coverslips and later placed into solution, the hydrophobic PMMA backbone associates with the glass coverslip, while the hydrophilic PEO side chains extend into solution [35]. This polymer can be designed to permit or resist nonspecific protein adsorption, by changing the percentage of PEO used to synthesize the polymer. Comb copolymers with greater than 30% PEO resist protein adsorption [35, 38-40], while polymers with greater than 45% PEO by weight are water soluble [35]. Polymers with lower percentages of PEO (~20% by weight) allow protein adsorption and non-specific cell adhesion [40, 41].

One of the key features of this co-polymer is that ligands of interest can be covalently tethered to the terminal ends of the PEO side chains, making them available for cell receptor binding interactions in a clustered, or locally dense manner [35, 39, 40, 42, 43]. The ability to present adhesive ligands in a clustered manner is necessary to enable integrin clustering, which is required for a number of cell responses including adhesion, motility, cytoskeletal organization, signaling, and adhesion strengthening [42, 44-46].

Using this system Maria Ufret and David Yin (M.Eng. 2006) showed that rat hepatocytes, which are reported to express the $\alpha 5\beta 1$ integrin but not $\alpha v\beta 3$, were able to attach and spread on comb copolymer substrates presenting the synergy-RGD peptide in a concentration dependent manner (Maria Ufret, unpublished data) [47]. Furthermore, hepatocyte spreading was inhibited when cells were treated with $\alpha 5$ and $\beta 1$ blocking antibodies. Maria Ufret, Ley Richardson (Ph.D. 2006) and William Kuhlman (Ph.D. 2007), also used the synergy-RGD peptide to promote the adhesion of NR6wt cells, a variant of the 3T3 murine fibroblast that is known to express both $\alpha 5\beta 1$ and $\alpha v\beta 3$, and observed that spreading and/or attachment increased on synergy-RGD in a concentration dependent manner [39, 40]. Interestingly, in antibody blocking experiments, Maria Ufret observed that NR6wt spreading was inhibited with αv blocking antibodies, but not with $\alpha 5$ blocking antibodies.

Maria Ufret and Ley Richardson also observed that NR6wt spreading was increased on synergy-RGD surfaces compared to a control RGD peptide that did not contain the PHSRN sequence. While this initially suggested that the PHSRN sequence enhanced cell adhesion, it is also possible that differences in surface peptide concentration may play a factor. While radiolabeling experiments were performed to enable the use of matching concentrations of the control RGD and synergy-RGD peptides in experiments comparing these ligands, measurements were made under the assumption that peptides could not penetrate into the polymer bulk, and that radiolabeling measurements represented only covalently bound ligand at the surface of the substrate. However, in subsequent work with the synergy-RGD peptide, William Kuhlman observed that the radiolabeling results varied with the thickness of the polymeric

substrates utilized in the experiments suggesting that these peptides could penetrate into the bulk of the polymer [39]. It is possible to determine the surface concentration of peptides by making measurements for films of multiple thicknesses, and extrapolating the surface concentration from this data. However, these extrapolations were not performed in the work comparing the control and synergy-RGD peptides. Therefore, it is possible that the surface concentrations of the two peptides may not have been identically matched in comparison experiments due to differences in the kinetics of the polymer penetration of the two peptides.

Taken together, this work clearly shows that the synergy-RGD peptide mediates robust cell attachment. However, it is unclear if the synergy-RGD peptide promotes increased cell adhesion or activity compared to conventional RGD peptides. In addition, the specificity of this peptide for $\alpha 5\beta 1$ vs. $\alpha v\beta 3$ is unclear. It has been reported that rat hepatocytes have $\alpha 5\beta 1$, but not $\alpha v\beta 3$. However, the hepatocytes utilized in this research are a heterogeneous population, and the integrin profile of these cells was not directly assessed, making it unclear as to which integrin was mediating hepatocyte attachment to the synergy-RGD peptide. And, as noted previously, αv blocking antibodies reduced NR6wt cell spreading.

Therefore, the goal of this work was to determine if synergy-RGD could mediate cellular adhesion through either, or both, $\alpha 5\beta 1$ and $\alpha v\beta 3$, using cells with well-defined integrin profiles. We further examined the effect of the PHSRN sequence on cell adhesion, by examining focal adhesion and actin stress fiber formation. Using a peptide with a scrambled synergy motif, we were able to circumvent differences in the coupling kinetics of a linear RGD peptide and the synergy-RGD peptide.

2.2 Materials and methods

2.2.1 Comb copolymer synthesis and functionalization

Thin-film substrates were made from a poly(methyl methacrylate)-graft-poly(ethylene oxide) (PMMA-g-PEO) amphiphilic comb copolymer, synthesized by summer technician Dan Pregibon, according to methods described previously [35]. The polymer was synthesized through free-radical polymerization of methyl methacrylate and polyethylene glycol methacrylate (HPOEM), using azo(bis)isobutyronitrile (AIBN) as an initiator (all reagents from Sigma Aldrich, St. Louis, MO). Because this polymer was designed to resist cell adhesion through non-specific protein adsorption, HPOEM with an average length of 10 PEO units (and $M_n=526$) was used, and the polymer comprised 32 wt% PEO, a composition highly resistant to cell adhesion [38-40, 43]. This polymer has a $M_n=142$ kDa and $PDI=3.2$, as measured by gel-permeation chromatography with in-line light scattering [39].

For coupling of thiol-terminated adhesion peptides, a portion of the polymer was reacted with N-[p-Maleimidophenyl]isocyanate (PMPI) (Pierce Biochemical, Rockford, IL) according to the method developed by Annunziato et al [48] by post-doctoral research associate Hyung-II Lee. This method has been previously used to couple adhesion peptides to comb copolymer substrates [39, 40, 43].

To accomplish the PMPI-activation, the comb copolymer was first freeze-dried from benzene to remove excess water from the polymer. Briefly, the polymer was dissolved in benzene in a round bottom flask and fitted with a three-way stop-cock. The polymer was then frozen by submerging the flask in liquid nitrogen, and rotating the flask to create a thin shell of frozen polymer. Vacuum was then applied to the flask, with a

liquid nitrogen trap. After reaching room temperature, the flask was removed from vacuum, and purged with nitrogen gas.

The polymer was then dissolved in anhydrous dimethyl sulfoxide (DMSO), and mixed with approximately 2.5 M excess of PMPI. The reaction was allowed to proceed overnight in the dark, and purified through repeated precipitation in diethyl ether. The reaction was characterized by nuclear magnetic resonance (NMR) spectroscopy of a sample of polymer dissolved in deuterated chloroform performed by post-doctoral research associate Shelly Peyton. NMR analysis revealed that approximately 50% of chain ends underwent reaction with PMPI. All surfaces made in this work consisted of polymer blends consisting of 25% PMPI-activated polymer and 75% unmodified polymer.

2.2.2 Surface preparation

12mm round glass coverslips (VWR International, Bridgeport, NJ) were cleaned using a 2% Chem-Solv solution (VWR). After cleaning, coverslips were rinsed thoroughly in deionized water, and treated with a 2% aqueous solution of Siliclad (Gelest Inc., Morrisville, PA). Surfaces were treated by being submerged in the Siliclad solution for 20s, rinsed in deionized water, cured at 100°C and stored in a vacuum oven under 20 in Hg vacuum at room temperature. For spin-coating, polymer blends were dissolved in toluene at a final concentration of 20mg/mL and filtered using a 20 µm pore-size syringe filter. Polymer thin films were spin-coated by completely covering the Siliclad prepared coverslips with polymer solution, and then spun at 2500 rpm for 30s using a Headway PWM32 spinner. All spin-coated surfaces were stored *in vacuo* prior to peptide coupling.

Schematics of the polymerization, PMPI-activation, and peptide coupling process are illustrated in Figures 2.3 and 2.4.

2.2.3 Synergy-RGD peptide

The synergy-RGD peptide designed by post-doctoral research associate Maria Ufret consists of the peptide sequence PHSRNGGGKGGRGDSP, with a GGC stem attached to the lysine. This results in a branched peptide with the PHSRN synergy motif on one branch as well as the GRGDSP on the other branch, and has a sulfhydryl associated with the cysteine to facilitate peptide coupling via the PMPI-activated comb copolymer. The peptide used here was synthesized and purified by the MIT Biopolymers Laboratory (peptide P7016). To evaluate any specific effects of the synergy site included on the peptide, a similar peptide was synthesized with a scrambled synergy motif. This peptide, referred to as scrambled synergy-RGD contains the peptide sequence HSPNRGGGKGGRGDSP, with a GGC stem attached to the lysine. This peptide is identical to the synergy-RGD peptide except that the synergy motif is replaced with the HSPNR sequence. This peptide was also synthesized and purified by the MIT Biopolymers Laboratory (peptide P7055). Schematics of both the active and scrambled synergy-RGD peptide are shown in Figure 2.2.

2.2.4 Ligand coupling

Surfaces were functionalized by reacting the spin-coated surfaces with either a 25 μ M or 100 μ M solution of the synergy-RGD peptide in phosphate buffered saline (PBS) at pH 7.5 at room temperature as described previously [40, 47, 49]. The coupling

solution also contained 10 mM Tris(2-Carboxyethyl) phosphine hydrochloride (TCEP) (Sigma Aldrich) as a reducing agent. The peptide was allowed to react for 2 hours, by placing polymer coated substrates face down on 40 μL of peptide solution on parafilm. The surfaces were then rinsed 3X with 250 μL of PBS, and stored *in vacuo* prior to use. Mock coupled control surfaces were also made by following the same procedure, using only PBS and TCEP in place of a peptide solution. Using film thickness considerations from William Kuhlman's work [39], the concentration of synergy-RGD and scrambled synergy-RGD peptide on the surface of comb copolymer films is estimated to be approximately 2×10^4 and 8×10^4 peptides/ μm^2 for the 25 and 100 μM solutions respectively. Having used 25% PMPI blends, the average nearest neighbor distance for ligands within a cluster on these surfaces is roughly 3.5 nm for 25 μM surfaces and 1.7 nm for the 100 μM surfaces. With an average radius of gyration of 9.2 nm for a comb copolymer molecule [43], an individual polymer molecule would create clusters that include 22 and 85 peptides respectively. These values only represent rough averages that will vary significantly, due to the polydispersity of the individual polymer molecules [43].

2.2.5 Cell culture

Three different variants of Chinese hamster ovary (CHO) cells were used to study cell attachment to the functionalized comb copolymer substrates. All variants were based upon the CHO-B2 cell line, which is a CHO clone selected for its inability to adhere to fibronectin, and is deficient in both the $\alpha 5$ integrin subunit as well as the $\beta 3$ intergin subunit [50-52]. The first variant is a CHO-B2 cell population that has been transfected

with the human $\alpha 5$ integrin subunit (CHO-B2 $\alpha 5\beta 1$), and expresses $\alpha 5\beta 1$ [53]. The second variant is a CHO-B2 population that has been transfected with the human $\beta 3$ integrin subunit and expresses $\alpha \nu \beta 3$ (CHO-B2 $\alpha \nu \beta 3$) [54, 55]. Finally, a control cell line was created by transfecting CHO-B2 cells with an unaltered pcDNA vector (CHO-B2 pcDNA). The CHO-B2 $\alpha 5\beta 1$ and pcDNA cells were a kind gift from Professor Siobhan A. Corbett at Robert Wood Johnson Medical School, and the CHO-B2 $\alpha \nu \beta 3$ cells were kindly provided by Professor Jean E. Schwarzbauer of Princeton University. These cell lines are not clonally derived and are heterogeneous populations of transfected cells. All three cell lines were maintained in the same basal growth medium, which consisted of high glucose Dulbecco's Modified Eagle Medium (DMEM) supplemented with 10% FetalClone II (Hyclone, Logan, UT), 1 mM sodium pyruvate, 0.1 mM MEM non-essential amino acids, 2 mM L-glutamine, 100 $\mu\text{g}/\text{ml}$ streptomycin sulfate, 100 units/ml penicillin G sodium and 0.25 $\mu\text{g}/\text{ml}$ amphotericin B. 500 $\mu\text{g}/\text{ml}$ Zeocin was added to the medium as a selection agent for the CHO-B2 $\alpha \nu \beta 3$ cells, and 250 $\mu\text{g}/\text{ml}$ G418 was added to the medium as a selection agent for both the $\alpha 5\beta 1$ and pcDNA cells. Except for FetalClone II, all products were from Invitrogen (Carlsbad, CA). For microscopic imaging, experiments were performed in media containing the same supplements, but with phenol-red free DMEM. Cells were maintained in 95% air/5% CO_2 at 37°C in tissue culture plates.

2.2.6 FACS analysis

Fluorescence activated cell sorting was used to check the expression of $\alpha 5\beta 1$ and $\alpha \nu \beta 3$ for all three CHO-B2 variants. Mouse anti-human integrin $\alpha \nu \beta 3$ monoclonal

antibody (MAB1976) and rat anti-mouse $\alpha 5\beta 1$ monoclonal antibody (MAB2514) were purchased from Chemicon (Temecula, Ca). Alexa Fluor 488 goat anti-rat IgG and Alexa Fluor 647 goat anti-mouse IgG $\alpha 5\beta 1$ were purchased from Invitrogen.

Cells were removed from tissue culture plates with trypsin-EDTA (Sigma, St. Louis, MO). The trypsin was inactivated with phosphate buffered saline (PBS) containing 2% FetalClone II. The cells were washed 2X by being spun-down at 1000 rpm for 5 minutes, and resuspended in PBS+2% FetalClone II. The cells were counted, spun-down, and resuspended in PBS+2% FetalClone II at a concentration of 10^7 cells/mL. 10^6 cells for each cell type and condition to be studied were then each added to an individual well in 96-well V-bottom plate.

Each CHO-B2 variant was incubated, in duplicate, with either anti- $\alpha 5\beta 1$, anti- $\alpha \nu \beta 3$, or no antibody. 2 μ L of each antibody was added to each necessary well, and the cells were incubated on ice for 30 minutes, and agitated every 10 minutes. 150 μ L of PBS+2% FetalClone II was then added to each well, and the cells were spun down in a plate centrifuge for 5 minutes at 1700 rpm, and resuspended in 100 μ L of PBS+2% FetalClone II. Each combination of cell type and primary antibody was then incubated with 20 μ L of a 1:150 dilution of either Alex Fluor 488 goat anti-rat or Alexa Fluor 647 goat anti-mouse secondary antibody for 30 minutes on ice, and agitated every 10 minutes. After the incubation, 200 μ L of PBS+2% FetalClone II was then added to each well, the cells were spun down, and resuspended in 200 μ L of PBS+2% FetalClone II for analysis. The cells were analyzed using a LSR II High Throughput Sampler (BD Biosciences, San Jose, CA), and data was analyzed with Flow Jo software (Tree Star, Ashland, OR).

2.2.7 CHO-B2 α v β 3 adhesion experiments

Spin-coated surfaces were coupled with either 25 μ M or 100 μ M of synergy-RGD or scrambled synergy-RGD peptide, or were mock coupled. Untreated glass coverslips, which allow cell attachment via non-specific protein adsorption, were also included as a positive control. The surfaces were placed in 24-well plates, and sterilized in PBS under ultraviolet light for approximately 30 minutes. 10^5 cells were seeded in each well, in 1 mL of microscopy medium. The cells were allowed to adhere for 4 hours in 95% air/5% CO₂ at 37°C, and then fixed in 4% paraformaldehyde in phosphate buffered saline containing Ca⁺⁺ and Mg⁺⁺ (PBS⁺⁺) for 20 min. The surfaces were then washed 2X in PBS⁺⁺ + .05% Tween-20, and the cells were permeabilized with PBS⁺⁺ + 0.1% Triton X100 for 3 minutes. The surfaces were washed 2X, and then stained for 20 minutes in PBS⁺⁺ containing 10 μ g/mL Hoechst 33342 trihydrochloride trihydrate (Invitrogen) and 5 units/mL Alexa Fluor 488 phalloidin (Invitrogen). The surfaces were then washed 2X, rinsed once in deionized water and then mounted on microscopy slides. The coverslips were mounted in medium consisting of 22.5 mg of 1,4-diazabicyclo[2.2.2]octane (DABCO) (Sigma) dissolved in .9 mL glycerol + .1 mL PBS at pH 8.0. The cells were imaged at 20X using a Zeiss Axiovert 135 and Zeiss Filter Set 10, and saved as tif files. Images were imported into Adobe Photoshop, and the Auto Levels command was used to adjust the contrast of each image. Occasionally, the brightness and contrast of images with very few cells were adjusted manually to allow the proper visualization of the image. To provide a semi-quantitative comparison of cell spreading between RGD

surface conditions, the percentage of area of an image covered by cells was measured using ImageJ. A t-test was used to examine statistical significance between conditions.

2.2.8 CHO-B2 $\alpha 5\beta 1$ adhesion experiments

Two distinct sets of conditions were used to examine the attachment of CHO-B2 $\alpha 5\beta 1$ or pcDNA cells to the synergy-RGD and scrambled synergy-RGD peptide. For the first set of conditions, CHO-B2 $\alpha 5\beta 1$ or pcDNA cells were seeded on surfaces that were coupled with 25 μM synergy-RGD, 25 μM scrambled synergy-RGD peptide, or were mock coupled. Untreated glass coverslips, which allow cell attachment via non-specific protein adsorption, were also included as a positive control. The surfaces were placed in 24-well plates, and sterilized in PBS under ultraviolet light for approximately 15 minutes. 10^5 cells were seeded in each well, in 1 mL of microscopy medium. The cells were allowed to adhere for 23 hours in 95% air/5% CO_2 at 37°C , and then fixed in 4% paraformaldehyde in phosphate buffered saline containing Ca^{++} and Mg^{++} (PBS^{++}) for 20 min. The surfaces were then washed 2X in PBS^{++} + .05% Tween-20, and the cells were permeabilized with PBS^{++} + 0.1% Triton X100 for 3 minutes. The surfaces were washed 2X, and then blocked in 5% donkey serum (Jackson ImmunoResearch Laboratories, West Grove, PA) in PBS^{++} for 30 minutes. The cells were then incubated for 1 hour at room temperature with monoclonal anti-vinculin clone hVIN-1 mouse ascites fluid (Sigma V9131) diluted 1:400 in blocking solution. The cells were washed 3X, and then incubated for 30 minutes at room temperature in the dark with Cy3-conjugated donkey anti-mouse IgG secondary antibody (Jackson ImmunoResearch) diluted 1:100 in PBS^{++} . The cells were then washed 3X and stained for 20 minutes in PBS^{++} containing 10 $\mu\text{g}/\text{mL}$

Hoechst 33342 trihydrochloride trihydrate (Invitrogen) and 5 units/mL Alexa Fluor 488 phalloidin (Invitrogen). The surfaces were then washed 2X, rinsed once in deionized water and then mounted on microscopy slides. The coverslips were mounted in medium consisting of 22.5 mg of 1,4-diazabicyclo[2.2.2]octane (DABCO) (Sigma) dissolved in .9 mL glycerol + .1 mL PBS at pH 8.0. The cells were imaged at 20X using a Zeiss Axiovert 135 and Zeiss Filter Set 10, and saved as tif files. Images were imported into Adobe Photoshop, and the Auto Levels command was used to adjust the contrast of each image. Occasionally, the brightness and contrast of images with very few cells were adjusted manually to allow the proper visualization of the image. Surfaces were also imaged at with a 60X oil objective using an Applied Precision DeltaVision deconvolution microscope using the SoftWorx Explorer software. Three-dimensional z-stacks were collected of individual cells using .15 μm sections, with an emphasis on imaging the cell membrane-substrate interface. Images were taken for each z-section using the DAPI, FITC, and rhodamine filters. Within an experiment, exposure times, and brightness and contrast levels were typically kept constant for each filter for all cells imaged. Z-stacks of cells were deconvolved using the “aggressive” algorithm for 10 iterations.

A second experiment was performed using the CHO-B2 $\alpha 5\beta 1$ cells. The experimental conditions were similar to the first experiment with 3 exceptions: 1) comb copolymer surfaces were coupled with 25 μM or 100 μM synergy-RGD scrambled synergy-RGD peptide; 2) 15,000 cells were seeded per well; 3) cells were fixed after 15 hours. Imaging on the Zeiss Axiovert was also performed as described above, but 10X images were taken in addition to 20X images. Similarly, images on the DeltaVision were taken as described, except that z-stacks consisted of sections were spaced every .20 μm .

2.3 Results

2.3.1 FACS confirms CHO-B2 $\alpha 5\beta 1$ and $\alpha v\beta 3$ integrin expression

To ensure that any observed cell attachment to the synergy-RGD peptide was mediated by either $\alpha 5\beta 1$ or $\alpha v\beta 3$, FACS analysis was used to examine the expression of both integrins in each of the three CHO-B2 cell variants. As shown in Figure 2.5, the CHO-B2 $\alpha 5\beta 1$ cells showed that 71.4% of the population expressed significant levels of the $\alpha 5\beta 1$ integrin, and only 0.7% expressed $\alpha v\beta 3$ integrin. Similarly, 91% of the CHO-B2 $\alpha v\beta 3$ were found to express significant levels of the $\alpha v\beta 3$ integrin, and only 0.2% expressed the $\alpha 5\beta 1$ integrin. None of the CHO-B2 pcDNA control cells were found to express significant levels of the $\alpha 5\beta 1$ integrin and only 0.7% expressed significant levels of the $\alpha v\beta 3$ integrin. These results confirmed that each CHO-B2 variant expressed only the integrin heterodimer expected as a result of transfection with either the $\alpha 5$ integrin subunit or the $\beta 3$ subunit.

2.3.2 Synergy-RGD peptide promotes rapid $\alpha v\beta 3$ -mediated CHO attachment and spreading

To determine if the synergy-RGD peptide could promote $\alpha v\beta 3$ -mediated cell adhesion we examined the attachment and spreading of CHO-B2 $\alpha v\beta 3$ cells on synergy-RGD substrates, and scrambled synergy-RGD substrates. Because the synergy-site is not present on vitronectin, and has not been observed to be an important component of $\alpha v\beta 3$ mediated adhesion, we hypothesized that CHO-B2 $\alpha v\beta 3$ attachment would be similar on both synergy-RGD and scrambled synergy-RGD substrates. As it is well established that

small linear peptides can promote robust $\alpha\beta3$ -mediated adhesion, here, we expected CHO-B2 $\alpha\beta3$ cells to attach and spread well on both RGD surfaces.

Figure 2.6 shows randomly selected fields of CHO-B2 $\alpha\beta3$ that were seeded at 100,000 cells per well in medium supplemented with 10% serum, fixed 4 hours after seeding, stained with Alexa Fluor 488 phalloidin, and imaged at 20X magnification. On mock tethered surfaces, only a small number of minimally spread cells, devoid of actin stress fibers, were observed. Conversely, many more cells attached to glass surfaces, compared to the mock tethered surfaces. Cells appeared to be in the process of spreading, but were not yet well spread, as most were rounded and devoid of stress fibers. However, on the synergy-RGD and scrambled synergy-RGD surfaces, all of the imaged fields contained a large number of well spread cells with an elongated morphology, with clearly evident actin stress fibers, suggesting that the synergy-RGD peptide could specifically promote $\alpha\beta3$ -mediated adhesion. Furthermore, we observed that the cells spread more rapidly on the synergy-RGD surfaces than on glass surfaces, where adhesion is mediated via serum adsorption.

2.3.3 $\alpha\beta3$ -mediated CHO attachment to synergy-RGD peptides are PHSRN-independent

Qualitatively, no significant differences were observed between cells on synergy-RGD or scrambled synergy-RGD at either 25 μM or 100 μM peptide coupling concentrations. To provide a semi-quantitative metric of cell spreading, the percentage of an image that contained cells was measured using ImageJ (Table 2.1). Using a t-test, no significant differences were observed in cell area between surface conditions. These

results suggest that that the PHSRN branch on the synergy-RGD peptide does not play an important role in promoting $\alpha\beta3$ -mediated attachment and spreading.

Table 2.1

Surface	25 μ M synergy-RGD	25 μ M scrambled synergy-RGD	100 μ M synergy-RGD	100 μ M scrambled synergy-RGD
Image 1	0.20	0.21	0.18	0.18
Image 2	0.18	0.17	0.19	0.23
Image 3	0.22	0.26	0.20	0.23
Image 4	0.18	0.25	0.13	0.29
Mean	0.19	0.22	0.17	0.23

t-test p-values				
25 μ M synergy-RGD	X	0.24422	0.35602	0.18069
25 μ M scrambled synergy-RGD	0.24422	X	0.12272	0.79408
100 μ M synergy-RGD	0.35602	0.12272	X	0.09641
100 μ M scrambled synergy-RGD	0.18069	0.79408	0.09641	X

2.3.4 Synergy-RGD peptide does not promote $\alpha5\beta1$ -mediated CHO attachment at short times

Because NR6wt cells express both $\alpha\beta3$ and $\alpha5\beta1$, previous results with $\alpha\beta3$ blocking antibodies and the rapid spreading of the CHO-B2 $\alpha\beta3$ cells demonstrated that the synergy-RGD peptide could promote $\alpha\beta3$ -mediated spreading. However, rat hepatocytes, which reportedly express $\alpha5\beta1$ but not $\alpha\beta3$, were observed to spread on the synergy-RGD peptide. Therefore, we chose to examine the attachment and spreading of CHO-B2 $\alpha5\beta1$ cells on the synergy-RGD peptide. We also examined cell attachment and spreading on scrambled synergy-RGD surfaces to parse any specific effects of the PHSRN synergy motif. Because the CHO-B2 $\alpha\beta3$ cells were well-spread after only 4 hours on surfaces that had been coupled with 25 μ M peptide solutions, we chose to use similar conditions to examine CHO-B2 $\alpha5\beta1$ cells. Cell attachment to mock coupled

surfaces as well as to untreated glass coverslips served as negative and positive controls. For this study CHO-B2 pcDNA control cells were used to determine if observed cell attachment to the comb copolymer surfaces was specifically $\alpha 5\beta 1$ -mediated. Cells were seeded at 10^5 cells per well on surfaces in 24-well plates. In contrast to the observed behavior of the CHO-B2 $\alpha \nu \beta 3$ cells, neither the CHO-B2 $\alpha 5\beta 1$ nor pcDNA control cells appeared to be well spread on any of the RGD surfaces at 4 and 7 hours after seeding. It has been shown that unlike $\alpha \nu \beta 3$ -mediated attachment, cell attachment through the $\alpha 5\beta 1$ integrin requires the engagement of syndecan-4 to promote focal adhesion and stress fiber formation [56, 57]. Although the native ligand for syndecan-4 is the heparin-binding domain of fibronectin, addition of a soluble heparin-binding fragment or clustering of syndecan-4 with antibodies has also been shown to promote focal adhesion and stress fiber formation in a RhoA dependent manner [58, 59]. Interestingly, RhoA-induced focal adhesion and stress fiber formation can be promoted in a syndecan-independent manner through the addition of lysophosphatidic acid (LPA), which is a component of serum [60, 61]. Because our medium contained serum, we therefore hypothesized that even without syndecan engagement, serum-induced RhoA activation could promote focal adhesion and stress fiber formation, and therefore cell attachment, at later time points on the synergy-RGD peptide. As a result, the cells were incubated (under 95% air/5% CO₂ at 37°C) overnight, and fixed after 23 hours, before being stained and mounted.

2.3.5 Synergy-RGD peptide promotes $\alpha 5\beta 1$ -mediated CHO attachment and spreading

Figure 2.7 shows randomly selected fields of CHO-B2 pcDNA cells on glass and synergy-RGD surfaces. Many CHO-B2 pcDNA cells, which were devoid of $\alpha v \beta 3$ and $\alpha 5 \beta 1$ integrins, attached and spread to a moderate degree to the untreated glass surfaces (Figure 2.7a). In comparison, very few cells attached to the synergy-RGD surfaces, and those that were present were extremely rounded (Figure 2.7b) and similar results were evident on the mock tethered and scrambled synergy-RGD surfaces (data not shown). Figures 2.8.1 and 2.8.2 show randomly selected fields of CHO-B2 $\alpha 5 \beta 1$ cells on mock tethered, glass, synergy-RGD, and scrambled synergy-RGD surfaces. Very little cell attachment was observed on the mock coupled surfaces (Figure 2.8.1a), and again, the few cells present were very poorly attached, as evident by their rounded morphology. Unlike the CHO-B2 pcDNA cells, however, the CHO-B2 $\alpha 5 \beta 1$ cells were observed to be well-spread on glass surfaces (Figure 2.8.1b) as evidenced by their elongated morphology. In contrast to the CHO-B2 pcDNA cells, however, many CHO-B2 $\alpha 5 \beta 1$ cells attached to the synergy-RGD and scrambled synergy-RGD surfaces (Figures 2.8.2c and 2.8.2d). These cells were moderately well spread, but not to the same extent as those on glass, and no qualitative differences in cell spreading were observed between the synergy-RGD and scrambled synergy-RGD surfaces. Because the CHO-B2 $\alpha 5 \beta 1$ cells adhered to the synergy-RGD surfaces, whereas the CHO-B2 pcDNA cells did not, it was clear that the synergy-RGD peptide could promote $\alpha 5 \beta 1$ -mediated cell attachment.

2.3.6 Synergy-RGD peptide promotes $\alpha 5 \beta 1$ -mediated CHO stress-fiber formation

Because attachment and spreading do not fully represent all of the processes involved with cell adhesion, we chose to examine synergy-RGD-mediated focal adhesion

and stress fiber formation, through the fluorescent staining of vinculin and actin. Figures 2.9.1 and 2.9.2 show individual CHO-B2 $\alpha 5\beta 1$ cells that have been stained for vinculin and actin that were chosen at random on the different surfaces. On the mock tethered surfaces (Figure 2.9.1a), the few attached cells were very poorly spread, and without evident stress fibers or focal adhesions. However, on glass (Figure 2.9.1b), synergy-RGD (Figure 2.9.1c), or scrambled synergy-RGD (Figure 2.9.2d), most CHO-B2 $\alpha 5\beta 1$ cells had formed focal adhesions and stress fibers. However, as shown in Figure 2.10, the very few CHO-B2 pcDNA cells attached to the synergy-RGD surfaces appeared similar to the CHO-B2 $\alpha 5\beta 1$ on the mock tethered surfaces: poorly spread, and without evident stress fibers or focal adhesions. These results clearly indicated that the synergy-RGD peptide was capable of inducing cell adhesion through an $\alpha 5\beta 1$ -dependent mechanism. However, our similar results with the scrambled synergy-RGD peptide appeared to indicate that the PHSRN motif was not playing an important role in any of the cell processes (spreading, attachment, focal adhesion formation, or stress fiber formation) that we had examined.

2.3.7 The PHSRN sequence in synergy-RGD does not enhance CHO-B2 $\alpha 5\beta 1$ focal adhesion formation or stress fiber formation

An important factor in cell adhesion is of course the density of adhesive ligands that are available on a surface. Therefore, we hypothesized that synergistic effects PHSRN sequence might not be evident on surfaces in which the overall concentration of synergy-RGD peptide was too low. We chose to further probe the effect of the PHSRN sequence using surfaces that had been prepared with synergy-RGD or scrambled

synergy-RGD using both 25 μM and 100 μM coupling solutions. As noted previously, the concentration of synergy-RGD and scrambled synergy-RGD peptide on the surface of comb copolymer films is estimated to be approximately 2×10^4 and 8×10^4 peptides/ μm^2 for the 25 and 100 μM solutions respectively. Glass surfaces were used as a positive control.

CHO-B2 $\alpha 5\beta 1$ were seeded at 15,000 cells per surface, to facilitate the imaging of individual cells, fixed after 15 hours, stained, and imaged at 10X and 20X (Figures 2.11, 2.12.1 and 2.12.2). Qualitatively, no obvious differences in the number of attached cells or cell spreading were immediately apparent between the different surfaces. Therefore, the DeltaVision was used to further examine focal adhesion and stress fiber formation in cells seeded on the synergy-RGD and scrambled synergy-RGD surfaces (Figures 2.13.1, 2.13.2, and 2.13.3). On all substrates, most cells that had attached displayed both focal adhesion formation, and stress fiber formation. Cells appeared to have increased spread area, as well as increased stress fiber and focal adhesion formation on the 100 μM synergy-RGD and 100 μM scrambled synergy-RGD surfaces compared to the 25 μM synergy-RGD surfaces, suggesting that both peptides could promote spreading in a dose-dependent manner. However, as observed previously, cells on the 100 μM synergy-RGD and 100 μM scrambled synergy-RGD surfaces displayed similar spreading, focal adhesion, and stress fiber formation

Taken together these results suggested that the synergy-RGD peptide can mediate cell adhesion, as well as focal adhesion formation and stress fiber formation via the $\alpha 5\beta 1$ integrin. However, no qualitative difference in cell attachment, focal adhesion formation, or stress fiber formation was evident between the synergy-RGD and scrambled synergy-

RGD surfaces, suggesting that the PHSRN synergy sequence within the synergy-RGD peptide was not influencing $\alpha 5\beta 1$ cell attachment, focal adhesion formation, or stress fiber formation.

2.4 Discussion

The promotion of specific cell-biomaterials interactions through RGD peptides in the presence of the PHSRN synergy domain has been studied through various methods, with conflicting results. Previous work performed in our laboratory using a synergy-RGD peptide based on the fibronectin structure has suggested that the use of the synergy-RGD peptide could promote enhanced cell attachment in multiple cell types compared to traditional linear RGD peptides. However, due to differences in surface concentrations, the effect of the ligand density could not be decoupled from these results. Different cell lines also gave conflicting results concerning the integrin specificity of these surfaces. Using variants of CHO-B2 cells that were transfected to express either $\alpha v\beta 3$ or $\alpha 5\beta 1$ alone, we found that synergy-RGD peptides could mediate cell adhesion and spreading through either $\alpha v\beta 3$ or $\alpha 5\beta 1$ integrin and lead to focal adhesion and stress-fiber formation. Focal adhesion and stress-fiber formation were integrin dependent, as CHO-B2 cells transfected with a control vector, and expressing minimal levels of $\alpha v\beta 3$ or $\alpha 5\beta 1$ integrin were unable to form either on peptide-conjugated surfaces. While CHO-B2 cells express $\alpha v\beta 1$ integrin which can mediate attachment to fibronectin surfaces [52], they do not appear to be functionally relevant in this system.

In this study, we found no differential effects of the synergy site on cell attachment, focal adhesion formation, or stress-fiber formation in comparison to a

scrambled synergy site (HSPNR) for either the $\alpha\beta3$ or $\alpha5\beta1$ expressing cells. Because the shape, overall composition, and molecular weight of both peptides were identical, there were no expected differences in terms of surface coupling efficiency between the two peptides, or penetration into the polymer bulk, as long as the peptide solution concentration used for coupling were the same.

One interpretation of this data is that the presence of the PHSRN motif in the synergy-RGD peptide is not having any direct effect on cellular adhesion. Because the exact role of the synergy-site is still unclear, it is possible that the structure of the synergy-RGD peptide does accurately replicate the structural relationship between the synergy-site and the RGD adhesion motif in native fibronectin, and therefore has no effect at all on integrin binding. Previous work has shown that the spacing between the PHSRN and RGD motifs in synthetic peptides is an important factor [34], suggesting that the spacing between the PHSRN and RGD motif in the synergy-RGD peptide may not be optimized. On the other hand, our previous observations with hepatocytes and NR6wt cells using this same system suggest that this may be a cell-type specific behavior. This is supported by the contrasting results observed by two groups using the same peptide, but examining different cell types [22, 33].

In comparison to previous studies which used cells with undetermined or heterogeneous integrin-expression profiles, we used variants of the CHO-B2 cell line that were transfected to express either $\alpha\beta3$ or $\alpha5\beta1$, but not both integrins and compared these to control cells which expressed neither $\alpha\beta3$ or $\alpha5\beta1$. The cell-surface expression of integrins on these cells were confirmed by FACS analysis. It should be noted that about 30% of the CHO-B2 $\alpha5\beta1$ cells did not express-significant levels of the $\alpha5\beta1$ -

integrin. However, these results were expected because the cell line was not clonally derived. Additionally, these numbers were consistent with FACS analysis performed on this cell line in the Corbett lab which kindly provided these cells (personal correspondence, Mohan Nair).

It is possible that because CHO-B2 cells in general are not functionally attached to fibronectin in nature, interactions between artificially expressed integrins and the synergy site are not functionally supported. Supporting this idea is evidence that the activation state of integrins has an effect on synergy site function, and differs among cell types [62]. While the mechanisms leading to integrin activation are poorly understood, recent evidence suggests that native ECM molecules may possess cryptic domains that can interact with other cell receptors, such as syndecans, to alter integrin activation state [63]. Therefore, it is plausible that CHO-B2 $\alpha 5\beta 1$ interactions with the PHSRN motif require other mechanisms that might be modulated by native ECM, but not by the synergy-RGD peptide.

In this study, we chose to examine cell attachment by staining cells for vinculin and actin to look for focal adhesion formation and/or stress fiber formation. This type of analysis would provide an appropriate evaluation of adhesion markers, particularly considering clinical applications of this biomaterial for selective cell-retention in bone tissue engineering (see Chapter 3). It is possible that the PHSRN motif may affect aspects of cell adhesion not studied in this work, specifically the adhesion strength of the cells to the surfaces. However, this seems unlikely since the synergy-site has generally been observed to play a role in cell spreading in other cell systems [33, 34], and cell-spreading and focal adhesion formation has a direct impact on adhesion strength [64].

Another possibility, however, is that both the PHSRN branch and the HSPNR branch are enhancing $\alpha 5\beta 1$ -mediated adhesion to a similar degree, compared to RGD alone. Previous work suggests that structural stability is a crucial component of the synergistic binding of $\alpha 5\beta 1$ and fibronectin [29]. Additionally, while it was shown that mutations to ninth and tenth domains of fibronectin can disrupt this synergistic affect [28], Takagi pointed out that 5 of 8 identified mutations were arginine to alanine mutations, including the arginine within PHSRN [30]. Takagi suggests that these mutations would lead to acidic residues within these fragments to cause a negative potential that would decrease the binding association rate. He further argues that the basic residues within the ninth fragment do not make contact with $\alpha 5\beta 1$, but instead mediate long range “steering” of the binding interactions. According to Takagi’s model, because the scrambled synergy-peptide contains the same basic arginine residue as synergy-RGD, and has a similar branched structure, it seems possible that both peptides are conferring a similar degree of “steering” and stability to the $\alpha 5\beta 1$ -binding interaction, which would account for the similar results observed for both peptides.

Another interesting observation from this work was that the CHO-B2 $\alpha \nu \beta 3$ cells spread more quickly than the CHO-B2 $\alpha 5\beta 1$ cells. In fact, at 4 hours, the CHO-B2 $\alpha \nu \beta 3$ cells were spread to a greater extent on RGD surfaces than on glass surfaces. On the other hand, the CHO-B2 $\alpha 5\beta 1$ cells spread more slowly, and at no point were observed to be spread to a greater degree on the RGD surfaces than on glass. One possible explanation is that the $\alpha \nu \beta 3$ integrin may bind to the RGD peptides with a higher affinity than the $\alpha 5\beta 1$ integrin. However, because the FACS analysis is not quantitative for comparing levels of expression of different integrins, it is also possible that differences in

receptor expression may result in the increased spreading observed in the CHO-B2 $\alpha\text{v}\beta\text{3}$ cells.

Finally, a third potential source of this difference may be a result of differential signaling cascade as promoted by each integrin. An example of differential signaling was reported by Danen et al. who observed that $\alpha\text{v}\beta\text{3}$ and $\alpha\text{5}\beta\text{1}$ differentially activated RhoA signaling which in turn affects the organization of matrix adhesions [65]. Similarly, both integrins have different requirements for focal adhesion formation. In serum-free culture, $\alpha\text{5}\beta\text{1}$ -mediated focal adhesion and stress fiber formation requires syndecan engagement (via integrins or the heparin-binding domain of fibronectin) or the exogenous addition of LPA to induce RhoA activity [56, 58]. Therefore, it is possible that $\alpha\text{5}\beta\text{1}$ -mediated adhesion could not be induced until serum factors such as fibronectin or LPA promoted RhoA activity. It should also be noted that during routine culture, the CHO-B2 $\alpha\text{v}\beta\text{3}$ cells appeared to spread more quickly than the CHO-B2 $\alpha\text{5}\beta\text{1}$ cells, also suggesting that multiple factors are likely involved for the differences observed in cell spreading on the RGD surfaces. Therefore, it is important to recognize that these experiments show that both integrins can mediate cell attachment to the RGD peptides we examined, but we were unable to observe *preferential* binding of either the $\alpha\text{v}\beta\text{3}$ or the $\alpha\text{5}\beta\text{1}$ integrin to the synergy-RGD peptide.

Future experiments using cell lines transfected with both integrins could be used in combination with blocking experiments and immunostaining to determine if cell adhesion was preferentially mediated to the synergy-RGD peptide through a specific integrin. It is likely that results would be cell line dependent, and thus would need to be examined in the context of a particular study. Direct studies of integrin affinity for the

synergy-RGD peptide could be performed using surface plasmon resonance studies or competitive binding experiments. However, from the perspective of tissue engineering applications, the cell adhesion studies are likely more informative as to the utility of the synergy-RGD peptide.

2.5 Conclusions

In this work, we have provided evidence that the synergy-RGD peptide can promote cellular adhesion via both the $\alpha\text{v}\beta\text{3}$ and the $\alpha\text{5}\beta\text{1}$ integrin. The PHSRN synergy motif did not increase cell spreading, focal adhesion formation, or stress fiber formation in CHO-B2 cells expressing either $\alpha\text{v}\beta\text{3}$ or $\alpha\text{5}\beta\text{1}$ only, suggesting that cell-type specific behavior or integrin activation or signaling may be important in mediating PHSRN synergy motif function. The crucial result of this work is that we have shown that the synergy-RGD peptide can be used in biomaterials applications to mediate adhesion of cells expressing either $\alpha\text{v}\beta\text{3}$ or $\alpha\text{5}\beta\text{1}$, but functionality of the synergy site must be determined independently.

2.6 References

1. Roach, P., et al., *Modern biomaterials: a review - bulk properties and implications of surface modifications*. J Mater Sci Mater Med, 2007. **18**(7): p. 1263-77.
2. Wilson, C.J., et al., *Mediation of biomaterial-cell interactions by adsorbed proteins: a review*. Tissue Eng, 2005. **11**(1-2): p. 1-18.
3. Cima, L.G., *Polymer substrates for controlled biological interactions*. J Cell Biochem, 1994. **56**(2): p. 155-61.
4. Hersel, U., C. Dahmen, and H. Kessler, *RGD modified polymers: biomaterials for stimulated cell adhesion and beyond*. Biomaterials, 2003. **24**(24): p. 4385-415.

5. Hynes, R.O., *Integrins: bidirectional, allosteric signaling machines*. Cell, 2002. **110**(6): p. 673-87.
6. Giancotti, F.G. and E. Ruoslahti, *Integrin signaling*. Science, 1999. **285**(5430): p. 1028-32.
7. Schwartz, M.A., *Integrin signaling revisited*. Trends Cell Biol, 2001. **11**(12): p. 466-70.
8. Pierschbacher, M.D. and E. Ruoslahti, *Cell attachment activity of fibronectin can be duplicated by small synthetic fragments of the molecule*. Nature, 1984. **309**(5963): p. 30-3.
9. Suzuki, S., et al., *Complete amino acid sequence of human vitronectin deduced from cDNA. Similarity of cell attachment sites in vitronectin and fibronectin*. EMBO J, 1985. **4**(10): p. 2519-24.
10. Ruoslahti, E., *RGD and other recognition sequences for integrins*. Annu Rev Cell Dev Biol, 1996. **12**: p. 697-715.
11. Pytela, R., M.D. Pierschbacher, and E. Ruoslahti, *Identification and isolation of a 140 kd cell surface glycoprotein with properties expected of a fibronectin receptor*. Cell, 1985. **40**(1): p. 191-8.
12. Pytela, R., M.D. Pierschbacher, and E. Ruoslahti, *A 125/115-kDa cell surface receptor specific for vitronectin interacts with the arginine-glycine-aspartic acid adhesion sequence derived from fibronectin*. Proc Natl Acad Sci U S A, 1985. **82**(17): p. 5766-70.
13. Charo, I.F., et al., *The vitronectin receptor alpha v beta 3 binds fibronectin and acts in concert with alpha 5 beta 1 in promoting cellular attachment and spreading on fibronectin*. J Cell Biol, 1990. **111**(6 Pt 1): p. 2795-800.
14. Hautanen, A., et al., *Effects of modifications of the RGD sequence and its context on recognition by the fibronectin receptor*. J Biol Chem, 1989. **264**(3): p. 1437-42.
15. Griffith, L.G., *Emerging design principles in biomaterials and scaffolds for tissue engineering*. Ann N Y Acad Sci, 2002. **961**: p. 83-95.
16. Griffith, L.G. and G. Naughton, *Tissue engineering--current challenges and expanding opportunities*. Science, 2002. **295**(5557): p. 1009-14.
17. Pierschbacher, M.D. and E. Ruoslahti, *Influence of Stereochemistry of the Sequence Arg-Gly-Asp-Xaa on Binding-Specificity in Cell-Adhesion*. Journal of Biological Chemistry, 1987. **262**(36): p. 17294-17298.

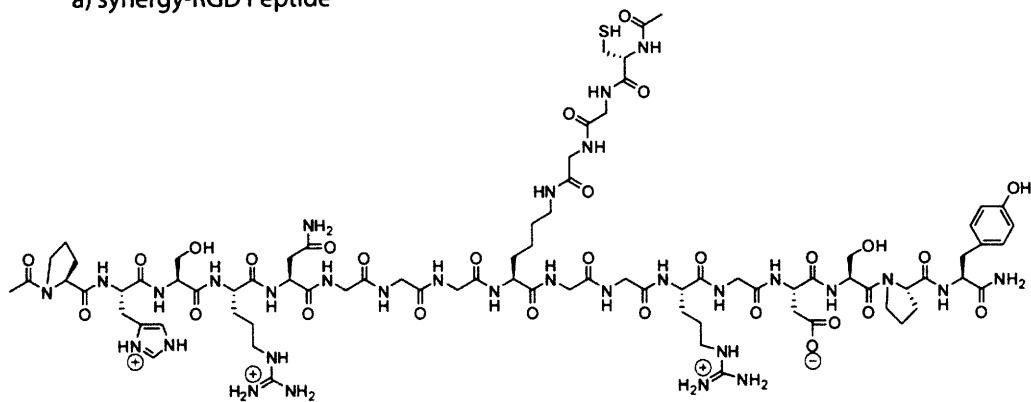
18. Ochsenhirt, S.E., et al., *Effect of RGD secondary structure and the synergy site PHSRN on cell adhesion, spreading and specific integrin engagement*. *Biomaterials*, 2006. **27**(20): p. 3863-74.
19. Dechantsreiter, M.A., et al., *N-methylated cyclic RGD peptides as highly active and selective alpha(v)beta(3) integrin antagonists*. *Journal of Medicinal Chemistry*, 1999. **42**(16): p. 3033-3040.
20. Pfaff, M., et al., *Selective recognition of cyclic RGD peptides of NMR defined conformation by alpha IIb beta 3, alpha V beta 3, and alpha 5 beta 1 integrins*. *J Biol Chem*, 1994. **269**(32): p. 20233-8.
21. Aota, S., M. Nomizu, and K.M. Yamada, *The short amino acid sequence Pro-His-Ser-Arg-Asn in human fibronectin enhances cell-adhesive function*. *J Biol Chem*, 1994. **269**(40): p. 24756-61.
22. Petrie, T.A., et al., *Integrin specificity and enhanced cellular activities associated with surfaces presenting a recombinant fibronectin fragment compared to RGD supports*. *Biomaterials*, 2006. **27**(31): p. 5459-70.
23. Garcia, A.J., J.E. Schwarzbauer, and D. Boettiger, *Distinct activation states of alpha5beta1 integrin show differential binding to RGD and synergy domains of fibronectin*. *Biochemistry*, 2002. **41**(29): p. 9063-9.
24. Yang, X.B., et al., *Human osteoprogenitor growth and differentiation on synthetic biodegradable structures after surface modification*. *Bone*, 2001. **29**(6): p. 523-31.
25. Aota, S., T. Nagai, and K.M. Yamada, *Characterization of regions of fibronectin besides the arginine-glycine-aspartic acid sequence required for adhesive function of the cell-binding domain using site-directed mutagenesis*. *J Biol Chem*, 1991. **266**(24): p. 15938-43.
26. Obara, M., M.S. Kang, and K.M. Yamada, *Site-directed mutagenesis of the cell-binding domain of human fibronectin: separable, synergistic sites mediate adhesive function*. *Cell*, 1988. **53**(4): p. 649-57.
27. Obara, M. and K. Yoshizato, *Possible involvement of the interaction of the alpha 5 subunit of alpha 5 beta 1 integrin with the synergistic region of the central cell-binding domain of fibronectin in cells to fibronectin binding*. *Exp Cell Res*, 1995. **216**(1): p. 273-6.
28. Redick, S.D., et al., *Defining fibronectin's cell adhesion synergy site by site-directed mutagenesis*. *J Cell Biol*, 2000. **149**(2): p. 521-7.
29. Altroff, H., L. Choulier, and H.J. Mardon, *Synergistic activity of the ninth and tenth FIII domains of human fibronectin depends upon structural stability*. *J Biol Chem*, 2003. **278**(1): p. 491-7.

30. Takagi, J., *Structural basis for ligand recognition by RGD (Arg-Gly-Asp)-dependent integrins*. *Biochem Soc Trans*, 2004. **32**(Pt3): p. 403-6.
31. Feng, Y. and M. Mrksich, *The synergy peptide PHSRN and the adhesion peptide RGD mediate cell adhesion through a common mechanism*. *Biochemistry*, 2004. **43**(50): p. 15811-21.
32. Dillow, A.K., et al., *Adhesion of alpha5beta1 receptors to biomimetic substrates constructed from peptide amphiphiles*. *Biomaterials*, 2001. **22**(12): p. 1493-505.
33. Benoit, D.S. and K.S. Anseth, *The effect on osteoblast function of colocalized RGD and PHSRN epitopes on PEG surfaces*. *Biomaterials*, 2005. **26**(25): p. 5209-20.
34. Mardilovich, A., et al., *Design of a novel fibronectin-mimetic peptide-amphiphile for functionalized biomaterials*. *Langmuir*, 2006. **22**(7): p. 3259-64.
35. Irvine, D.J., A.M. Mayes, and L.G. Griffith, *Nanoscale clustering of RGD peptides at surfaces using Comb polymers. 1. Synthesis and characterization of Comb thin films*. *Biomacromolecules*, 2001. **2**(1): p. 85-94.
36. Leckband, D., S. Sheth, and A. Halperin, *Grafted poly(ethylene oxide) brushes as nonfouling surface coatings*. *J Biomater Sci Polym Ed*, 1999. **10**(10): p. 1125-47.
37. Tessmar, J.K. and A.M. Gopferich, *Customized PEG-derived copolymers for tissue-engineering applications*. *Macromol Biosci*, 2007. **7**(1): p. 23-39.
38. Au, A., et al., *Formation of osteogenic colonies on well-defined adhesion peptides by freshly isolated human marrow cells*. *Biomaterials*, 2007. **28**(10): p. 1847-61.
39. Kuhlman, W., et al., *Interplay between PEO tether length and ligand spacing governs cell spreading on RGD-modified PMMA-g-PEO comb copolymers*. *Biomacromolecules*, 2007. **8**(10): p. 3206-13.
40. Richardson, L.B. "EGF receptor-mediated fibroblast signaling and motility : role of nanoscale spatial ligand organization." Ph.D. Thesis. Massachusetts Institute of Technology, 2005.
41. Fan, V.H., et al., *Tethered epidermal growth factor provides a survival advantage to mesenchymal stem cells*. *Stem Cells*, 2007. **25**(5): p. 1241-51.
42. Koo, L.Y., et al., *Co-regulation of cell adhesion by nanoscale RGD organization and mechanical stimulus*. *J Cell Sci*, 2002. **115**(Pt 7): p. 1423-33.
43. Kuhlman, W.A., et al., *Chain Conformations at the Surface of a Polydisperse Amphiphilic Comb Copolymer Film*. *Macromolecules*, 2006. **39**(15): p. 5122-5126.

44. Miyamoto, S., S.K. Akiyama, and K.M. Yamada, *Synergistic roles for receptor occupancy and aggregation in integrin transmembrane function*. Science, 1995. **267**(5199): p. 883-5.
45. Maheshwari, G., et al., *Cell adhesion and motility depend on nanoscale RGD clustering*. J Cell Sci, 2000. **113 (Pt 10)**: p. 1677-86.
46. Yauch, R.L., et al., *Mutational evidence for control of cell adhesion through integrin diffusion/clustering, independent of ligand binding*. J Exp Med, 1997. **186**(8): p. 1347-55.
47. Yin, D. "The applications of comb polymer to the study of liver cell adhesion and signaling." M. Eng. Thesis. Massachusetts Institute of Technology, 2004.
48. Annunziato, M.E., et al., *p-maleimidophenyl isocyanate: a novel heterobifunctional linker for hydroxyl to thiol coupling*. Bioconjug Chem, 1993. **4**(3): p. 212-8.
49. Kuhlman, W.A. and Massachusetts Institute of Technology. Dept. of Materials Science and Engineering. "Presentation and accessibility of surface bound ligands on amphiphilic graft copolymer films." Thesis Ph. D. --Massachusetts Institute of Technology Dept. of Materials Science and Engineering 2007. 2007.
50. Schreiner, C.L., et al., *Isolation and characterization of Chinese hamster ovary cell variants deficient in the expression of fibronectin receptor*. J Cell Biol, 1989. **109**(6 Pt 1): p. 3157-67.
51. Bauer, J.S., et al., *Motility of fibronectin receptor-deficient cells on fibronectin and vitronectin: collaborative interactions among integrins*. J Cell Biol, 1992. **116**(2): p. 477-87.
52. Zhang, Z., et al., *The alpha v beta 1 integrin functions as a fibronectin receptor but does not support fibronectin matrix assembly and cell migration on fibronectin*. J Cell Biol, 1993. **122**(1): p. 235-42.
53. Robinson, E.E., et al., *Alpha5beta1 integrin mediates strong tissue cohesion*. J Cell Sci, 2003. **116**(Pt 2): p. 377-86.
54. Ly, D.P., K.M. Zazzali, and S.A. Corbett, *De novo expression of the integrin alpha5beta1 regulates alphavbeta3-mediated adhesion and migration on fibrinogen*. J Biol Chem, 2003. **278**(24): p. 21878-85.
55. Mao, Y. and J.E. Schwarzbauer, *Accessibility to the fibronectin synergy site in a 3D matrix regulates engagement of alpha5beta1 versus alphavbeta3 integrin receptors*. Cell Commun Adhes, 2006. **13**(5-6): p. 267-77.

56. Morgan, M.R., M.J. Humphries, and M.D. Bass, *Synergistic control of cell adhesion by integrins and syndecans*. Nature Reviews Molecular Cell Biology, 2007. **8**(12): p. 957-969.
57. Mostafavi-Pour, Z., et al., *Integrin-specific signaling pathways controlling focal adhesion formation and cell migration*. Journal of Cell Biology, 2003. **161**(1): p. 155-167.
58. Saoncella, S., et al., *Syndecan-4 signals cooperatively with integrins in a Rho-dependent manner in the assembly of focal adhesions and actin stress fibers*. Proceedings of the National Academy of Sciences of the United States of America, 1999. **96**(6): p. 2805-2810.
59. Woods, A., et al., *Adhesion and cytoskeletal organisation of fibroblasts in response to fibronectin fragments*. EMBO J, 1986. **5**(4): p. 665-70.
60. Ridley, A.J., *Rho family proteins: coordinating cell responses*. Trends Cell Biol, 2001. **11**(12): p. 471-7.
61. Wilcox-Adelman, S.A., F. Denhez, and P.F. Goetinck, *Syndecan-4 modulates focal adhesion kinase phosphorylation*. J Biol Chem, 2002. **277**(36): p. 32970-7.
62. Danen, E.H., et al., *Requirement for the synergy site for cell adhesion to fibronectin depends on the activation state of integrin alpha 5 beta 1*. J Biol Chem, 1995. **270**(37): p. 21612-8.
63. Saito, Y., et al., *A peptide derived from tenascin-C induces beta1 integrin activation through syndecan-4*. J Biol Chem, 2007. **282**(48): p. 34929-37.
64. Garcia, A.J. and N.D. Gallant, *Stick and grip: measurement systems and quantitative analyses of integrin-mediated cell adhesion strength*. Cell Biochem Biophys, 2003. **39**(1): p. 61-73.
65. Danen, E.H.J., et al., *The fibronectin-binding integrins alpha 5 beta 1 and alpha v beta 3 differentially modulate RhoA-GTP loading, organization of cell matrix adhesions, and fibronectin fibrillogenesis*. Journal of Cell Biology, 2002. **159**(6): p. 1071-1086.

a) synergy-RGD Peptide



b) scrambled synergy-RGD Peptide

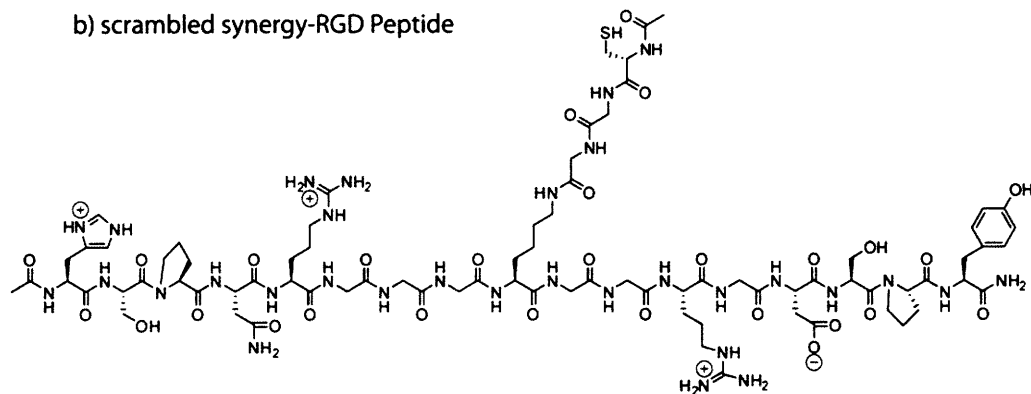


Figure 2.2 Structure of a) synergy-RGD and b) scrambled synergy-RGD peptide.

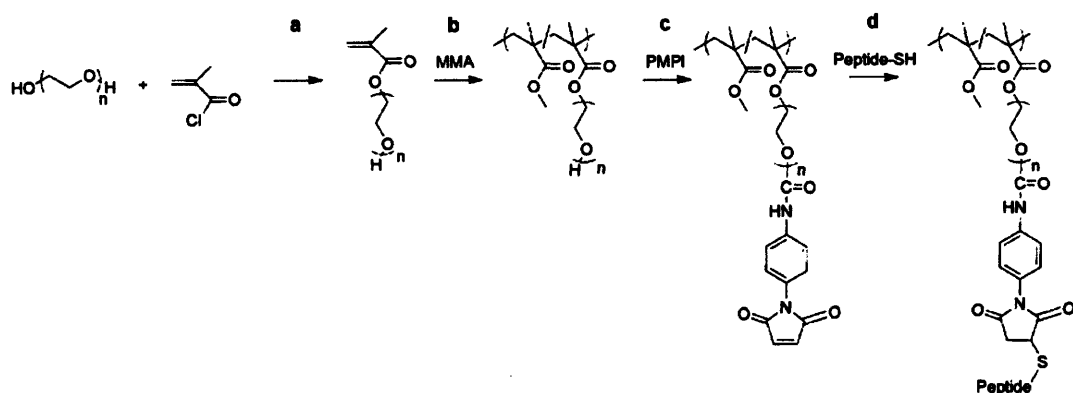


Figure 2.3 Synthesis of PEO macromonomer (a), synthesis of PMMA-g-PEO (b), reaction of PMMA-g-PEO with PMPI (c), and coupling of a thiol-bearing peptide to PMMA-g-PEO through PMPI (d). Reprinted with permission from Biomacromolecules, 8, Kuhlman W, Taniguchi I, Griffith LG, Mayes AM, Interplay between PEO tether length and ligand spacing governs cell spreading on RGD-modified PMMA-g-PEO comb copolymers, p. 3206-13, 2007. Copyright 2007 American Chemical Society.

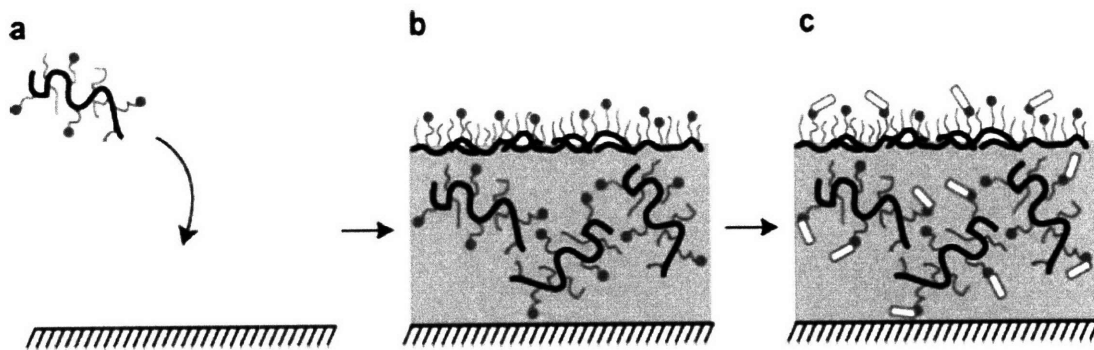


Figure 2.4 Schematic illustration of surface preparation. Surfaces are spin cast from PMPI-activated PMMA-g-PEO (a) and then exposed to peptide solution (b) to produce the peptide-bearing surface (c). Reprinted with permission from *Biomacromolecules*, 8, Kuhlman W, Taniguchi I, Griffith LG, Mayes AM, Interplay between PEO tether length and ligand spacing governs cell spreading on RGD-modified PMMA-g-PEO comb copolymers, p. 3206-13, 2007. Copyright 2007 American Chemical Society.

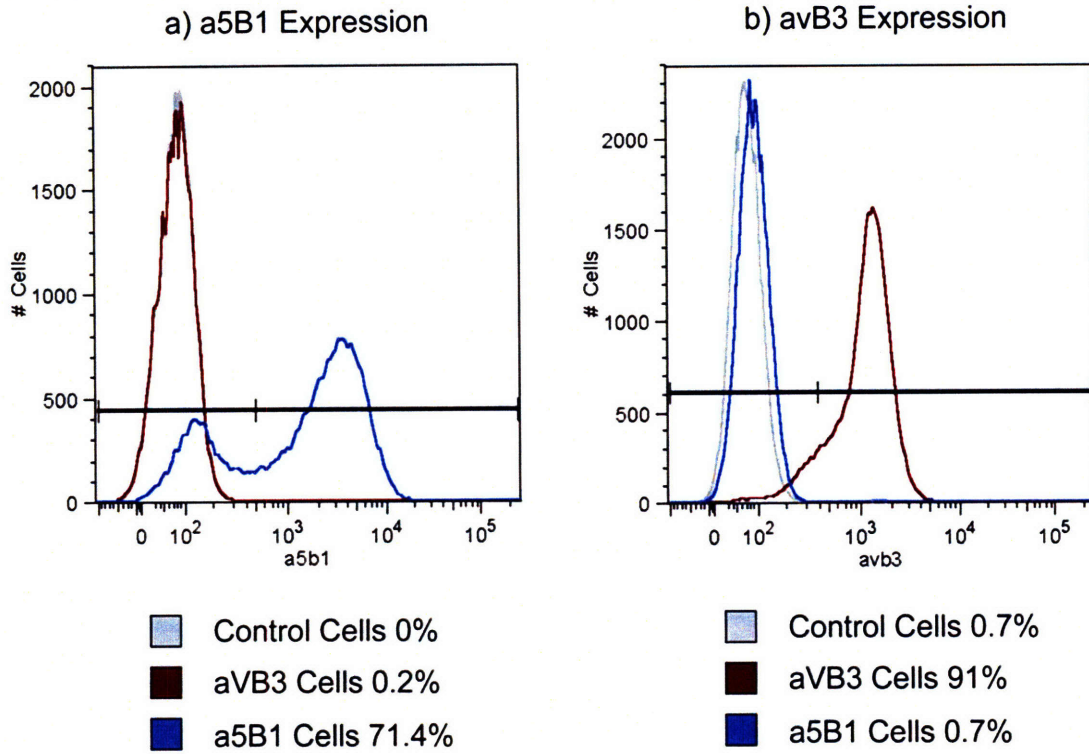


Figure 2.5 Percentage of cells expressing a) $\alpha 5\beta 1$ and b) $\alpha v\beta 3$ integrins in CHO-B2 cell lines transfected with control vector (Control Cells), or vector containing $\alpha 5$ integrin subunit (a5B1 Cells), or $\beta 3$ integrin subunit (avB3 Cells). $\alpha 5\beta 1$ expression was only detected in CHO-B2 $\alpha 5\beta 1$ cells and $\alpha v\beta 3$ was only detected in CHO-B2 $\alpha v\beta 3$ cells.

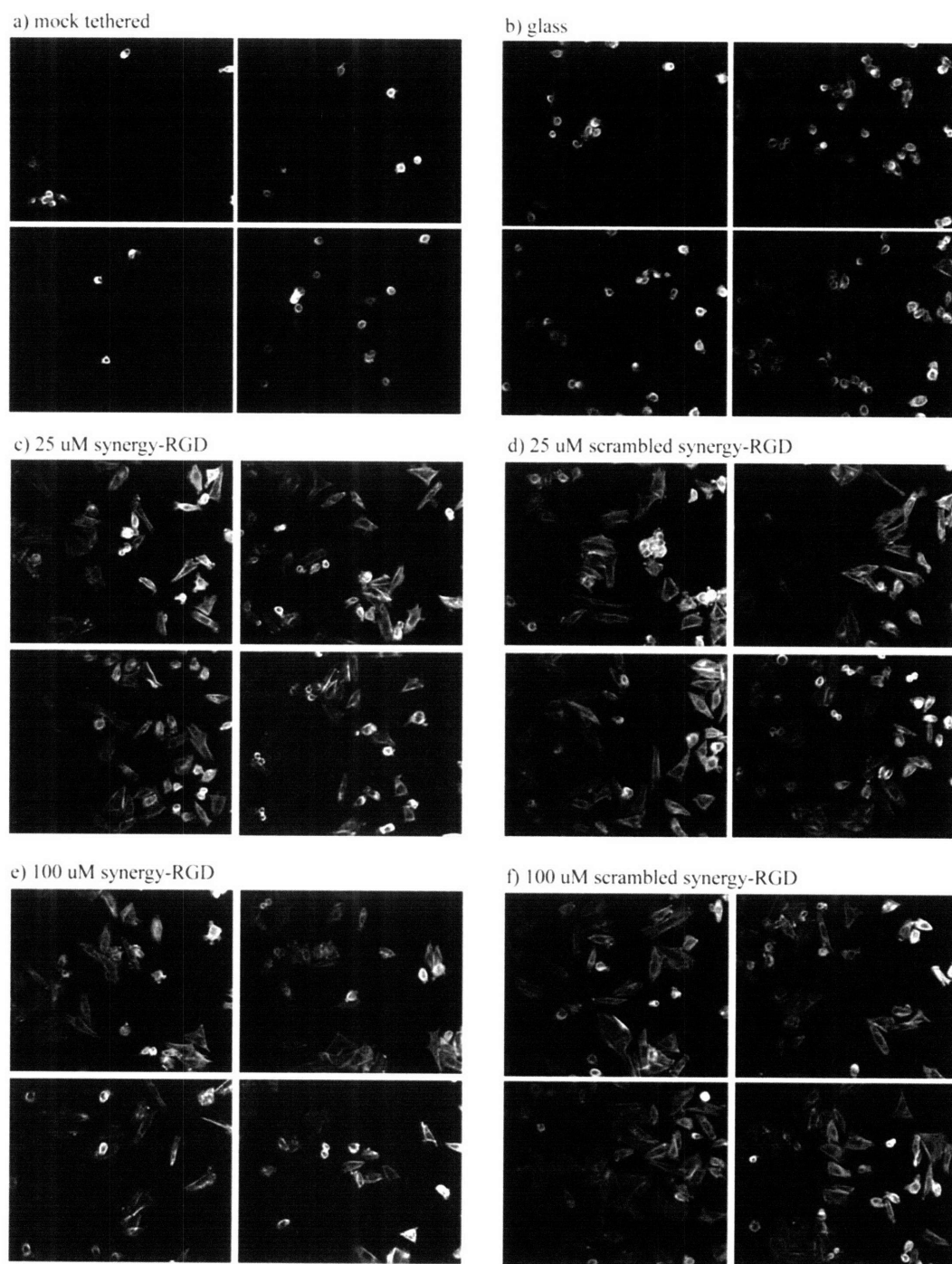
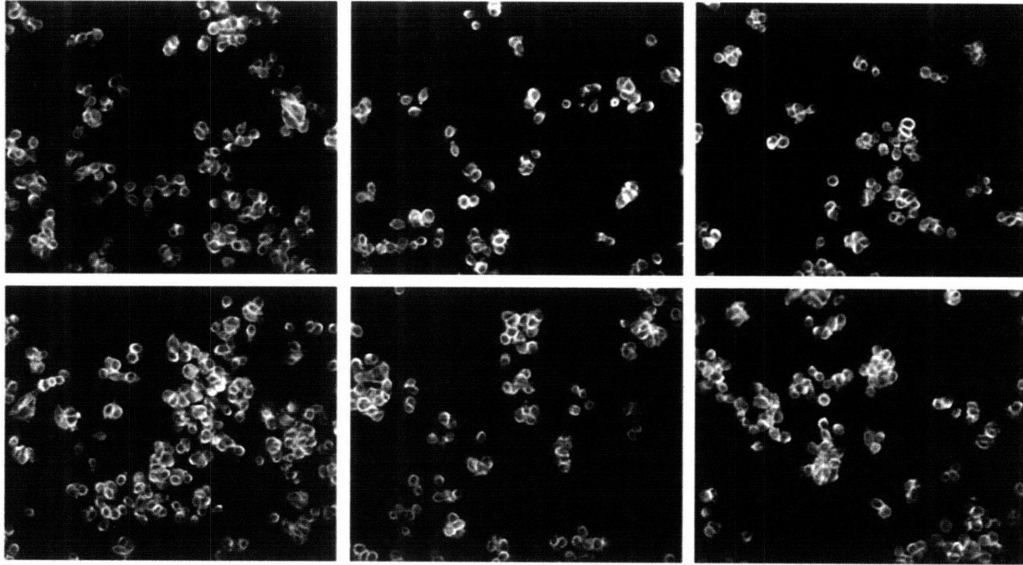


Figure 2.6 20X Images of actin-stained CHO-B2 α v β 3 cells on a) mock tethered, b) glass, c) 25 μ M synergy-RGD, and d) 25 μ M scrambled synergy-RGD surfaces.

a) Glass



b) 25 μ m synergy-RGD

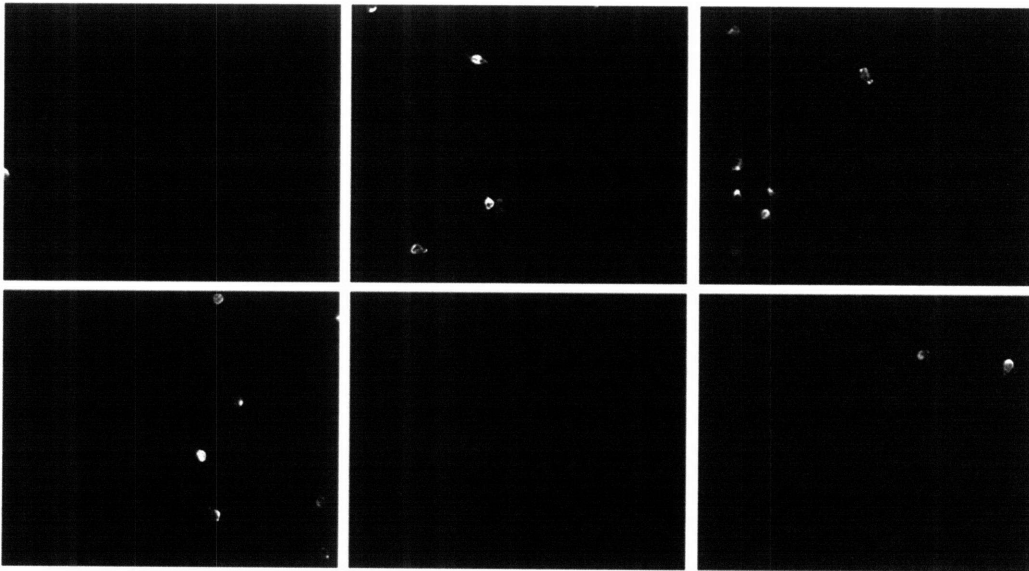
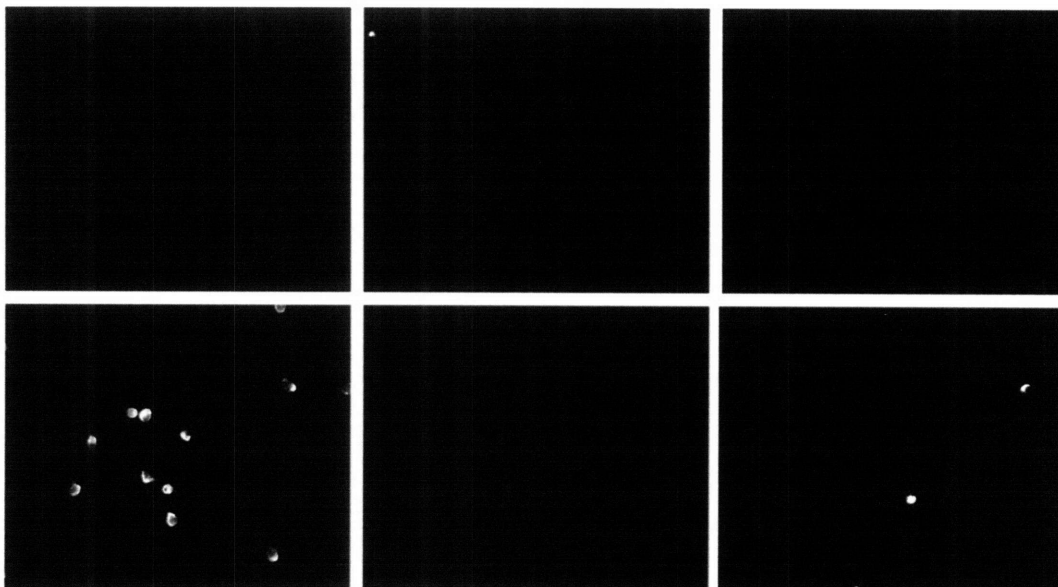


Figure 2.7 20X Images of actin-stained CHO-B2 pcDNA control cells on a) glass and b) 25 μ m synergy-RGD surfaces.

a) Mock Tethered



b) Glass

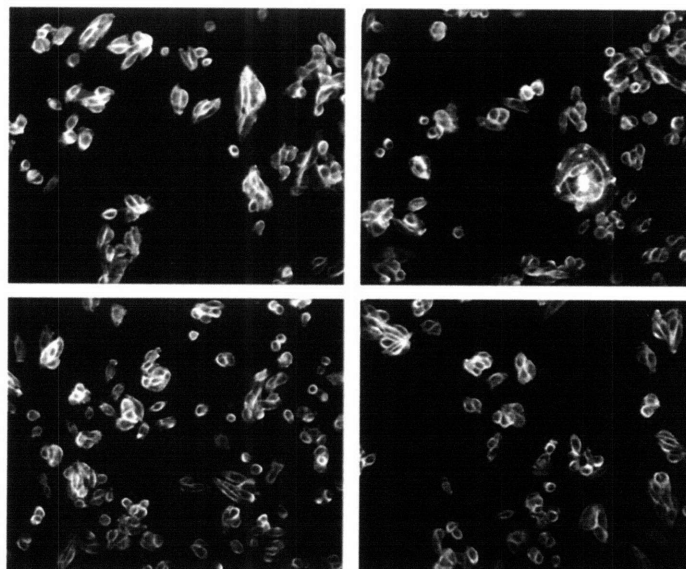
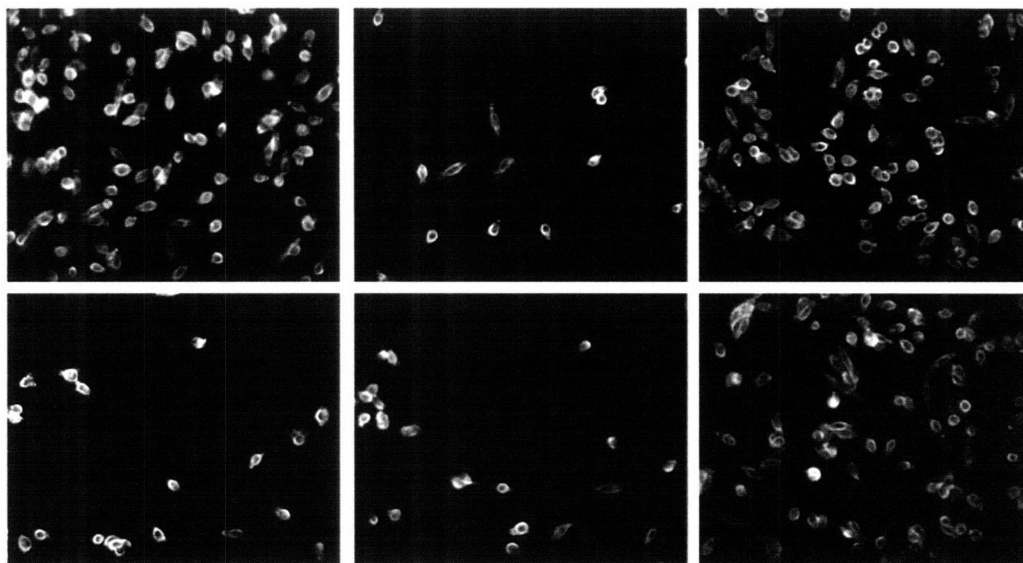


Figure 2.8.1 20X Images of actin-stained CHO-B2 $\alpha 5\beta 1$ cells on a) mock tethered, b) glass surfaces.

c) 25 μ m synergy-RGD



d) 25 μ m scrambled synergy-RGD

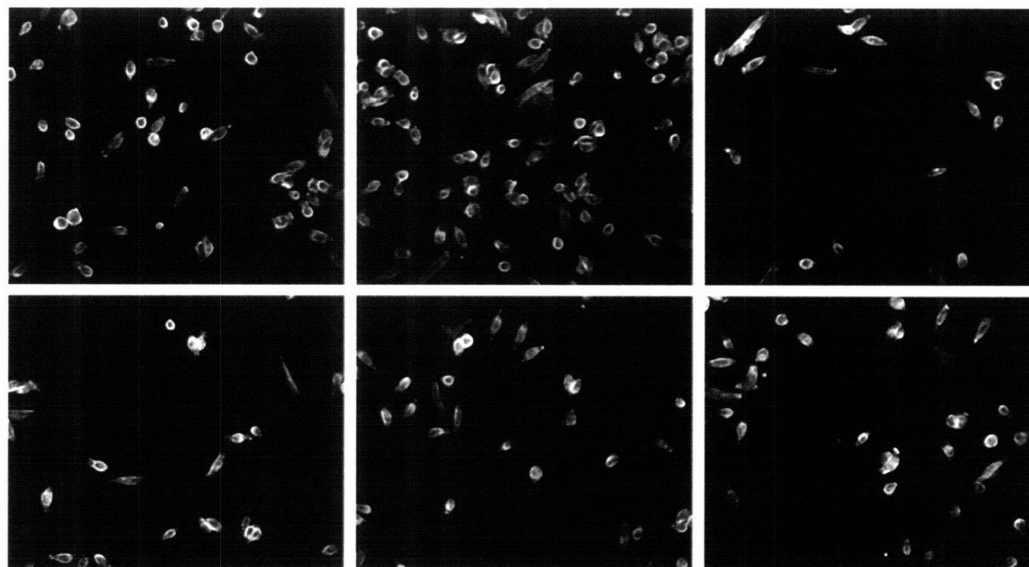
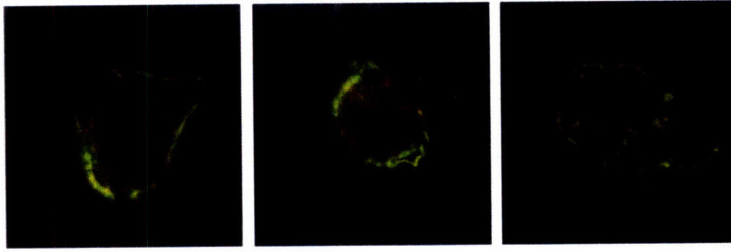
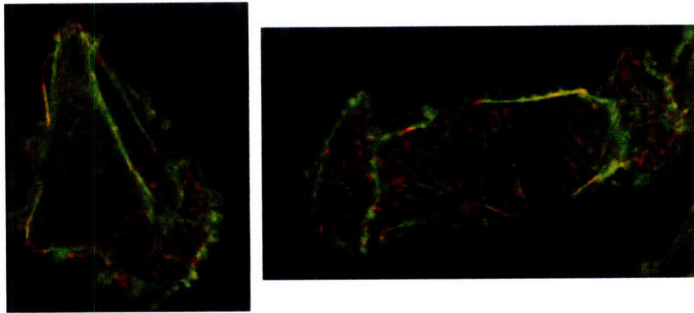


Figure 2.8.2 20X Images of actin-stained CHO-B2 α 5 β 1 cells on c) 25 μ M synergy-RGD, and d) 25 μ M scrambled synergy-RGD surfaces.

a) mock tethered



b) glass



c) 25 μ M synergy-RGD

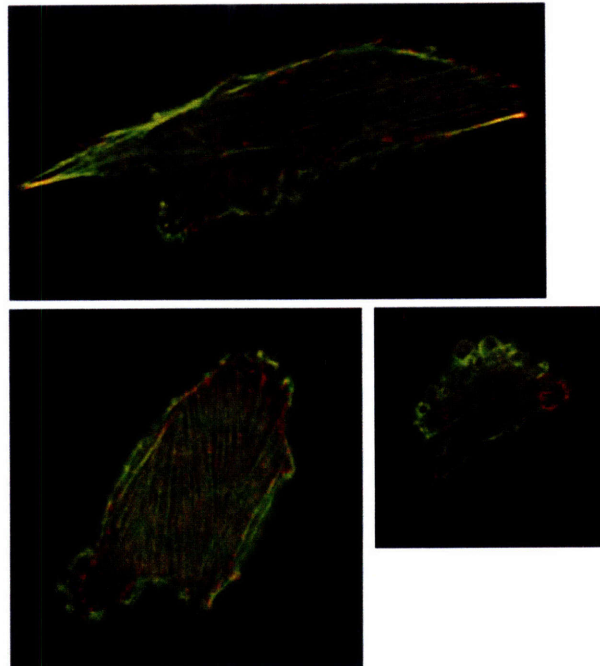


Figure 2.9.1 60X deconvolved images of vinculin (red) and actin-stained (green) (CHO-B2 α 5 β 1 cells on a) mock tethered, b) glass, c) 25 μ M synergy-RGD surfaces.

d) 25 μ M scrambled synergy-RGD

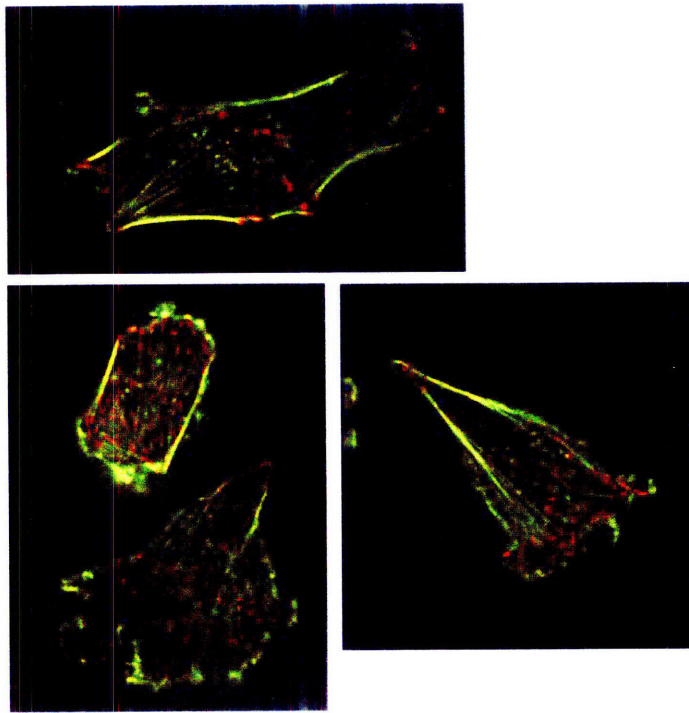


Figure 2.9.2 60X deconvolved images of vinculin (red) and actin-stained (green) CHO-B2 α 5 β 1 cells on d) 25 μ M scrambled synergy-RGD surfaces.

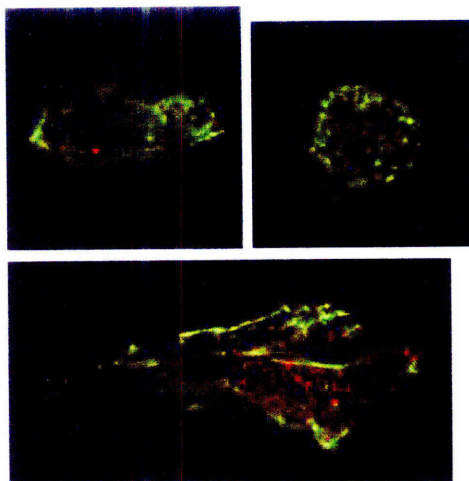
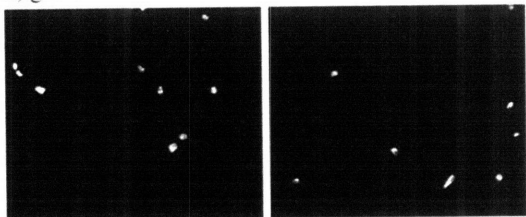
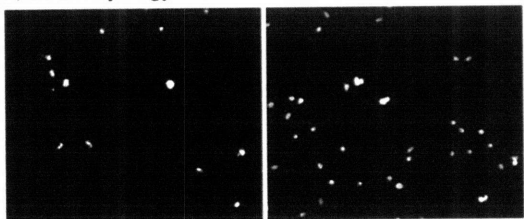


Figure 2.10 60X deconvolved images of vinculin (red) and actin-stained (green) CHO-B2 pcDNA control cells on 25 μ M synergy-RGD.

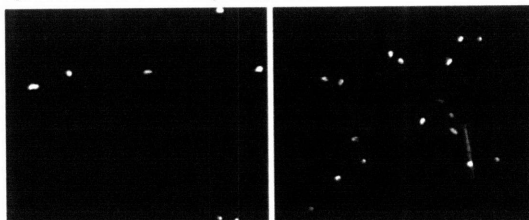
a) glass



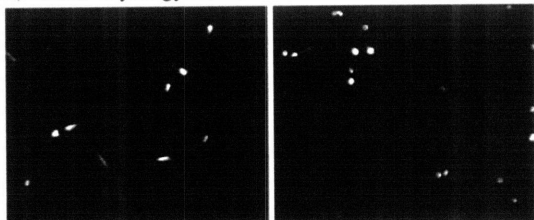
b) 25 μ M synergy-RGD



c) 25 μ M scrambled synergy-RGD



d) 100 μ M synergy-RGD



e) 100 μ M scrambled synergy-RGD

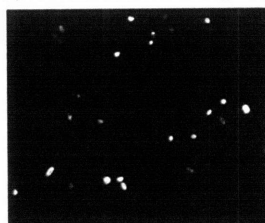
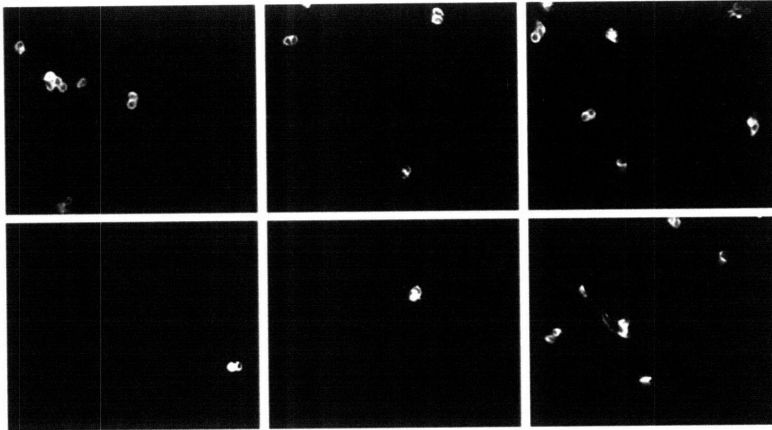
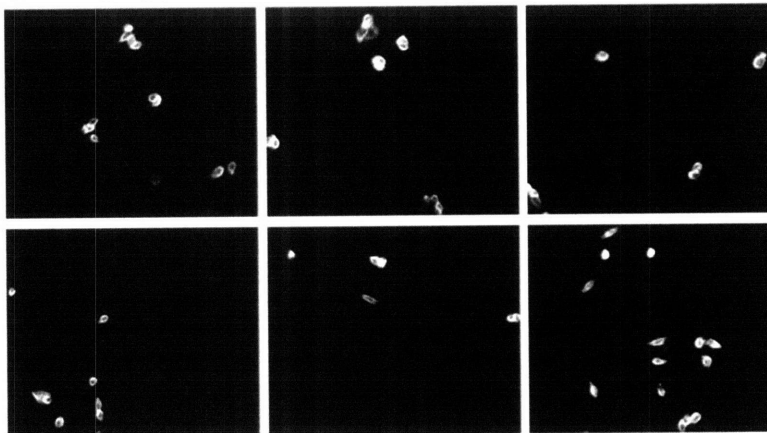


Figure 2.11 10X images of actin-stained CHO-B2 $\alpha 5 \beta 1$ cells on a) glass, b) 25 μ M synergy-RGD, c) 25 μ M scrambled synergy-RGD surfaces, d) 100 μ M synergy-RGD, and e) 100 μ M scrambled synergy-RGD surfaces.

a) glass



b) 25 μ M synergy-RGD



c) 25 μ M scrambled synergy-RGD

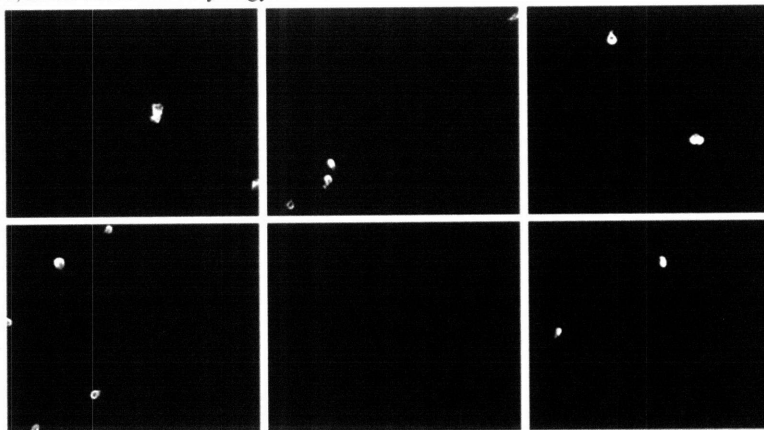
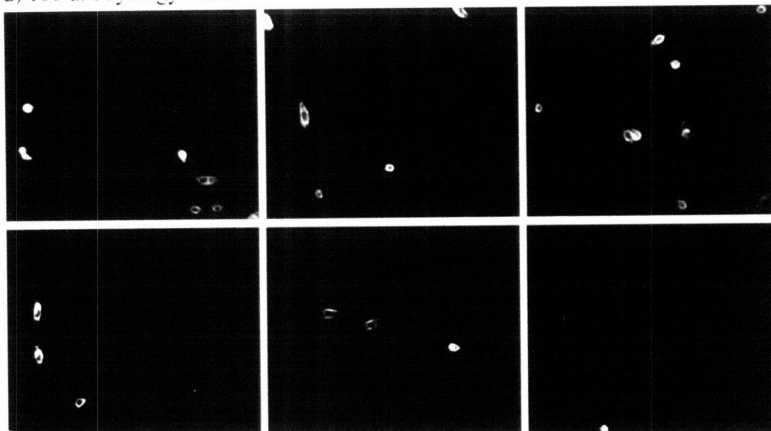


Figure 2.12.1 20X images of actin-stained CHO-B2 $\alpha 5 \beta 1$ cells on a) glass, b) 25 μ M synergy-RGD, c) 25 μ M scrambled synergy-RGD surfaces.

d) 100 μ M synergy-RGD



e) 100 μ M scrambled synergy-RGD

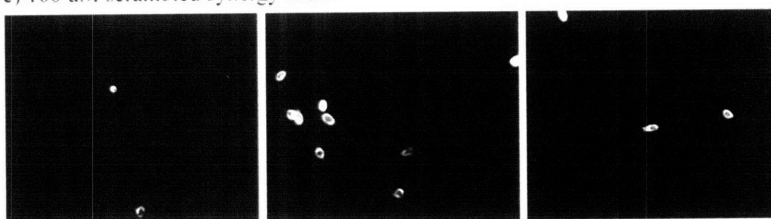


Figure 2.12.2 20X images of actin-stained CHO-B2 α 5 β 1 cells on d) 100 μ M synergy-RGD and e) 100 μ M scrambled synergy-RGD surfaces.

a) 25 μ M synergy-RGD

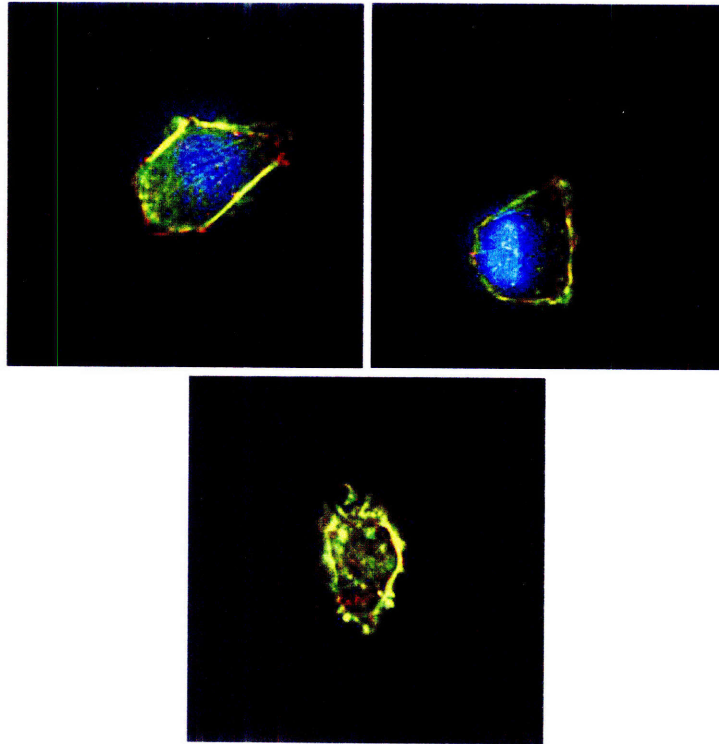


Figure 2.13.1 60X deconvolved images of vinculin (red) and actin-stained (green) CHO- α 5 β 1 cells on a) 25 μ M synergy-RGD surfaces.

b) 100 μ M synergy-RGD

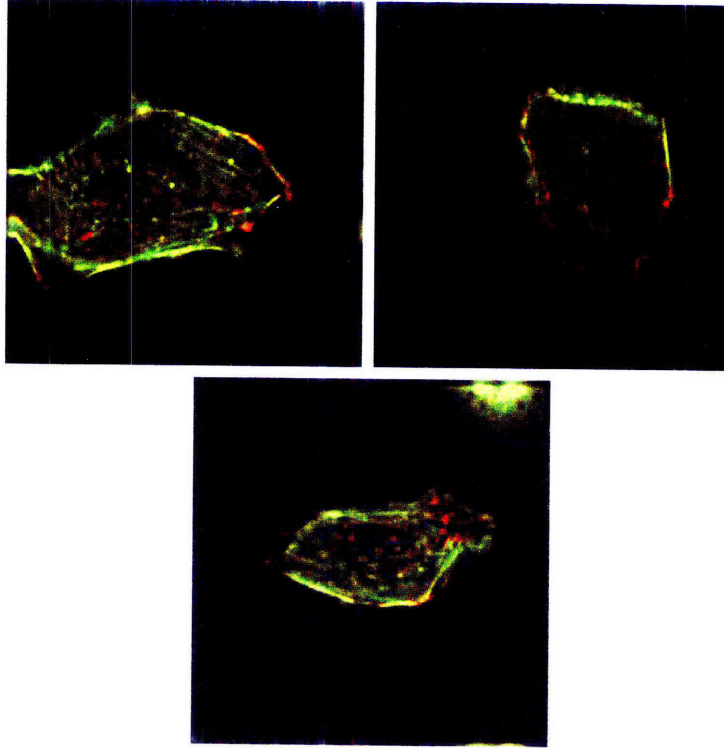


Figure 2.13.2 60X deconvolved images of vinculin (red) and actin-stained (green) CHO-B2 α 5 β 1 cells on b) 100 μ M synergy-RGD surfaces.

c) 100 μ M scrambled synergy-RGD

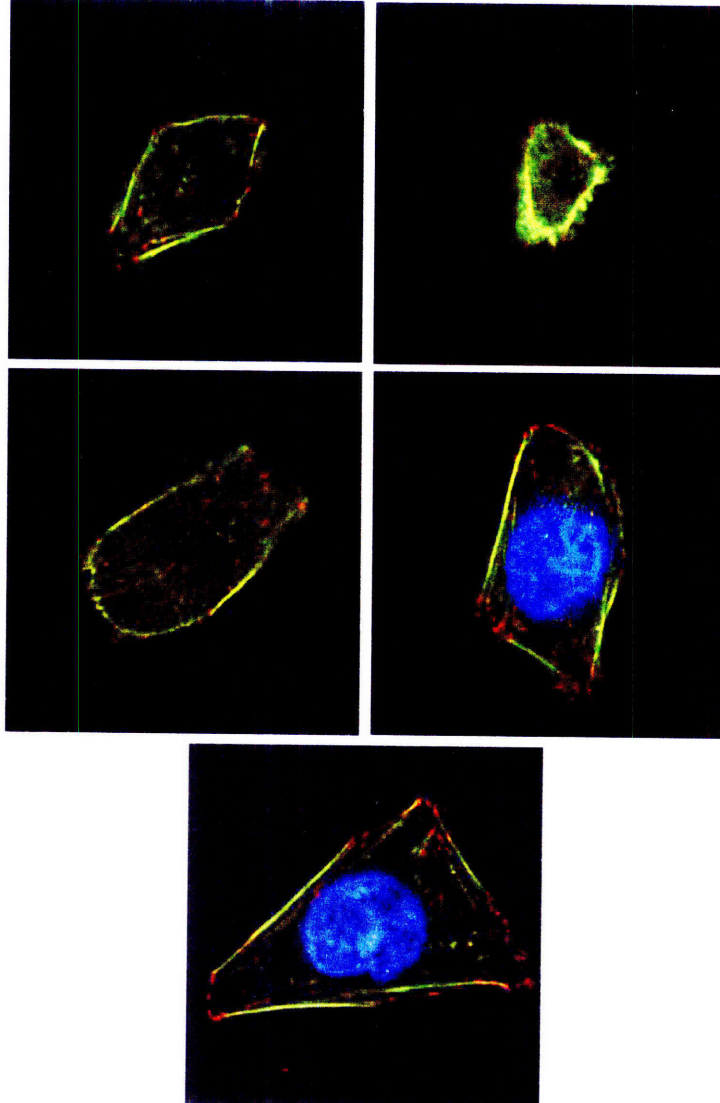


Figure 2.13.3. 60X deconvolved images of vinculin (red) and actin-stained (green) CHO-B2 α 5 β 1 cells on c) 100 μ M scrambled synergy-RGD surfaces.

Chapter 3. Tethered EGF enhances connective tissue progenitor osteogenic colony formation

3.1 Introduction

Bone marrow contains a diverse population of connective tissue stem and progenitor cells that contribute to the formation of new tissues after injury [1-5]. When marrow aspirate is plated in culture, these cells adhere, exhibit fibroblastic morphology, and proliferate to form colonies (Figure 3.1) with multilineage differentiation potential [6-13]. Such colony-forming cells -- about one out of 20,000 nucleated marrow aspirate cells [14-16] -- can form bone, cartilage and fat when transplanted *in vivo* [7, 8, 17]. Colonies formed from marrow aspirates are heterogeneous in size and appearance, likely reflecting a spectrum of stem-to-early progenitor properties in the population giving rise to colonies. Various terminologies have been employed to describe this marrow-resident population and their culture-expanded progeny, including mesenchymal stem cells (MSCs) [18], bone marrow stromal cells [6], skeletal stem cells [19] adult multipotential progenitor cells [20, 21], and connective tissue progenitors (CTPs). The present work concerns properties of adherent marrow cells that form colonies, and we use the term CTP in deference to both the heterogeneity and the range of differentiation potential [22, 23].

Among the many potential regenerative applications of marrow-derived CTPs that are envisioned, regeneration of bone by intraoperative addition of autologous bone marrow aspirate to bone grafts (including ceramics and demineralized bone matrix) is already clinically practiced [24-28], though not as a routine replacement for autograft bone. Recently, it has been shown in canine models of spinal fusion and segmental defect repair that the success of bone grafts can be enhanced using an approach that filters marrow through the graft and results in both selective

retention of CTPs over other nucleated cells and concentration of CTPs to a greater number per unit volume [29-31]. While the mechanisms underlying enhanced healing in these studies are not yet known, these results motivate additional studies aimed at understanding and manipulating the CTP population in marrow-supplemented grafts to improve healing.

Survival and function of CTPs following implantation are influenced by local environmental cues. The scaffold or matrix used in the graft provides not only mechanical support, but is a source of adhesive molecules and soluble factors that regulate CTP behavior. While natural scaffolds such as demineralized bone provide such cues, such scaffolds also have inherent limitations in size, mechanical properties, biological activity from lot-to-lot, and other features, thus motivating design of synthetic scaffolds with precise properties for particular indications [32-37]. In this regard, much attention has focused on the use of bone morphogenetic proteins (BMPs) in grafts, and clinical efficacy of BMP 2 and BMP-7 have been demonstrated in several indications, though results are not uniformly successful [38-41]. BMP-2 acts on early progenitors to induce a program leading to osteogenic differentiation, and its actions in humans can be antagonized by signaling from growth factors activating Map kinase pathway [42, 43].

In scenarios where marrow aspirates are transplanted, providing signals that act on CTPs to enhance survival and proliferation, upstream of where BMPs act to induce differentiation programs, may enhance overall healing by increasing the number of cells that are capable of forming bone. Ligands for the epidermal growth factor (EGF) receptor are candidates for such cues, as the EGF receptor plays important roles in bone development and homeostasis [44-48], and is in particular an important regulator of CTP behavior [49-54]. When stro-1 positive cells from human marrow are plated on fibronectin and maintained in serum-free medium,

supplementation with soluble EGF in a physiological range (~2 nM) fosters the same extent of colony formation as does serum supplementation [53]. In the presence of serum, EGF receptor ligands stimulate proliferation of culture-expanded CTPs without inhibiting subsequent differentiation [49, 55]. Under some experimental conditions, EGF may also influence osteoblastic differentiation. EGF was shown to increase the number of mineralized nodules formed by rat calvarial cells at low density, but decrease nodule formation at higher densities [56]. When added to osteogenic culture medium, EGF was also observed to increase alkaline phosphatase activity in culture expanded MSC [50].]

Although *in vitro* studies typically employ soluble EGF, there are several potential advantages in presenting EGF as a matrix-tethered molecule for applications in tissue engineering [57]; i.e., in linking EGF to the scaffold so that it is competent to bind and activate the EGF receptor, but not internalized and degraded. This mode mimics features of the physiological presentation of EGF receptor ligands that act in juxtacrine fashion or are matrix-bound. The potential advantages include better control of local EGF concentration, reduction in receptor downregulation, and prolonging overall signaling [57]. Tethered EGF may also alter the balance of downstream signaling pathways activated by the EGFR compared to activation by soluble EGF. Indeed, tethered EGF, but not soluble EGF, enhances cell spreading and protects culture-expanded human CTPs from pro-death inflammatory cues [58].

We therefore hypothesized that tethered EGF might also act beneficially on CTPs in fresh human bone marrow aspirates. We tested the ability of tethered EGF to increase the number of osteogenic CTP colonies generated from freshly aspirated human bone marrow plated in serum-containing medium, and whether the effects of tethered EGF were influenced by variation of the adhesive properties of the substrate. Our results indicate that tethered EGF provides an

advantage in colony formation *in vitro*, and hence delivery of EGF in tethered format *in vivo* may provide cues beneficial for survival and proliferation of CTPs in bone healing indications.

3.2 Materials and methods

3.2.1 Ligand-modified culture substrates

Substrates were prepared to present tethered EGF against an adhesion background of adsorbed fibronectin (Fn), adsorbed serum proteins, or a branched minimal Fn-derived adhesion peptide designed to mimic the adhesion sites in the 9th-10th domains of Fn. This peptide, which we designate “synergy-RGD” contains two lysine-linked branches, one containing a RGD-adhesion domain and the other a PHSRN-synergy sequence, a GGC stem attached to the lysine side chain for covalent linkage to the polymer [59]. Polymer-coated glass slides modified with ligands of interest were prepared as described earlier [58] with minor modifications to expand the range of adhesive ligands presented with tethered EGF. All substrates were prepared from blends of two different poly(methyl methacrylate)-graft-poly(ethylene oxide) (PMMA-g-PEO) amphiphilic comb copolymers [60]: CC1 (32 wt% PEO) resists cell adhesion unless modified with adhesion peptides and fosters high-density ligand clustering; [60, 61]; CC2 (20 wt% PEO) allows cell attachment mediated by serum protein adsorption [58]. CC1 was activated with 4-nitrophenyl chloroformate (NPC) (Alpha Aesar, Ward Hill, MA) [58, 61] to target the N-terminal amine of murine EGF, and with N-[p-Maleimidophenyl]isocyanate (PMPI) (Pierce Biochemical, Rockford, IL) to target thiol-terminated adhesion peptides, as described previously [59, 62]. Unmodified CC1, unmodified CC2, PMPI-activated CC1, and NPC-activated CC1 were blended in specific proportions to give a 20 mg/mL solution in toluene, spin-coated onto 18 mm square glass coverslips pre-treated with Siliclad (Gelest Inc., Morrisville, PA) to a thickness

of ~75 nm, vacuum-dried, then modified by adhesion ligands and/or EGF (see below) to create 4 unique polymer surfaces (Table 3.1), some of which were further treated by adhesion of fibronectin or serum.

Table 3.1

Blend	Adhesion Mediating Component	Percentage	Tethered Growth Factor Component	Percentage	Bulk	Percentage
1	Non-Resistant CC2	100%	None			
2	Non-Resistant CC2	60%	EGF-modified CC1	40%		
3	Synergy-RGD-modified CC1	25%	None		Resistant CC1	75%
4	Synergy-RGD-modified CC1	25%	EGF-modified CC1	40%	Resistant CC1	35%

Covalent linkage of the synergy-RGD peptide was accomplished by reacting substrates with a 25 μ M solution of the peptide in phosphate buffered saline (PBS) containing 10 mM Tris(2-Carboxyethyl) phosphine hydrochloride (TCEP; Sigma, St. Louis, MO) at pH 7.5 for 2 hr at room temperature [59]. The peptide density was about 20,000 RGD/ μ m² based on measurements made previously [59]. Covalent linkage of murine EGF (PeproTech, Rocky Hill, NJ) to substrates, through the N-terminal amine of the EGF, was accomplished by incubating substrates for 20-24 hr with a 25 μ g/mL solution of EGF in 100 mM phosphate buffer (pH 8.5-8.7) at room temperature, followed by rinsing 3X and blocking unreacted sites with 100 mM Tris buffer [58]. Substrates presenting tethered EGF against the synergy-RGD adhesion background were produced by sequential reaction of each ligand, because the PMPI reaction with thiols and the NPC reaction with amines proceed at different values of pH [58, 59]. All surfaces containing tethered EGF were stored in PBS and used within 3 weeks of EGF coupling. Where indicated, Fn (Sigma, St. Louis, MO) was adsorbed to substrates 1 and 2 (Table 3.1) by incubating substrates with a 10 μ g/mL solution in PBS for 2 hr at room temperature, rinsing 3X with PBS, then

blocking for 1 hour at room temperature with 1% bovine serum albumin (Sigma, St. Louis, MO), and rinsing 3X. Fn coating was performed within a day of use.

3.2.2 Bone marrow aspiration

Human bone marrow was obtained from 39 normal donors and patients presenting to Dr. G.F. Muschler prior to an elective orthopedic procedure. All subjects were enrolled with full informed consent under a protocol, which was approved by the Institutional Review Board of the Cleveland Clinic. 2 mL of bone marrow was isolated from the iliac crest of volunteers as described previously [15, 61]. Briefly, bone marrow was aspirated into a 10-ml plastic syringe containing 1 ml of saline containing 1000 units of heparin. Subsequent aspirates were taken using identical technique through separate cortical perforations separated by at least 1 cm, moving posteriorly along the iliac crest. Four aspirates were harvested from each side. The heparinized marrow sample from each site was suspended into 20 ml of MEM- α containing 2 unit/ml Na-heparin and sealed in a 50-ml test tube for transportation to the cell culture laboratory. All samples were harvested by Dr. G.F. Muschler.

The aspirated bone marrow was centrifuged for 10 minutes at 1500 RPM. The buffy coat was isolated and re-suspended in complete medium, MEM- α containing, 50 mg/ml sodium ascorbate, antibiotic-antimycotic (Invitrogen, Chicago, IL), and 10% fetal bovine serum (BioWhittaker, Walkersville, MD, USA), using a lot that was selected on the basis of enhancing osteogenic differentiation.

3.2.3 CTP/CFU assay

Treated coverslips were placed in the wells of 2-chamber Lab-Tek culture slides (Nunc, Rochester, NY), with one coverslip covering the bottom of each chamber on the slide, sterilized under UV for 30 min, and seeded with 0.5 million cells (approximately 1.5×10^5 nucleated cells/cm²) in complete medium.

For each individual donor, 4 coverslips for each surface condition being examined were seeded with bone marrow cells. In addition to comb copolymer surfaces, untreated glass surfaces were also seeded, and served as the positive control for each donor.

Cultures were maintained at 37°C in a humidified atmosphere of 5% CO₂ in air. The culture medium was changed 48 h after plating and the non-adherent cells from each chamber were replated on glass slide surfaces. Where indicated, soluble EGF was added at 10 ng/mL at plating and with each medium change.

The initial and replated cultures were maintained for 4 and 6 additional days, respectively. Cultures were then washed twice with PBS and fixed. After fixation, cells were stained with DAPI and for alkaline phosphatase with VectorRed (Vector Labs, Burlingame, CA). Clusters of 8 or more cells staining positive for alkaline phosphatase were scored as an osteogenic colony. Colonies on original substrates were defined as “early adherent colonies”, as they originated from cells that adhered to the test surfaces within 48 h of plating. Colonies formed on glass slides from the re-plating of cells that were non-adherent at 48 h were defined as “late adherent colonies.” Figure 3.2 shows the schematic of the colony-forming unit (CFU) assay for CTP colony formation.

3.2.4 Surface conditions

Over the course of 3 experiments, 9 experimental surface conditions were studied. Three individual adhesion conditions were studied. Polymeric scaffolds promoted adhesion either via synergy-RGD peptide, pre-adsorbed fibronectin, or adsorbed serum. These adhesion conditions were then studied in concert with 3 different EGF conditions: no EGF, tethered EGF, or soluble EGF. The conditions are illustrated in Figure 3.3.

3.2.5 Statistical analysis

For each of the 3 experiments, bone marrow from a given donor was used to study each surface condition, so that data could be analyzed in the context of an individual patient. For each experimental condition, the prevalence of osteogenic colonies that formed was calculated by dividing the total number of colonies that formed on all of the surfaces per million seeded cells. The prevalence for each experimental surface was then normalized to the prevalence of colonies that formed on the glass control surface for each individual donor. The normalized prevalence of early-adherent colonies normalized to the prevalence of early-adherent colonies formed on glass controls is colony forming unit efficiency (CFE). The same procedure was applied with the late-adherent colonies to determine the normalized number of late-adherent colonies that formed on glass after being removed from a given experimental surface. Each data point for CFE was log base-2 transformed and a mean CFE and 95% confidence levels for each experimental condition were calculated across all patients in log base-2 space. It should be noted that 3 data points had a CFE equal to 0. Therefore, these values were set to $\frac{1}{2}$ the smallest non-zero CFE for the rest of the data set for that condition, prior to the log transformation. A Shapiro-Wilk test was used to assess the normality of each data set, and data sets were assumed to be normal if $p > .05$. To test for statistical differences between surface conditions, a two-way matched pair t-test was

performed in log-2 space. In the event that a data set for a surface condition was non-normally distributed, a Wilcoxon Signed-rank test was also used to test for significant differences between surface conditions. Using a $p=.05$ as the cutoff for significance, no differences in statistical conclusions were observed for any comparison with non-normally distributed data sets using either the matched pair t-test or the Wilcoxon Signed-Rank test.

The same procedure was performed for the normalized number of late-adherent colonies. For two donors, the glass control surfaces had 0 colonies, making normalization impossible. This data was therefore not included in the calculation of mean and confidence levels for each surface condition.

3.2.6 Image analysis

Quantitative image analysis (Figure 3.4) was performed on data from 9 donors using a procedure described previously [63]. All surfaces were visually reviewed after the software was used to automatically outline colonies. Colonies that were incorrectly outlined due to debris were adjusted manually by the reviewer. The number of colonies was also assessed, to calculate CFE as measured by image analysis. Additionally, the following metrics were analyzed for each colony: the area of the colony expressing alkaline phosphatase, total colony area as defined by the colony outline, and the number of cells per colony. For each patient, the median value for each particular metric was assessed for all colonies (across all coverslips), and normalized to the median of those metrics for colonies formed on glass controls. Each normalized data point was log-2 transformed and an average value for each experimental condition was calculated across all patients. 95% confidence levels were calculated and matched pair t-tests were performed in log-2 space. As above, the Shapiro-Wilk test was used to assess the normality of each data set, and a

Wilcoxon signed-rank test was applied in addition to the matched pair t-test where appropriate. As above, using a $p=.05$ as the cutoff for significance, no differences in statistical conclusions were observed for any comparison with non-normally distributed data sets using either the matched pair t-test or the Wilcoxon signed-rank test.

3.3 Results

3.3.1 Tethered EGF enhances osteogenic colony formation on minimal adhesion peptides

Formation of osteogenic colonies in culture requires cell adhesion, proliferation, and expression of differentiation markers. In the CFU assay, marrow aspirates are plated at a density of 1.5×10^5 nucleated cells/cm², non-adherent cells are removed after 48 hr, and the number of colonies (8 or more cells in a cluster) formed, along with determination of differentiation status, are counted after 6 total days of culture. Differences in the final colony number may arise from differences in the number of CTPs adhering initially, or differences in proliferation. These processes are both influenced by cues from the culture substrate and cues from soluble medium components.

We first asked whether tethered EGF could enhance colony formation under conditions where adhesion was expected to be the limiting process in colony formation, as tethered EGF has been shown to enhance spreading of culture-expanded CTPs [58]. We therefore used substrates that foster adhesion through the minimal peptide adhesion moiety RGD (using the synergy-RGD peptide). Substrates presenting minimal RGD-containing peptides support proliferation of culture-expanded CTPs [61]. However, formation of colonies from human marrow aspirates on these substrates is very significantly diminished compared to control adhesion environments, even though CTPs express integrins known to interact with RGD-containing matrix proteins

[61]. We observed here an average CFE of 0.27 on RGD substrates, confirming that colony formation on RGD is significantly diminished compared to glass controls (Figure 3.5). However, tethered EGF increased colony formation on RGD almost 3-fold, resulting in an average CFE of 0.73. The minimal RGD adhesion sequence is not sufficient to engender full adhesion and spreading by all integrins that recognize the RGD sequence [64-68] and tethered EGF might be substituting for additional adhesion signals present in full-length matrix proteins such as Fn or the mixture of adhesion molecules present in serum. We thus next sought to determine whether tethered EGF would increase colony formation on substrates presenting a more extensive array of adhesion sites.

3.3.2 Tethered EGF enhances osteogenic colony formation on adsorbed serum and Fn

Osteogenic colony formation is typically assessed by plating cells in serum-containing medium onto glass or plastic substrates so that adhesion is mediated by adsorbed serum proteins [14, 16, 54, 69, 70]. Plating marrow in serum on control substrate (Blend 1 in Table 3.1), we observed a significant increase in colony formation (CFE=0.41), compared to minimal RGD peptide (0.27, $p=.01164$) in the absence of tethered EGF (Figure 3.5). Further, tethered EGF nearly doubled colony formation for cells plated in serum (CFE=0.74, $p=.00003$). Because average CFE was <1.0 (suggesting that CTP availability was not depleted), we would expect the magnitude of the increase in colony formation to be similar on serum and synergy-RGD, if tethered EGF was increasing colony formation primarily through activation and proliferation. In the presence of tethered EGF, CFE was statistically similar on synergy-RGD and adsorbed serum ($p=.90039$), suggesting that the mechanism by which tethered EGF increases colony formation is associated with initial cell adhesion and survival.

CTPs are also present in the “non-adherent” cell population removed after the initial 48 hr, and form “late-adherent” colonies when this cell population is replated on glass [71-73]. We observed no significant differences between any conditions in the prevalence of late-adherent colony-forming CTPs (Figure 3.6). Therefore, additional analyses to parse the effects of tethered EGF on colony formation focused on early adherent CTPs. We also confirmed that, despite the substantial variability among donors in the total prevalence of colonies (early+late) [16], there was no obvious correlation between the total number of colonies formed on control substrates and the CFE observed on the experimental substrates (Figure 3.7), suggesting that the observed increase in colony formation as result of tethered EGF was not associated with differences in total CTP prevalence among donors.

Among the adhesion molecules in serum, Fn has been shown to foster colony formation in serum-free medium in a manner comparable to serum-supplemented medium [53, 74-78]. In addition to the PHSRN and RGD sites in the 9th-10th domains, Fn contains binding sites for integrin $\alpha 4\beta 1$ and syndecans, hence would be expected to foster colony formation to a greater extent than the minimal synergy-RGD peptide. Using a different cohort of donors than those studied in Figure 3.5, we found that colony formation on Fn (CFE = 0.46) was statistically similar to that for cells plated in serum (CFE=0.37, $p=.09868$), and greater than on synergy-RGD (CFE=0.23, $p=.00311$) (Figure 3.8); CFE for cells plated in serum were similar for cohorts presented in Figures 3.5 and 3.8. Notably, as with other adhesion environments, tethered EGF increased colony formation for cells on Fn (CFE=0.59, $p=.00488$). When compared to the other surfaces with tethered EGF, interestingly, colony formation was similar to that on the synergy-RGD surfaces (CFE=0.58, $p=.72426$) but greater than on serum (CFE=0.47, $p=.03676$). This result may indicate that there is a synergistic effect of tethered EGF and synergy-RGD-mediated

adhesion on colony formation. However, considering that CFE was statistically similar on synergy-RGD and serum in the presence of tethered EGF in our initial study which included a larger donor population, it is more likely that this result is specific to this smaller cohort of donors. Even though CFE was much greater on fibronectin than on synergy-RGD in the absence of tethered EGF, when EGF was tethered to the substrate, CFE was similar on fibronectin and on synergy-RGD, lending further support to our hypothesis that tethered EGF is increasing the attachment and survival of CTPs, rather than increasing proliferation.

3.3.3 Soluble EGF is less effective than tethered EGF in fostering colony formation

The EGF receptor initiates multiple intracellular signaling pathways and is subject to ligand-mediated internalization and downregulation. Restricting internalization of the ligand-bound EGF receptor (for example via external tethering of ligand or mutation of the receptor) alters the balance of signaling pathways compared to the canonical soluble EGF ligand, and can dramatically alter downstream phenotypic responses [58, 79-81]. In culture-expanded human CTPs and in an immortalized human MSC cell line, soluble EGF is far less effective than tethered EGF in promoting cell spreading and in protecting cells from FasL-mediated cell death [58] and decreases colony formation from rabbit marrow cells plated in the presence of serum [54]. However, soluble EGF promotes colony formation from human cells on fibronectin in serum-free medium to a degree comparable to serum-supplemented medium [52, 53]. When we add soluble EGF (10 ng/mL) to cells plated on Fn in serum-containing medium, colony formation is significantly decreased compared to the control no EGF case (CFE=0.32, $p=0.00200$), whereas tethered EGF significantly increased colony formation.

This large difference in CFE led us to further investigate the effect of soluble EGF on colony formation, on both serum and synergy-RGD, in a cohort of 9 donors with an average age of 58.25. As shown in Figure 3.9, tethered EGF again enhanced colony formation on both synergy-RGD ($p=.03079$) and serum ($p=.00204$). Unlike tethered EGF, however, soluble EGF did not appear to affect colony formation on either synergy-RGD ($p=.39254$) or serum ($p=.18492$). While differences in local concentration can arise when comparing ligand presentation in 2D and 3D, it has been previously shown that the restriction of EGFR signaling to the surface of cells can lead to differential cell behaviors [80, 82]. Furthermore, previous work using similar conditions showed that the restriction of EGFR signaling to the surface of MSC increased ERK-mediated cell spreading and survival [58]. Therefore, our results appear to indicate that the modality of EGF presentation can play an important role in promoting osteogenic colony formation.

3.3.4 Tethered EGF enhances CFE in multiple donor populations

Because number of CTPs available within a bone marrow sample is affected by factors such as age and health [16], we asked if tethered EGF-induced colony formation might be affected by different donor populations. While the majority of bone marrow donors in this study suffered from osteoarthritis, several donors were healthy volunteers, enabling us to retrospectively compare the data from these two populations. Because a number of donors presented with multiple indications, we restricted our analysis to donors who suffered from only osteoarthritis. This population consisted of 24 donors with an average age of 62.8, whereas the volunteers included 7 donors with an average age of 39. As shown in Figures 3.10 and 3.11, tethered EGF significantly increased CFE in both donor populations, on both synergy-RGD and

serum ($p < .01$ for all comparisons between surfaces with tethered EGF vs. those without tethered EGF). While there hasn't been any reported systemic bone marrow abnormalities associated with osteoarthritis [16], this data emphasizes the robustness of the observed CFE enhancement associated with tethered EGF.

3.3.5 Tethered EGF increases colony size on serum

A retrospective analysis on the colony formation of bone marrow from all 39 donors included in this study (Figure 3.12) confirms our observations from the original cohort of 18 donors. Without tethered EGF, colony formation is slightly increased on serum (CFE=0.33) compared to synergy-RGD (CFE=0.23, $p = .00536$). However, with tethered EGF, CFE is enhanced on both synergy-RGD (CFE=0.62, $p < .00001$) and serum (CFE=0.57, $p < .00001$). Also, as observed previously, in the presence of tethered EGF, CFE was similar on serum and synergy-RGD ($p = .2759$), supporting our hypothesis that tethered EGF was enhancing the adhesion and survival of CTPs. However, we did not rule out the possibility that tethered EGF might also be influencing the proliferation of CTPs. While an initial enhancement of CTP activation and proliferation would likely lead to an increase in colony number, induction of proliferation at a later point would lead to an increase in colony size. Therefore, we used quantitative image analysis to further study CTP proliferation by examining colony size.

Quantitative image analysis (QIA) was used to examine data from 9 of the donors. We first examined CFE to ensure that the analysis was consistent with the hand-counted data. For one donor, the CFE for all experimental surfaces was extremely high (in the range of 3.3-5.7), which was significantly different from the hand-counted data for this patient, suggesting that some of the colonies on the glass control surfaces were lost in the processing for QIA. As a

result, data from this donor is not included in the analysis, to prevent all data from being improperly skewed. Therefore, only data from the other 8 donors, with an average age of 65, was considered for QIA. As shown in Figure 3.13, QIA revealed a similar increase in CFE on both serum and synergy-RGD in the presence of tethered EGF. Interestingly, as shown in Figure 3.14, QIA indicated that tethered EGF increased the median area of colonies formed on serum, compared to all other conditions ($p < .01$ for all comparisons). However, median colony area was similar on the other 3 conditions. Because an increase in colony area could be a result of increased cell number resulting from proliferation, or increased migration, we also used QIA to assess the number of cells within a colony. QIA (Figure 3.15) revealed that colonies formed on serum in the presence of tethered EGF consisted of more cells compared to those formed without tethered EGF ($p = .00130$) suggesting an increase in CTP proliferation in the presence of tethered EGF. However, cell number was similar on synergy-RGD in the presence or absence of tethered EGF. A surprising result was that cell number was similar in colonies formed on serum+tethered EGF and colonies formed on both synergy-RGD surfaces, even though colony area on serum+tethered EGF was larger. This suggests the possibility that a complex interplay exists between tethered EGF and adhesive ligands, which might affect both CTP migration and proliferation. Further studies are needed to elucidate these interactions.

3.3.6 Tethered EGF does not affect the number of cells expressing alkaline phosphatase within a colony

CFE as measured by QIA differs from the hand-counting procedure, in that the QIA measures all colonies, whereas the hand-count procedure measures only colonies expressing alkaline phosphatase. In the hand-counted data, colonies that do not express alkaline

phosphatase are not included in the CFE measurements. A possible interpretation of the hand-count data could therefore be that tethered EGF was not increasing colony formation, but was promoting a higher percentage of colonies to express alkaline phosphatase. However, the CFE as measured by QIA (Figure 3.13) reflects all attached colonies, regardless of alkaline phosphatase expression. Therefore, the increase in CFE observed with QIA supports our hypothesis that tethered EGF is increasing CFE through the adhesion and survival of CTPs. However, we did not rule out the possibility that tethered EGF might also be affecting osteogenic differentiation, as has been observed in other studies with MSCs [50].

On all surfaces, approximately 80-90% of colonies appeared to express alkaline phosphatase, regardless of the surface condition (Cynthia Boehm, personal communication), which is similar to previous studies [61]. In the hand-counted data, colonies are scored as positive or negative for alkaline phosphatase expression, even though individual colonies may express different levels of alkaline phosphatase activity. Therefore, we asked if tethered EGF was affecting alkaline phosphatase expression in a manner that was not obvious in the hand-counted data. With QIA, it is possible to examine the number of cells expressing alkaline phosphatase within a colony by measuring the area of a colony expressing alkaline phosphatase, and normalizing it to the number of cells within that colony. However, Figure 3.16 shows that the number of cells expressing alkaline phosphatase within a colony was similar across all conditions ($p > .05$ for all comparisons). Because the intensity of alkaline phosphatase expression is not being quantified in this procedure, it is possible that tethered EGF may increase the level of alkaline phosphatase expression within a colony. It should also be pointed out, that for the colonies formed on synergy-RGD, 6 of the 8 donors showed a decrease in the number of cells expressing alkaline phosphatase with tethered EGF. This suggests that under some conditions,

tethered EGF may act to suppress osteogenic differentiation, and that this effect is abrogated when adhesion is mediated by native extracellular matrix proteins. These results also suggest that additional experiments are needed to elucidate the effects of tethered EGF on the osteogenic differentiation of CTPs.

3.4 Discussion

In this study, we examined the effect of tethered EGF on osteogenic connective tissue progenitor (CTP) colony formation from freshly aspirated human bone marrow for potential tissue engineering applications. Our results showed that tethered EGF increased the number of osteogenic colonies that formed on comb copolymer substrates across multiple adhesion conditions. In the absence of tethered EGF, serum proteins increased the number of osteogenic colonies that formed comb copolymer substrates compared to a small adhesion peptide; however, this increase was smaller than the increase observed on substrates with tethered EGF. A key observation was that this increase was not evident when cells were treated with soluble EGF at 10 ng/mL, suggesting that the modality of EGF presentation has a major effect on CTP colony formation.

Muschler and Midura have modeled CTP differentiation towards an osteoblastic phenotype as a series of steps including stem cell activation, proliferation, migration, and terminal differentiation [83]. Activation essentially implies a transition of a stem cell from a resting state to a proliferate state, which involves the birth of a progenitor cell. Because colony formation is a product of these different cellular behaviors, the exact mechanism by which tethered EGF promotes osteogenic colony formation is difficult to isolate. According to this model, however, the number of osteoblasts formed within a region can be modeled as:

$$N_{ob} = N_s \epsilon 2^\mu$$

where N_s is the number of stem cells available for activation, ϵ is the probability that a stem cell will be activated, and μ is the mean number of mitotic events between the time of activation and terminal differentiation. Extending this model to the CFU assay, the number of colonies formed on a substrate could be considered to be equal to $N_s \times \epsilon$. For a first-pass analysis, it might be assumed that tethered EGF could influence either activation (Figure 3.17) or adhesion and survival (Figure 3.18). Assuming that the effects of tethered EGF and adhesion peptides are decoupled, if tethered EGF increased ϵ to a similar degree across all surface conditions, and N_s was constant for a surface condition, we would expect tethered EGF to increase colony formation on all adhesive substrates to the same extent. Instead, we observed that the number of colonies was statistically similar across all adhesive conditions in the presence of tethered EGF. This is consistent with the hypothesis that tethered EGF maximized N_s on all surfaces, and ϵ remained constant. While it is simplistic to assume that the effects of tethered EGF and adhesion ligands are decoupled, or that adhesion and activation are decoupled, our hypothesis that tethered EGF is enhancing CTP attachment and survival is additionally supported by previous work [58].

Several previous studies have examined the effect of soluble EGF on CTP colony formation. Using stro-1 purified [70, 84] bone marrow mononuclear cells, Gronthos and Simmons showed that under serum-deprived conditions, clonogenic colony growth required platelet derived growth factor (PDGF) and EGF at 10 ng/mL [53]. Kimura et al. similarly observed that PDGF and EGF increased colony formation in the presence of human plasma derived serum [52]. In contrast, our studies showed that in the presence of serum-containing media, soluble EGF at 10 ng/mL failed to enhance osteogenic CTP colony formation; however, Owen et al. observed a decrease in rabbit-derived colonies when cultured in media containing 40

ng/mL EGF in addition to 10% FBS [54] suggesting that the presence of serum may play a significant role in modulating the effect that EGF exerts upon colony formation. The inclusion of serum better approximates a wound healing scenario in vivo, and the ability of tethered EGF to promote colony formation in serum-containing media demonstrates its potential for use in clinical applications. Further studies are required to elucidate the specific cellular mechanism responsible for tethered EGF-induced enhancement of osteogenic colony formation in contrast to soluble EGF. However, our studies suggest that tethered EGF is enhancing CTP attachment and survival.

The direct and downstream signaling interactions that occur between growth factor receptors and integrins has been studied extensively, and in most cases, adhesion is considered to be a requirement for full EGFR-mediated signaling [85-89]. However, a few studies have also shown that EGF-like repeats of tenascin-C and laminin can serve to promote EGFR-mediated signaling and adhesion, demonstrating that the presentation of insoluble EGFR-ligands can affect cell adhesion [76, 79]. Additionally, evidence exists showing EGFR-mediated effects on adhesion-related behavior that is not strictly integrin-mediated. Kempiak et al. showed that EGF-coated beads, which were coupled via a biotin-streptavidin linkage to minimize the release of EGF, promoted localized adhesion-independent actin polymerization and ERK-activation, when brought in contact with cells overexpressing EGFR [81]. These results strongly support previous work showing that tethered EGF promoted the spreading of culture expanded CTPs in an EGFR-dependent, ERK-mediated manner.

In this work, we have not distinguished between adhesion and survival because of the inability to separate the individual contributions of these behaviors to colony formation, from both limitations in the CFU assay, as well as the importance that adhesion has on cell survival

[90]. However, much evidence has implicated both EGF-induced signaling and ERK as effectors of cell survival, supporting our hypothesized mechanism underlying our results [91-93].

Due to the inherent limitations in working with donated marrow, we did not perform the CFU assay using inhibitors to verify the dependence of colony formation on EGFR phosphorylation or ERK-signaling. Therefore, we cannot definitively rule out other possible underlying mechanisms that are not induced by EGFR-signaling. One possibility would be that increased colony formation was solely a result of an increase in the mechanical attachment of cells resulting from a large number of EGF-EGFR binding events. This is unlikely due to the fact that the density of EGF on the polymer surfaces is significantly lower than the density of synergy-RGD. Furthermore, an enhancement in colony formation was observed even on highly-adhesive Fn substrates. Another possibility is that the tethered EGF is promoting the selective adsorption of serum factors that can then promote differential cell signaling. However, previous results with culture expanded CTPs using a similar experimental system suggest that our observed effects are EGFR-mediated [58].

Recently, Tamama et al. showed that EGF induced the proliferation and motility of immortalized MSCs under low serum conditions, but did not affect differentiation, suggesting that EGF could be used for the *ex vivo* expansion of MSCs [49]. Our observation that tethered EGF increased colony size and the number of cells per colony on serum suggests that tethered EGF may have a similar proliferative effect on CTPs, at a time point that occurs after a CTP activation step. Because CTP differentiation proceeds as the cells within the colony proliferate, it is unclear, however, if this proliferative effect is dependent upon the differentiated state of the cells within a colony. Interestingly we did not see a tethered EGF-induced increase in colony area or cell number per colony on synergy-RGD which might imply a synergistic effect between

tethered EGF and native ECM molecules, but needs to further investigated. When all donors were considered, our results also suggested that at early time points, tethered EGF was not increasing the number of cells expressing alkaline phosphatase, an early marker for osteogenic activity. However, because the QIA used to assess alkaline phosphatase expression is not quantitative for staining intensity, it is unclear if tethered EGF may be affecting the expression levels of alkaline phosphatase, which may provide a better indicator of osteogenic activity. Interestingly, in 6 of 8 donors, tethered EGF was observed to decrease the number of cells expressing alkaline phosphatase within colonies formed on synergy-RGD. However, this was not evident for colonies formed on serum. These results suggest that for at least some donor cell populations, tethered EGF might affect CTP differentiation, and that this effect may be influenced by the adhesive environment. This is consistent with previous work suggesting that both EGFR-mediated signaling and different adhesion molecules can affect differentiation under certain culture conditions in a time-dependent manner [50, 76, 77].

It is clear that additional studies of signaling mechanisms are necessary to elucidate the way in which tethered EGF enhances osteogenic colony formation. Due to the limitations in acquiring freshly aspirated bone marrow, initial studies on culture expanded CTP populations can guide more focused studies with primary cell sources. Some studies are currently being performed in our laboratory, by Manu Platt and Shan Wu. When passage 3 CTPs are seeded on serum-adsorbed surfaces, tethered EGF has been observed to increase the number of cells adhering to substrates at 4 hours (communications with Manu Platt, unpublished data) supporting our hypothesis that tethered EGF is enhancing of the attachment and survival of freshly aspirated CTPs. The signaling mechanisms underlying this effect are still being elucidated, but considerable attention is focused on focal adhesion kinase which is known to integrate EGFR-

and integrin-mediated signals [85, 86]. Additionally, tethered EGF has been observed to promote the proliferation of passage 3 CTPs on serum-adsorbed surfaces, in both basal growth medium and osteogenic medium, as well as to increase alkaline phosphatase expression for CTPs cultured in osteogenic medium (communications with Manu Platt, unpublished data). Clearly, the observation that tethered EGF increases attachment and proliferation on serum-adsorbed surfaces strongly supports the increased colony number and colony size observed in our results. While we did not observe an increased number of cells expressing alkaline phosphatase, it is likely that differences in the assays utilized can account for our different observations.

The effects of tethered EGF induced-migration CTPs derived from freshly aspirated marrow, however, are less clear. Interestingly, total colony area was greater on serum in the presence of tethered EGF compared to both synergy-RGD surfaces even though cell number per colony was similar, suggesting that the observed increase in area may be a result of tethered EGF-migration on serum. However, because of the relationship between adhesive substrate and migration speed [94, 95], additional experiments are needed to distinguish these individual effects. However, there is substantial evidence for tethered-EGF induced migration [96], as well as EGFR-mediated migration of immortalized MSCs [49]

Initial signaling studies with passage 3 CTPs suggest that tethered EGF is increasing the levels of ERK (communications with Manu Platt, unpublished data), which is again similar to previous studies [58], and supports the work by Kempiak et al. described previously [81]. Interestingly, tethered EGF was also seen to increase Akt, but decrease total levels of EGFR, suggesting a possible negative feedback mechanism resulting from the inability of tethered EGF to be internalized. Future work will attempt to identify additional important signals, and more direct effectors regulating the cell behavior induced by tethered-EGF. Once these signals and

effectors have been identified in culture expanded CTP systems, these molecules can be targeted in assays of freshly aspirated CTPs to further elucidate the mechanisms responsible for tethered EGF-enchanted CTP colony formation. At this point in time, however, evidence supports our hypothesis that tethered EGF is increasing the adhesion and survival of freshly aspirated CTPs, and may also promote the proliferation of cells with colonies formed on serum.

3.5 Conclusion

In conclusion, this study has shown that tethered EGF enhances CTP osteogenic colony formation across multiple adhesion conditions. We have shown that by tethering EGF to a biomaterial surface, we are able to achieve an increase in CFE not achievable through the use of soluble EGF, which has particular importance from the perspective of clinically applicable biomaterials

3.6 References

1. Burwell, R.G., *Studies in the Transplantation of Bone. Vii. The Fresh Composite Homograft-Autograft of Cancellous Bone; an Analysis of Factors Leading to Osteogenesis in Marrow Transplants and in Marrow-Containing Bone Grafts.* J Bone Joint Surg Br, 1964. **46**: p. 110-40.
2. Beresford, J.N., *Osteogenic stem cells and the stromal system of bone and marrow.* Clin Orthop Relat Res, 1989(240): p. 270-80.
3. Friedenstein, A.J., et al., *Stromal cells responsible for transferring the microenvironment of the hemopoietic tissues. Cloning in vitro and retransplantation in vivo.* Transplantation, 1974. **17**(4): p. 331-40.
4. Owen, M., *Marrow stromal stem cells.* J Cell Sci Suppl, 1988. **10**: p. 63-76.
5. Bianco, P., et al., *Bone marrow stromal stem cells: nature, biology, and potential applications.* Stem Cells, 2001. **19**(3): p. 180-92.
6. Owen, M. and A.J. Friedenstein, *Stromal stem cells: marrow-derived osteogenic precursors.* Ciba Found Symp, 1988. **136**: p. 42-60.

7. Kuznetsov, S.A., et al., *Single-colony derived strains of human marrow stromal fibroblasts form bone after transplantation in vivo*. Journal of Bone and Mineral Research, 1997. **12**(9): p. 1335-1347.
8. Friedenstein, A.J., *Stromal mechanisms of bone marrow: cloning in vitro and retransplantation in vivo*. Haematol Blood Transfus, 1980. **25**: p. 19-29.
9. Friedenstein, A.J., et al., *Marrow Micro-Environment Transfer by Heterotopic Transplantation of Freshly Isolated and Cultured-Cells in Porous Sponges*. Experimental Hematology, 1982. **10**(2): p. 217-227.
10. Ashton, B.A., et al., *Formation of bone and cartilage by marrow stromal cells in diffusion chambers in vivo*. Clin Orthop Relat Res, 1980(151): p. 294-307.
11. Berry, L., et al., *Bone-marrow-derived chondrogenesis in vitro*. J Cell Sci, 1992. **101** (Pt 2): p. 333-42.
12. Herbertson, A. and J.E. Aubin, *Cell sorting enriches osteogenic populations in rat bone marrow stromal cell cultures*. Bone, 1997. **21**(6): p. 491-500.
13. Pittenger, M.F., et al., *Multilineage potential of adult human mesenchymal stem cells*. Science, 1999. **284**(5411): p. 143-7.
14. Majors, A.K., et al., *Characterization of human bone marrow stromal cells with respect to osteoblastic differentiation*. J Orthop Res, 1997. **15**(4): p. 546-57.
15. Muschler, G.F., C. Boehm, and K. Easley, *Aspiration to obtain osteoblast progenitor cells from human bone marrow: the influence of aspiration volume*. J Bone Joint Surg Am, 1997. **79**(11): p. 1699-709.
16. Muschler, G.F., et al., *Age- and gender-related changes in the cellularity of human bone marrow and the prevalence of osteoblastic progenitors*. J Orthop Res, 2001. **19**(1): p. 117-25.
17. Friedenstein, A.J., R.K. Chailakhyan, and U.V. Gerasimov, *Bone marrow osteogenic stem cells: in vitro cultivation and transplantation in diffusion chambers*. Cell Tissue Kinet, 1987. **20**(3): p. 263-72.
18. Caplan, A.I., *Mesenchymal stem cells*. J Orthop Res, 1991. **9**(5): p. 641-50.
19. Bianco, P., et al., *Postnatal skeletal stem cells*. Methods Enzymol, 2006. **419**: p. 117-48.
20. Jiang, Y., et al., *Pluripotency of mesenchymal stem cells derived from adult marrow*. Nature, 2002. **418**(6893): p. 41-9.
21. Reyes, M. and C.M. Verfaillie, *Characterization of multipotent adult progenitor cells, a subpopulation of mesenchymal stem cells*. Ann N Y Acad Sci, 2001. **938**: p. 231-3; discussion 233-5.

22. Muschler, G.F. and R.J. Midura, *Connective tissue progenitors: practical concepts for clinical applications*. Clin Orthop Relat Res, 2002(395): p. 66-80.
23. Patterson, T.E., et al., *Cellular strategies for enhancement of fracture repair*. J Bone Joint Surg Am, 2008. **90 Suppl 1**: p. 111-9.
24. Healey, J.H., et al., *Percutaneous bone marrow grafting of delayed union and nonunion in cancer patients*. Clin Orthop Relat Res, 1990(256): p. 280-5.
25. Tiedeman, J.J., et al., *Healing of a large nonossifying fibroma after grafting with bone matrix and marrow. A case report*. Clin Orthop Relat Res, 1991(265): p. 302-5.
26. Connolly, J.F., et al., *Autologous marrow injection as a substitute for operative grafting of tibial nonunions*. Clin Orthop Relat Res, 1991(266): p. 259-70.
27. Garg, N.K. and S. Gaur, *Percutaneous autogenous bone-marrow grafting in congenital tibial pseudarthrosis*. J Bone Joint Surg Br, 1995. **77(5)**: p. 830-1.
28. Garg, N.K., S. Gaur, and S. Sharma, *Percutaneous autogenous bone marrow grafting in 20 cases of ununited fracture*. Acta Orthop Scand, 1993. **64(6)**: p. 671-2.
29. Muschler, G.F., et al., *Selective retention of bone marrow-derived cells to enhance spinal fusion*. Clin Orthop Relat Res, 2005(432): p. 242-51.
30. Muschler, G.F., et al., *Spine fusion using cell matrix composites enriched in bone marrow-derived cells*. Clin Orthop Relat Res, 2003(407): p. 102-18.
31. Brodke, D., et al., *Bone grafts prepared with selective cell retention technology heal canine segmental defects as effectively as autograft*. J Orthop Res, 2006. **24(5)**: p. 857-66.
32. Bauer, T.W. and G.F. Muschler, *Bone graft materials. An overview of the basic science*. Clin Orthop Relat Res, 2000(371): p. 10-27.
33. Muschler, G.F., C. Nakamoto, and L.G. Griffith, *Engineering principles of clinical cell-based tissue engineering*. J Bone Joint Surg Am, 2004. **86-A(7)**: p. 1541-58.
34. Khan, Y., et al., *Tissue engineering of bone: material and matrix considerations*. J Bone Joint Surg Am, 2008. **90 Suppl 1**: p. 36-42.
35. Hutmacher, D.W., et al., *State of the art and future directions of scaffold-based bone engineering from a biomaterials perspective*. J Tissue Eng Regen Med, 2007. **1(4)**: p. 245-60.
36. Bonzani, I.C., J.H. George, and M.M. Stevens, *Novel materials for bone and cartilage regeneration*. Curr Opin Chem Biol, 2006. **10(6)**: p. 568-75.

37. Carson, J.S. and M.P. Bostrom, *Synthetic bone scaffolds and fracture repair*. Injury, 2007. **38 Suppl 1**: p. S33-7.
38. Johnson, E.E., M.R. Urist, and G.A. Finerman, *Bone morphogenetic protein augmentation grafting of resistant femoral nonunions. A preliminary report*. Clin Orthop Relat Res, 1988(230): p. 257-65.
39. Govender, S., et al., *Recombinant human bone morphogenetic protein-2 for treatment of open tibial fractures: a prospective, controlled, randomized study of four hundred and fifty patients*. J Bone Joint Surg Am, 2002. **84-A(12)**: p. 2123-34.
40. Gautschi, O.P., S.P. Frey, and R. Zellweger, *Bone morphogenetic proteins in clinical applications*. ANZ J Surg, 2007. **77(8)**: p. 626-31.
41. Robinson, Y., et al., *Evidence supporting the use of bone morphogenetic proteins for spinal fusion surgery*. Expert Rev Med Devices, 2008. **5(1)**: p. 75-84.
42. Osyczka, A.M. and P.S. Leboy, *Bone morphogenetic protein regulation of early osteoblast genes in human marrow stromal cells is mediated by extracellular signal-regulated kinase and phosphatidylinositol 3-kinase signaling*. Endocrinology, 2005. **146(8)**: p. 3428-37.
43. Ryoo, H.M., M.H. Lee, and Y.J. Kim, *Critical molecular switches involved in BMP-2-induced osteogenic differentiation of mesenchymal cells*. Gene, 2006. **366(1)**: p. 51-57.
44. Wang, K., et al., *Epidermal growth factor receptor-deficient mice have delayed primary endochondral ossification because of defective osteoclast recruitment*. J Biol Chem, 2004. **279(51)**: p. 53848-56.
45. Omi, M., et al., *Studies on epidermal growth factor receptor signaling in vertebrate limb patterning*. Dev Dyn, 2005. **233(2)**: p. 288-300.
46. Sibilias, M., et al., *Mice humanised for the EGF receptor display hypomorphic phenotypes in skin, bone and heart*. Development, 2003. **130(19)**: p. 4515-25.
47. Qin, L., et al., *Amphiregulin is a novel growth factor involved in normal bone development and in the cellular response to parathyroid hormone stimulation*. J Biol Chem, 2005. **280(5)**: p. 3974-81.
48. Chan, S.Y. and R.W. Wong, *Expression of epidermal growth factor in transgenic mice causes growth retardation*. J Biol Chem, 2000. **275(49)**: p. 38693-8.
49. Tamama, K., et al., *Epidermal growth factor as a candidate for ex vivo expansion of bone marrow-derived mesenchymal stem cells*. Stem Cells, 2006. **24(3)**: p. 686-95.
50. Kratchmarova, I., et al., *Mechanism of divergent growth factor effects in mesenchymal stem cell differentiation*. Science, 2005. **308(5727)**: p. 1472-7.

51. Kuznetsov, S.A., A.J. Friedenstein, and P.G. Robey, *Factors required for bone marrow stromal fibroblast colony formation in vitro*. Br J Haematol, 1997. **97**(3): p. 561-70.
52. Kimura, A., O. Katoh, and A. Kuramoto, *Effects of platelet derived growth factor, epidermal growth factor and transforming growth factor-beta on the growth of human marrow fibroblasts*. Br J Haematol, 1988. **69**(1): p. 9-12.
53. Gronthos, S. and P.J. Simmons, *The growth factor requirements of STRO-1-positive human bone marrow stromal precursors under serum-deprived conditions in vitro*. Blood, 1995. **85**(4): p. 929-40.
54. Owen, M.E., J. Cave, and C.J. Joyner, *Clonal analysis in vitro of osteogenic differentiation of marrow CFU-F*. J Cell Sci, 1987. **87** (Pt 5): p. 731-8.
55. Krampera, M., et al., *HB-EGF/HER-1 signaling in bone marrow mesenchymal stem cells: inducing cell expansion and reversibly preventing multilineage differentiation*. Blood, 2005. **106**(1): p. 59-66.
56. Antosz, M.E., C.G. Bellows, and J.E. Aubin, *Biphasic effects of epidermal growth factor on bone nodule formation by isolated rat calvaria cells in vitro*. J Bone Miner Res, 1987. **2**(5): p. 385-93.
57. Kuhl, P.R. and L.G. Griffith-Cima, *Tethered epidermal growth factor as a paradigm for growth factor-induced stimulation from the solid phase*. Nat Med, 1996. **2**(9): p. 1022-7.
58. Fan, V.H., et al., *Tethered epidermal growth factor provides a survival advantage to mesenchymal stem cells*. Stem Cells, 2007. **25**(5): p. 1241-51.
59. Kuhlman, W., et al., *Interplay between PEO tether length and ligand spacing governs cell spreading on RGD-modified PMMA-g-PEO comb copolymers*. Biomacromolecules, 2007. **8**(10): p. 3206-13.
60. Irvine, D.J., A.M. Mayes, and L.G. Griffith, *Nanoscale clustering of RGD peptides at surfaces using Comb polymers. 1. Synthesis and characterization of Comb thin films*. Biomacromolecules, 2001. **2**(1): p. 85-94.
61. Au, A., et al., *Formation of osteogenic colonies on well-defined adhesion peptides by freshly isolated human marrow cells*. Biomaterials, 2007. **28**(10): p. 1847-61.
62. Kuhlman, W.A., et al., *Chain Conformations at the Surface of a Polydisperse Amphiphilic Comb Copolymer Film*. Macromolecules, 2006. **39**(15): p. 5122-5126.
63. Powell, K.A., et al., *Quantitative image analysis of connective tissue progenitors*. Anal Quant Cytol Histol, 2007. **29**(2): p. 112-21.
64. Garcia, A.J., J.E. Schwarzbauer, and D. Boettiger, *Distinct activation states of alpha5beta1 integrin show differential binding to RGD and synergy domains of fibronectin*. Biochemistry, 2002. **41**(29): p. 9063-9.

65. Hautanen, A., et al., *Effects of modifications of the RGD sequence and its context on recognition by the fibronectin receptor*. J Biol Chem, 1989. **264**(3): p. 1437-42.
66. Petrie, T.A., et al., *Integrin specificity and enhanced cellular activities associated with surfaces presenting a recombinant fibronectin fragment compared to RGD supports*. Biomaterials, 2006. **27**(31): p. 5459-70.
67. Saoncella, S., et al., *Syndecan-4 signals cooperatively with integrins in a Rho-dependent manner in the assembly of focal adhesions and actin stress fibers*. Proceedings of the National Academy of Sciences of the United States of America, 1999. **96**(6): p. 2805-2810.
68. Morgan, M.R., M.J. Humphries, and M.D. Bass, *Synergistic control of cell adhesion by integrins and syndecans*. Nature Reviews Molecular Cell Biology, 2007. **8**(12): p. 957-969.
69. Friedenstein, A.J., *Precursor cells of mechanocytes*. Int Rev Cytol, 1976. **47**: p. 327-59.
70. Gronthos, S., et al., *The STRO-1+ fraction of adult human bone marrow contains the osteogenic precursors*. Blood, 1994. **84**(12): p. 4164-73.
71. Clarke, E. and S.R. Mccann, *Stromal Colonies Can Be Grown from the Nonadherent Cells in Human Long-Term Bone-Marrow Cultures*. European Journal of Haematology, 1991. **46**(5): p. 296-300.
72. Baksh, D., P.W. Zandstra, and J.E. Davies, *A non-contact suspension culture approach to the culture of osteogenic cells derived from a CD49e(low) subpopulation of human bone marrow-derived cells*. Biotechnology and Bioengineering, 2007. **98**(6): p. 1195-1208.
73. Wan, C., et al., *Nonadherent cell population of human marrow culture is a complementary source of mesenchymal stem cells (MSCs)*. Journal of Orthopaedic Research, 2006. **24**(1): p. 21-28.
74. Docheva, D., et al., *Human mesenchymal stem cells in contact with their environment: surface characteristics and the integrin system*. J Cell Mol Med, 2007. **11**(1): p. 21-38.
75. Gronthos, S., et al., *Integrin-mediated interactions between human bone marrow stromal precursor cells and the extracellular matrix*. Bone, 2001. **28**(2): p. 174-81.
76. Klees, R.F., et al., *Laminin-5 induces osteogenic gene expression in human mesenchymal stem cells through an ERK-dependent pathway*. Mol Biol Cell, 2005. **16**(2): p. 881-90.
77. Salasznyk, R.M., et al., *Adhesion to Vitronectin and Collagen I Promotes Osteogenic Differentiation of Human Mesenchymal Stem Cells*. J Biomed Biotechnol, 2004. **2004**(1): p. 24-34.

78. Chastain, S.R., et al., *Adhesion of mesenchymal stem cells to polymer scaffolds occurs via distinct ECM ligands and controls their osteogenic differentiation*. J Biomed Mater Res A, 2006. **78**(1): p. 73-85.
79. Swindle, C.S., et al., *Epidermal growth factor (EGF)-like repeats of human tenascin-C as ligands for EGF receptor*. J Cell Biol, 2001. **154**(2): p. 459-68.
80. Wells, A., et al., *Ligand-induced transformation by a noninternalizing epidermal growth factor receptor*. Science, 1990. **247**(4945): p. 962-4.
81. Kempiak, S.J., et al., *Local signaling by the EGF receptor*. J Cell Biol, 2003. **162**(5): p. 781-7.
82. Reddy, C.C., A. Wells, and D.A. Lauffenburger, *Receptor-mediated effects on ligand availability influence relative mitogenic potencies of epidermal growth factor and transforming growth factor alpha*. J Cell Physiol, 1996. **166**(3): p. 512-22.
83. Muschler, G.F., R.J. Midura, and C. Nakamoto, *Practical Modeling Concepts for Connective Tissue Stem Cell and Progenitor Compartment Kinetics*. J Biomed Biotechnol, 2003. **2003**(3): p. 170-193.
84. Simmons, P.J. and B. Torok-Storb, *Identification of stromal cell precursors in human bone marrow by a novel monoclonal antibody, STRO-1*. Blood, 1991. **78**(1): p. 55-62.
85. Cabodi, S., et al., *Integrin regulation of epidermal growth factor (EGF) receptor and of EGF-dependent responses*. Biochem Soc Trans, 2004. **32**(Pt3): p. 438-42.
86. Giancotti, F.G. and G. Tarone, *Positional control of cell fate through joint integrin/receptor protein kinase signaling*. Annu Rev Cell Dev Biol, 2003. **19**: p. 173-206.
87. Miranti, C.K. and J.S. Brugge, *Sensing the environment: a historical perspective on integrin signal transduction*. Nature Cell Biology, 2002. **4**(4): p. E83-E90.
88. Schwartz, M.A. and M.H. Ginsberg, *Networks and crosstalk: integrin signalling spreads*. Nat Cell Biol, 2002. **4**(4): p. E65-8.
89. Yamada, K.M. and S. Even-Ram, *Integrin regulation of growth factor receptors*. Nat Cell Biol, 2002. **4**(4): p. E75-6.
90. Meredith, J.E., Jr., B. Fazeli, and M.A. Schwartz, *The extracellular matrix as a cell survival factor*. Mol Biol Cell, 1993. **4**(9): p. 953-61.
91. Ballif, B.A. and J. Blenis, *Molecular mechanisms mediating mammalian mitogen-activated protein kinase (MAPK) kinase (MEK)-MAPK cell survival signals*. Cell Growth Differ, 2001. **12**(8): p. 397-408.

92. Sato, H., et al., *Epidermal growth factor receptor-transfected bone marrow stromal cells exhibit enhanced migratory response and therapeutic potential against murine brain tumors*. *Cancer Gene Ther*, 2005. **12**(9): p. 757-68.
93. Roux, P.P. and J. Blenis, *ERK and p38 MAPK-activated protein kinases: a family of protein kinases with diverse biological functions*. *Microbiol Mol Biol Rev*, 2004. **68**(2): p. 320-44.
94. Maheshwari, G., et al., *Cell adhesion and motility depend on nanoscale RGD clustering*. *J Cell Sci*, 2000. **113** (Pt 10): p. 1677-86.
95. Maheshwari, G., et al., *Biophysical integration of effects of epidermal growth factor and fibronectin on fibroblast migration*. *Biophys J*, 1999. **76**(5): p. 2814-23.
96. Richardson, L.B. "EGF receptor-mediated fibroblast signaling and motility : role of nanoscale spatial ligand organization." Ph.D. Thesis. Massachusetts Institute of Technology, 2005.

3.7 Figures

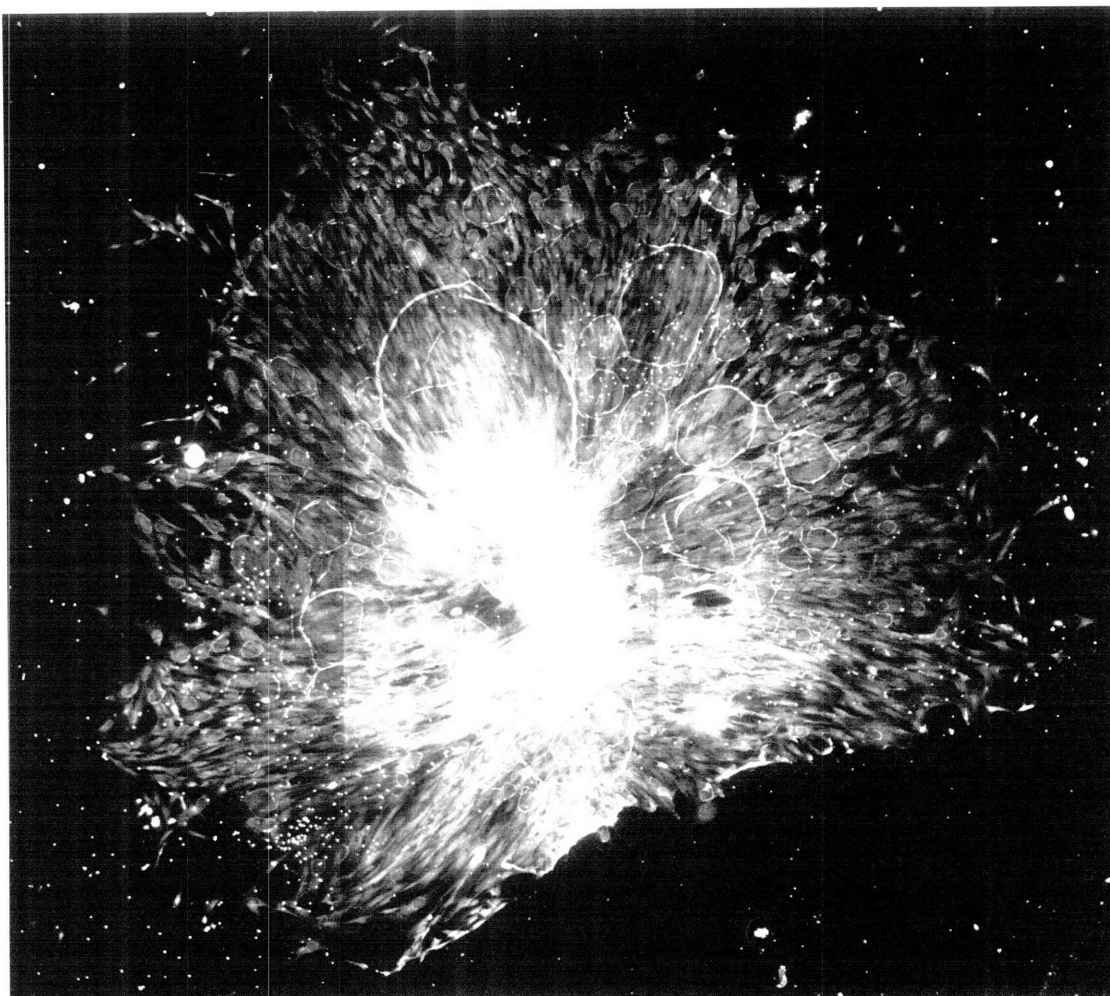


Figure 3.1 Image of alkaline phosphatase positive connective tissue progenitor colony.

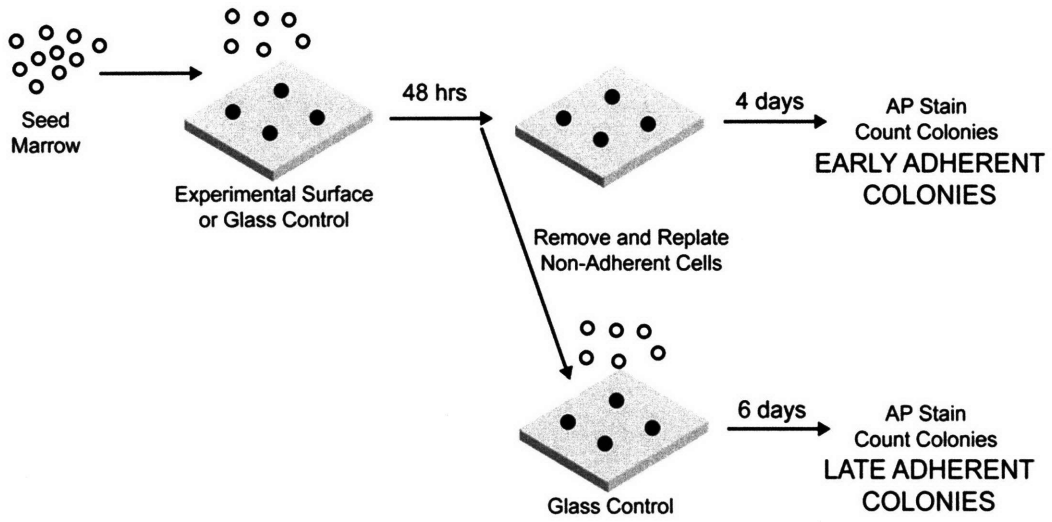


Figure. 3.2 Protocol for bone marrow aspirate colony forming unit (CFU) assay. Open circle: non-adherent bone marrow cells. Closed circle: colonies of adherent cells derived from adherent CTPs.

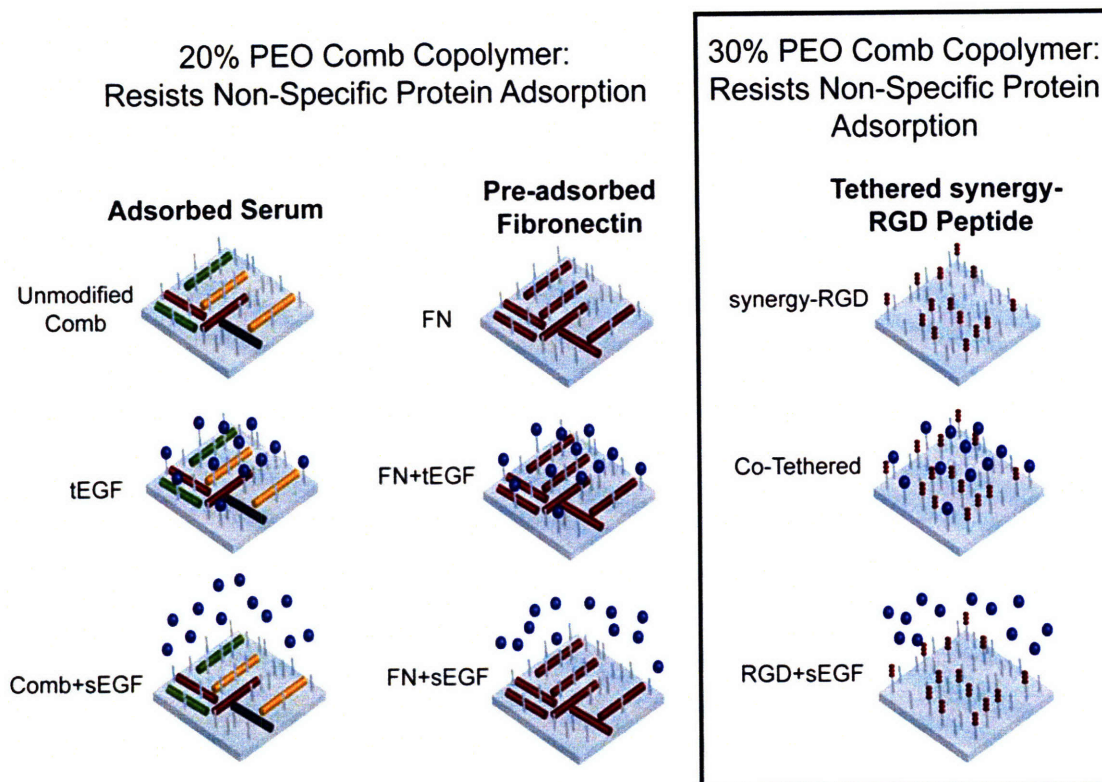


Figure 3.3 Schematic of surface conditions used in colony forming unit assay and abbreviations used for data plots. Top row: no epidermal growth factor (EGF). Middle row: tethered EGF. Bottom row: soluble EGF at 10 ng/mL.

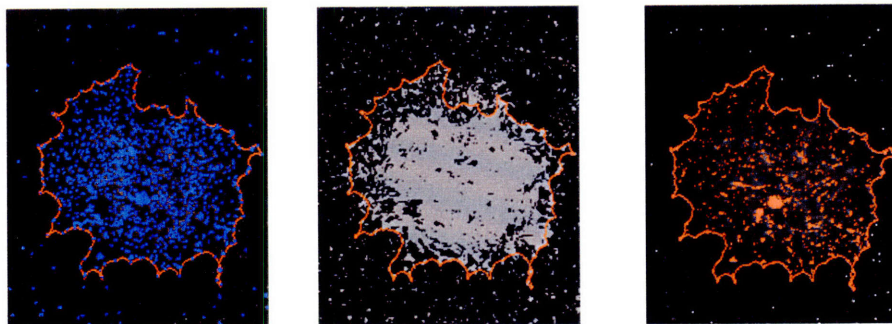
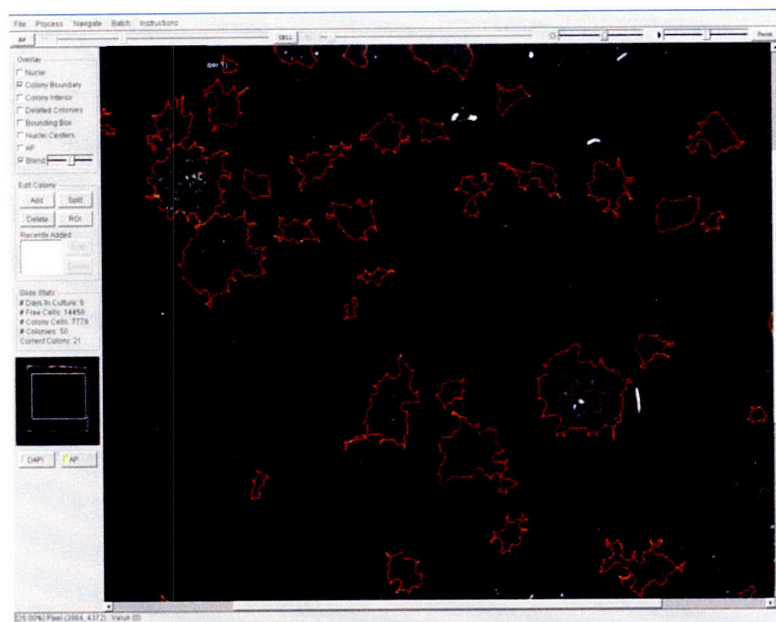
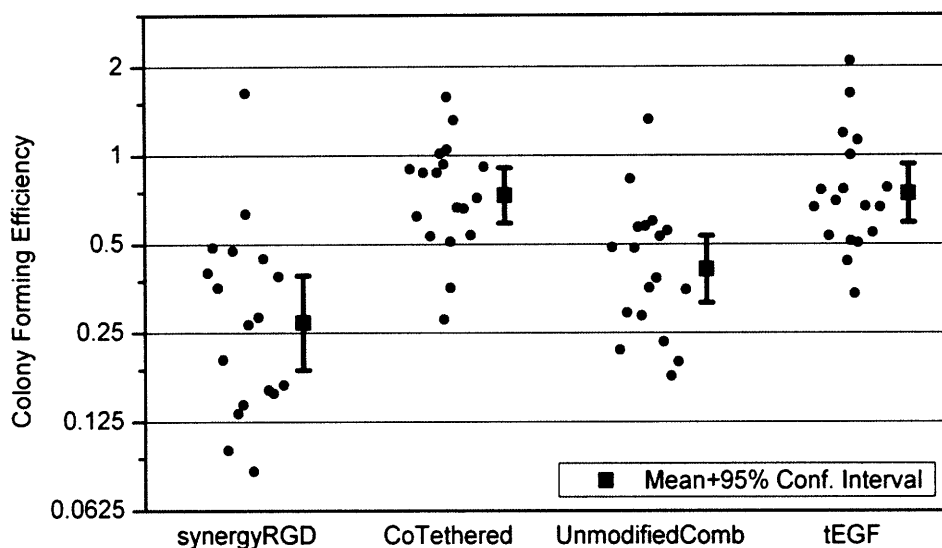


Figure 3.4 Example of quantitative image analysis of connective tissue progenitor osteogenic colony formation, showing quantification of cell nuclei, cell area, and alkaline phosphatase.

a)

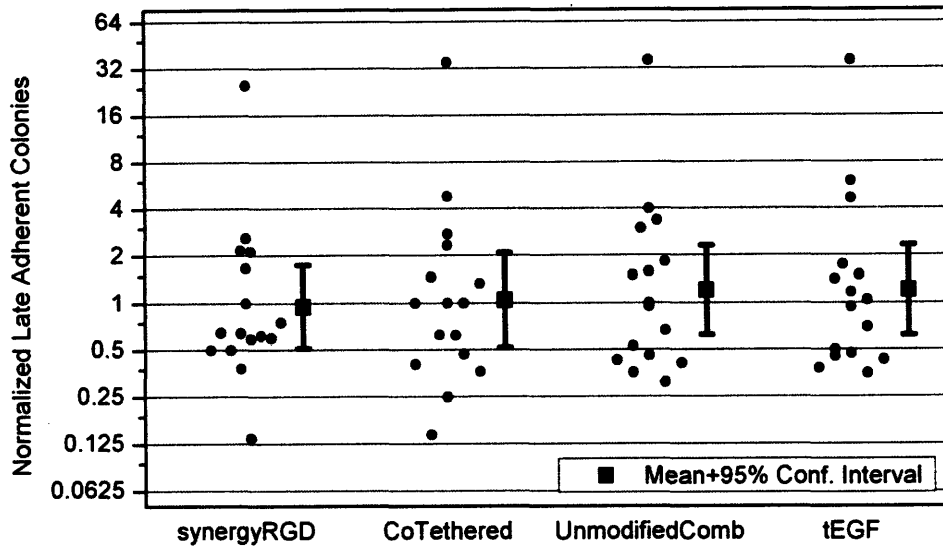


b)

Surface	synergy-RGD	Co-Teth	Unmodified Comb	tEGF
Mean CFE	0.27	0.73	0.41	0.74
Lower 95% Conf. Level	0.19	0.59	0.32	0.59
Upper 95% Conf. Level	0.39	0.91	0.53	0.93
p-values: Shapiro-Wilk Normality Test	0.56105	0.74279	0.68768	0.54184
p-values: Matched-Pairs t-test				
synergy-RGD	X	0.00001	0.01164	0.00007
Co-Teth	0.00001	X	0.00038	0.90039
Unmodified Comb	0.01164	0.00038	X	0.00003
tEGF	0.00007	0.90039	0.00003	X

Figure 3.5 a) Colony forming efficiency (CFE) of bone marrow aspirates seeded onto synergy-RGD peptide conjugated surfaces (synergy-RGD), synergy-RGD peptide + tethered EGF surfaces (CoTethered), serum-adsorptive surfaces (unmodified comb), and serum-adsorptive surfaces + tethered EGF (tEGF) for a cohort of 18 donors with an average age of 62. b) Table of statistical comparisons of CFE between the different surfaces. Tethered EGF surfaces (CoTeth and tEGF) showed significant increases in CFE in comparison to their respective controls ($p < .05$).

a)



b)

Surface	synergy-RGD	Co-Teth	Unmodified Comb	tEGF
Mean CFE	0.95	1.05	1.20	1.20
Lower 95% Conf. Level	0.51	0.52	0.62	0.62
Upper 95% Conf. Level	1.75	2.10	2.32	2.32
p-values: Shapiro-Wilk Normality Test	0.02042	0.2145	0.03432	0.01081
p-values: Matched-Pairs t-test				
synergy-RGD	X	0.62385	0.12401	0.18378
Co-Teth	0.62385	X	0.07807	0.27050
Unmodified Comb	0.12401	0.07807	X	0.99091
tEGF	0.18378	0.27050	0.99091	X
p-values: Wilcoxon Signed-Rank Test				
synergy-RGD	X	0.05370	0.23100	0.30300
Unmodified Comb	0.23100	0.06500	X	0.80400
tEGF	0.30300	0.34200	0.80400	X

Figure 3.6 a) Normalized number of late-adherent connective tissue progenitor colonies formed on glass, after being removed from synergy-RGD peptide conjugated surfaces (synergy-RGD), synergy-RGD peptide + tethered EGF surfaces (CoTethered), serum-adsorptive surfaces (unmodified comb), and serum-adsorptive surfaces + tethered EGF (tEGF). b) Table of statistical comparisons of late adherent colony formation between the different surfaces. No significant differences were observed between any surfaces ($p > .05$).

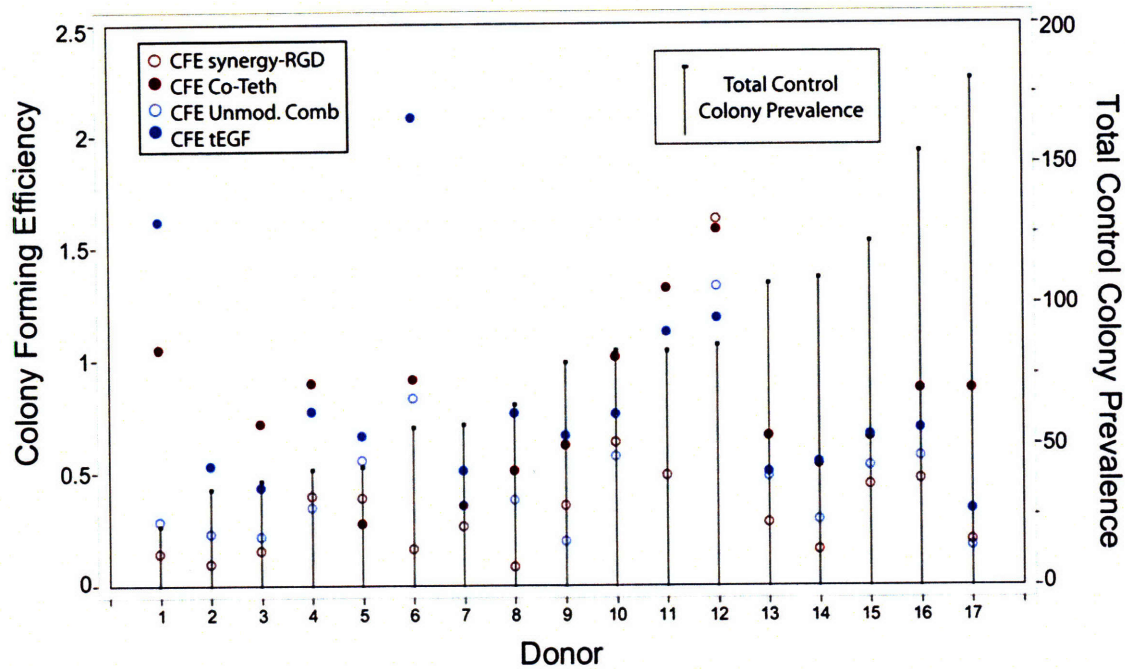
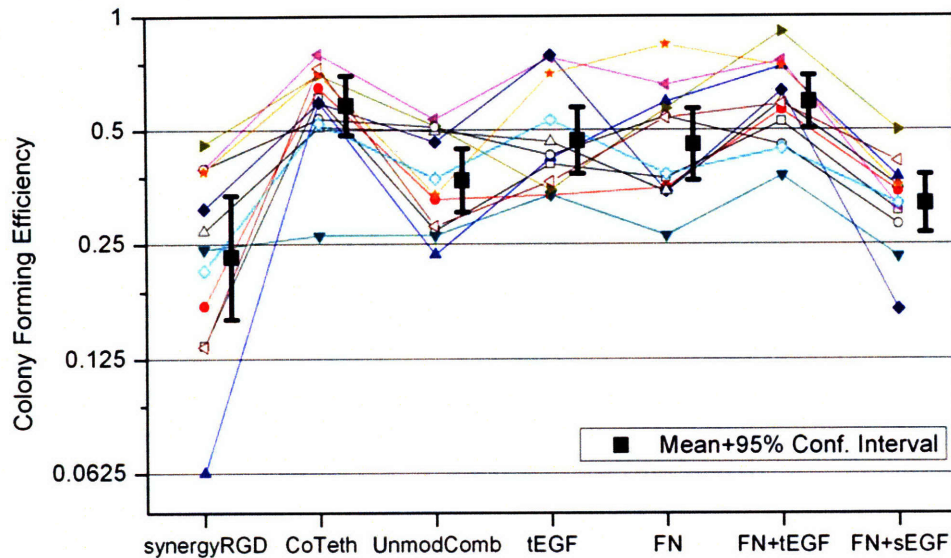


Figure 3.7 Left axis: colony forming efficiency for synergy-RGD peptide conjugated surfaces (synergy-RGD), synergy-RGD peptide + tethered EGF surfaces (CoTethered), serum-adsorptive surfaces (unmodified comb), and serum-adsorptive surfaces + tethered EGF (tEGF). Right axis: total number of early- and late-adherent colonies per million cells seeded on glass control surfaces for each donor.

a)

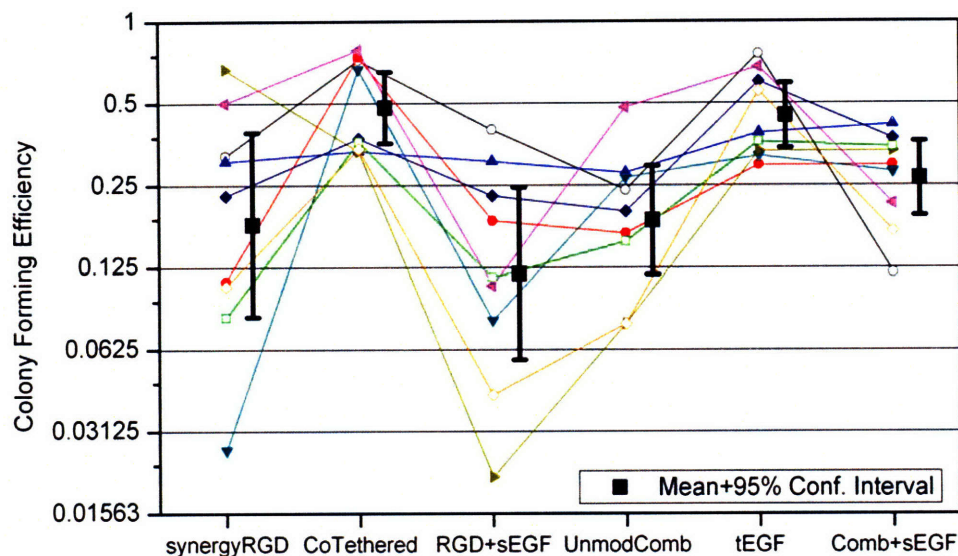


b)

Surface	synergy-RGD	Co-Teth	Unmodified Comb	tEGF	FN	FN+tEGF	FN+sEGF
Mean CFE	0.23	0.58	0.37	0.47	0.46	0.59	0.32
Lower 95% Conf. Level	0.16	0.48	0.30	0.38	0.37	0.50	0.27
Upper 95% Conf. Level	0.34	0.70	0.45	0.57	0.57	0.70	0.38
p-values: Shaprio-Wilk Normality Test	0.24669	0.00657	0.14252	0.05965	0.52966	0.95856	0.40579
p-values: Matched-Pairs t-test							
synergy-RGD	X	0.00041	0.00155	0.00097	0.00311	0.00023	0.1296
Co-Teth	0.00041	X	0.00095	0.05610	0.00688	0.72426	0.00002
Unmodified Comb	0.00155	0.00095	X	0.02856	0.09868	0.00044	0.27309
tEGF	0.00097	0.05610	0.02856	X	0.83739	0.03676	0.02327
FN	0.00311	0.00688	0.09868	0.83739	X	0.00488	0.002
FN+tEGF	0.00023	0.72426	0.00044	0.03676	0.00488	X	0.00001
FN+sEGF	0.1296	0.00002	0.27309	0.02327	0.002	0.00001	X
p-values: Wilcoxon Signed-Rank Test							
Co-Teth	0.000	X	0.001	0.067	0.010	0.733	0.000

Figure 3.8. a) Colony forming efficiency (CFE) of bone marrow aspirates seeded onto synergy-RGD peptide conjugated surfaces (synergy-RGD), synergy-RGD peptide + tethered EGF surfaces (CoTethered), serum-adsorptive surfaces (unmodified comb), serum-adsorptive + tethered EGF surfaces (tEGF), fibronectin surfaces (FN), fibronectin + tethered EGF surfaces (FN+tEGF), and fibronectin + soluble EGF surfaces (FN+sEGF) for a cohort of 12 donors with an average age of 51. b) Table of statistical comparisons of CFE between the different surfaces. Tethered EGF surfaces (CoTeth, tEGF, and FN+tEGF) showed significant increases in CFE in comparison to their respective controls ($p < .05$). FN+sEGF showed a significant decrease in CFE compared to FN only ($p < .05$).

a)

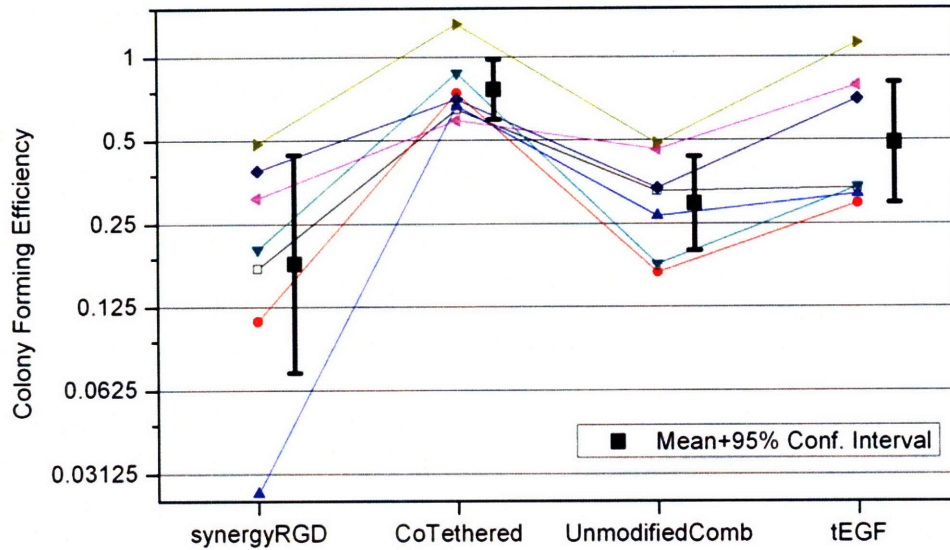


b)

Surface	synergy-RGD	Co-Teth	RGD+sEGF	Unmodified Comb	tEGF	Comb+sEGF
Mean CFE	0.18	0.48	0.12	0.19	0.45	0.27
Lower 95% Conf. Level	0.08	0.36	0.06	0.12	0.34	0.19
Upper 95% Conf. Level	0.39	0.65	0.25	0.29	0.59	0.36
p-values: Shapiro-Wilk Normality Test	0.7234	0.00931	0.8228	0.54297	0.2406	0.3002
p-values: Matched-Pairs t-test						
synergy-RGD	X	0.03079	0.39254	0.9248	0.01693	0.32327
Co-Teth	0.03079	X	0.00156	0.0003	0.6769	0.03114
synergy-RGD+sEGF	0.39254	0.00156	X	0.10179	0.00205	0.05154
Unmodified Comb	0.9248	0.0003	0.10179	X	0.00204	0.18492
tEGF	0.01693	0.6769	0.00205	0.00204	X	0.05129
Comb+sEGF	0.32327	0.03114	0.05154	0.18492	0.05129	X
p-values: Wilcoxon Signed-Rank Test						
Co-Teth	0.027	X	0.0004	0.004	0.938	0.047

Figure 3.9. a) Colony forming efficiency (CFE) of bone marrow aspirates seeded onto synergy-RGD peptide conjugated surfaces (synergy-RGD), synergy-RGD peptide + tethered EGF surfaces (CoTethered), synergy-RGD peptide + soluble EGF surfaces (RGD+sEGF), serum-adsorptive surfaces (unmodified comb), serum-adsorptive + tethered EGF surfaces (tEGF), serum-adsorptive + soluble EGF surfaces (Comb+sEGF) for a cohort of 9 donors with an average age of 58. b) Table of statistical comparisons of CFE between the different surfaces. Tethered EGF surfaces (CoTeth and tEGF) showed significant increases in CFE in comparison to their respective controls ($p < .05$). Surfaces with soluble EGF (RGD+sEGF and Comb+sEGF) were statistically similar to controls ($p > .05$).

a)



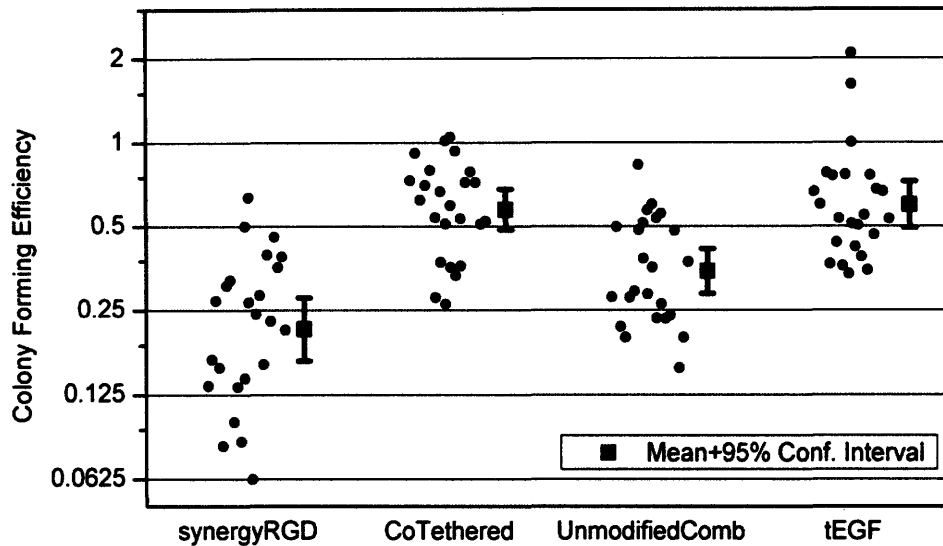
b)

Surface	synergy-RGD	Co-Teth	Unmodified Comb	tEGF
Mean CFE	0.18	0.77	0.30	0.49
Lower 95% Conf. Level	0.07	0.60	0.20	0.30
Upper 95% Conf. Level	0.45	0.98	0.44	0.81
p-values: Shaprio-Wilk Normality Test	0.31649	0.11313	0.41479	0.07558

	synergy-RGD	Co-Teth	Unmodified Comb	tEGF
p-values: Matched-Pairs t-test				
synergy-RGD	X	0.00552	0.17236	0.00782
Co-Teth	0.00552	X	0.00174	0.05115
Unmodified Comb	0.17236	0.00174	X	0.00402
tEGF	0.00782	0.05115	0.00402	X

Figure 3.10 a) Colony forming efficiency (CFE) of bone marrow aspirates seeded onto synergy-RGD peptide conjugated surfaces (synergy-RGD), synergy-RGD peptide + tethered EGF surfaces (CoTethered), serum-adsorptive surfaces (unmodified comb), and serum-adsorptive surfaces + tethered EGF (tEGF) for a retrospective study of 7 healthy donors with an average age of 39. b) Table of statistical comparisons of CFE between the different surfaces. Tethered EGF surfaces (CoTeth and tEGF) showed significant increases in CFE in comparison to their respective controls ($p < .05$).

a)

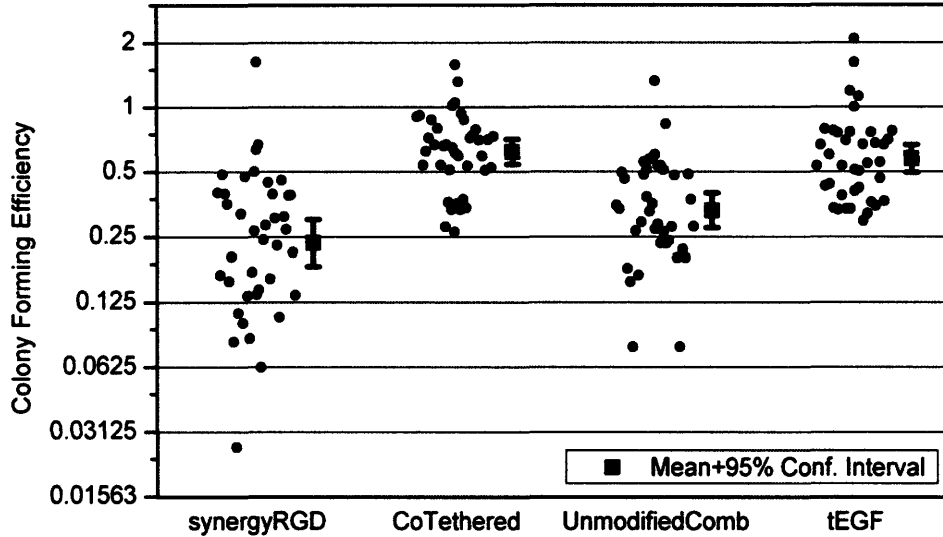


b)

Surface	synergy-RGD	Co-Teth	Unmodified Comb	tEGF
Mean CFE	0.21	0.57	0.34	0.60
Lower 95% Conf. Level	0.17	0.49	0.29	0.49
Upper 95% Conf. Level	0.28	0.68	0.41	0.72
p-values: Shaprio-Wilk Normality Test	0.83371	0.25417	0.41879	0.0229
p-values: Matched-Pairs t-test				
synergy-RGD	X	0.00000	0.00057	0.00000
Co-Teth	0.00000	X	0.00002	0.63342
Unmodified Comb	0.00057	0.00002	X	0.00001
tEGF	0.00000	0.63342	0.00001	X
p-values: Wilcoxon Signed-Rank Test				
tEGF	0.000	0.626	0.000	X

Figure 3.11 a) Colony forming efficiency (CFE) of bone marrow aspirates seeded onto synergy-RGD peptide conjugated surfaces (synergy-RGD), synergy-RGD peptide + tethered EGF surfaces (CoTethered), serum-adsorptive surfaces (unmodified comb), and serum-adsorptive surfaces + tethered EGF (tEGF) for a retrospective study of 24 donors with osteoarthritis with an average age of 63. b) Table of statistical comparisons of CFE between the different surfaces. Tethered EGF surfaces (CoTeth and tEGF) showed significant increases in CFE in comparison to their respective controls ($p < .05$).

a)

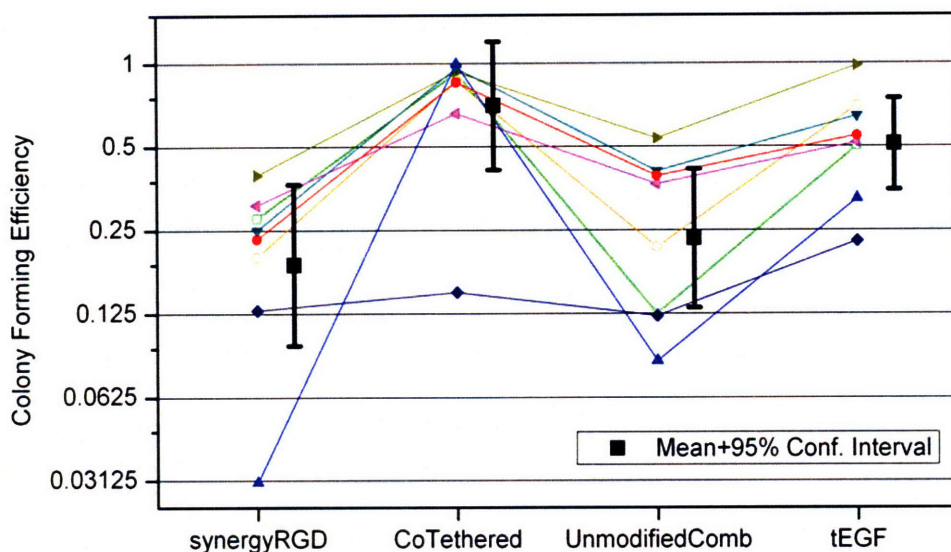


b)

Surface	synergy-RGD	Co-Teth	Unmodified Comb	tEGF
Mean CFE	0.23	0.62	0.33	0.57
Lower 95% Conf. Level	0.18	0.54	0.27	0.50
Upper 95% Conf. Level	0.30	0.71	0.40	0.67
p-values: Shapiro-Wilk Normality Test	0.83015	0.39558	0.28459	0.0413
p-values: Matched-Pairs t-test				
synergy-RGD	X	0.00000	0.00536	0.00000
Co-Teth	0.00000	X	0.00000	0.27586
Unmodified Comb	0.00536	0.00000	X	0.00000
tEGF	0.00000	0.27586	0.00000	X
p-values: Wilcoxon Signed-Rank Test				
tEGF	0.000	0.301	0.000	X

Figure 3.12 a) Colony forming efficiency (CFE) of bone marrow aspirates seeded onto synergy-RGD peptide conjugated surfaces (synergy-RGD), synergy-RGD peptide + tethered EGF surfaces (CoTethered), serum-adsorptive surfaces (unmodified comb), and serum-adsorptive surfaces + tethered EGF (tEGF) for a retrospective study of all 39 donors used in previous studies, with an average age of 58. b) Table of statistical comparisons of CFE between the different surfaces. Tethered EGF surfaces (CoTeth and tEGF) showed significant increases in CFE in comparison to their respective controls ($p < .05$).

a)



b)

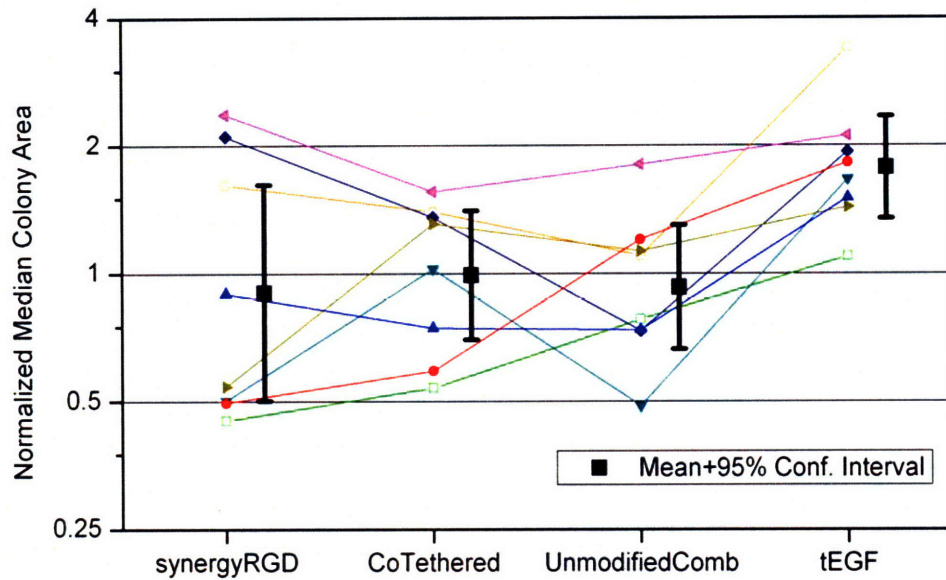
Surface	synergy-RGD	Co-Teth	Unmodified Comb	tEGF
Mean CFE	0.19	0.70	0.23	0.51
Lower 95% Conf. Level	0.10	0.41	0.13	0.35
Upper 95% Conf. Level	0.37	1.20	0.41	0.75
p-values: Shapiro-Wilk Normality Test	0.02164	0.00013	0.3006	0.76842

	synergy-RGD	Co-Teth	Unmodified Comb	tEGF
p-values: Matched-Pairs t-test				
synergy-RGD	X	0.00623	0.27589	0.00213
Co-Teth	0.00623	X	0.00527	0.08666
Unmodified Comb	0.27589	0.00527	X	0.00162
tEGF	0.00213	0.08666	0.00162	X

	synergy-RGD	Co-Teth	Unmodified Comb	tEGF
p-values: Wilcoxon Signed-Rank Test				
synergy-RGD	X	0.008	0.195	0.008
Co-Teth	0.008	X	0.008	0.109

Figure 3.13. a) Colony forming efficiency (CFE) of bone marrow aspirates seeded onto synergy-RGD peptide conjugated surfaces (synergy-RGD), synergy-RGD peptide + tethered EGF surfaces (CoTethered), serum-adsorptive surfaces (unmodified comb), and serum-adsorptive surfaces + tethered EGF (tEGF) as measured with quantitative image analysis for 8 donors with an average age of 65. b) Table of statistical comparisons of CFE between the different surfaces. Tethered EGF surfaces (CoTeth and tEGF) showed significant increases in CFE in comparison to their respective controls ($p < .05$).

a)

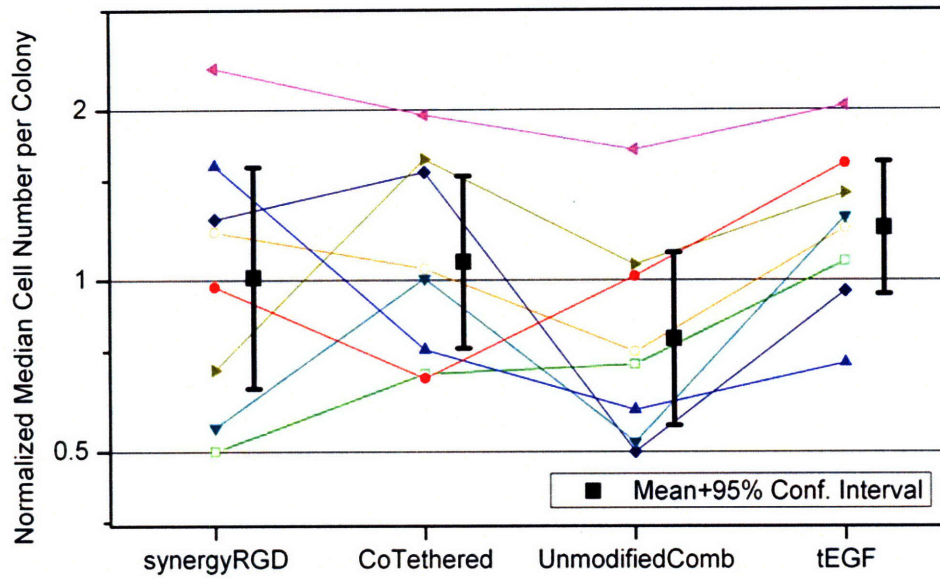


b)

Surface	synergy-RGD	Co-Teth	Unmodified Comb	tEGF
Mean CFE	0.90	0.99	0.93	1.78
Lower 95% Conf. Level	0.50	0.70	0.66	1.35
Upper 95% Conf. Level	1.62	1.41	1.30	2.34
p-values: Shapiro-Wilk Normality Test	0.07471	0.17924	0.81895	0.73512
p-values: Matched-Pairs t-test				
synergy-RGD	X	0.60531	0.90393	0.00924
Co-Teth	0.60531	X	0.71355	0.00184
Unmodified Comb	0.90393	0.71355	X	0.00326
tEGF	0.00924	0.00184	0.00326	X

Figure 3.14 a) Normalized median area of colonies formed on synergy-RGD peptide conjugated surfaces (synergy-RGD), synergy-RGD peptide + tethered EGF surfaces (CoTethered), serum-adsorptive surfaces (unmodified comb), and serum-adsorptive surfaces + tethered EGF (tEGF) as measured with quantitative image analysis for 8 donors with an average age of 65. b) Table of statistical comparisons between the different surfaces. Serum-adsorptive surfaces + tethered EGF (tEGF) showed significant increases in median colony area in comparison to all other surfaces ($p < 0.05$).

a)

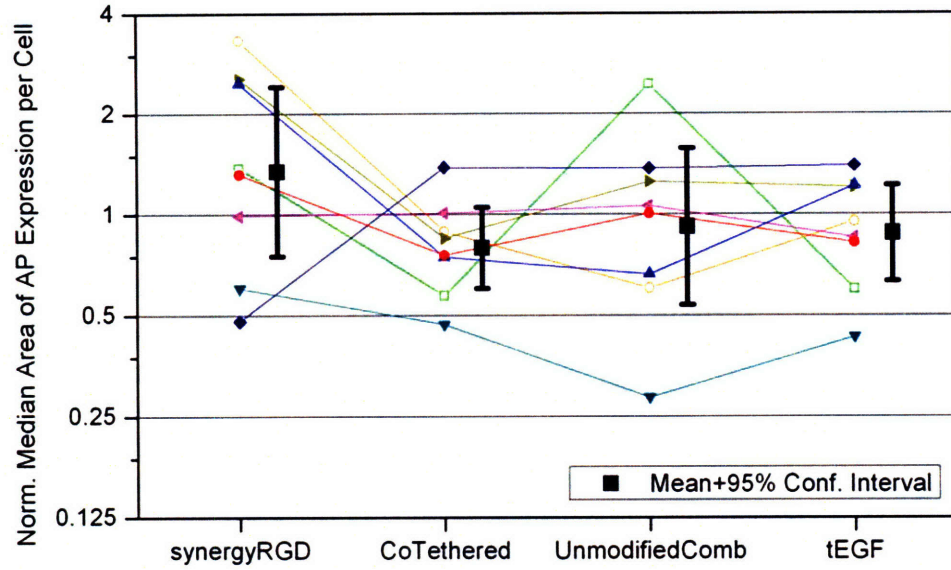


b)

Surface	synergy-RGD	Co-Teth	Unmodified Comb	tEGF
Mean CFE	1.01	1.08	0.79	1.24
Lower 95% Conf. Level	0.64	0.76	0.56	0.95
Upper 95% Conf. Level	1.58	1.53	1.12	1.62
p-values: Shapiro-Wilk Normality Test	0.83596	0.31296	0.50553	0.99844
p-values: Matched-Pairs t-test				
synergy-RGD	X	0.74262	0.23352	0.37221
Co-Teth	0.74262	X	0.09787	0.37050
Unmodified Comb	0.23352	0.09787	X	0.00130
tEGF	0.37221	0.37050	0.00130	X

Figure 3.15 a) Normalized median number of cells per colony formed on synergy-RGD peptide conjugated surfaces (synergy-RGD), synergy-RGD peptide + tethered EGF surfaces (CoTethered), serum-adsorptive surfaces (unmodified comb), and serum-adsorptive surfaces + tethered EGF (tEGF) as measured with quantitative image analysis for 8 donors with an average age of 65. b) Table of statistical comparisons between the different surfaces. Serum-adsorptive surfaces + tethered EGF (tEGF) showed significant increases in cell number in comparison to control (Unmodified Comb) ($p < .05$).

a)



b)

Surface	synergy-RGD	Co-Teth	Unmodified Comb	tEGF
Mean CFE	1.35	0.80	0.92	0.88
Lower 95% Conf. Level	0.75	0.60	0.54	0.63
Upper 95% Conf. Level	2.42	1.05	1.58	1.22
p-values: Shapiro-Wilk Normality Test	0.65093	0.95906	0.88013	0.59055
p-values: Matched-Pairs t-test				
synergy-RGD	X	0.10238	0.28425	0.12438
Co-Teth	0.10238	X	0.52092	0.23428
Unmodified Comb	0.28425	0.52092	X	0.84409
tEGF	0.12438	0.23428	0.84409	X

Figure 3.16 a) Normalized median area of alkaline phosphatase per cell on synergy-RGD peptide conjugated surfaces (synergy-RGD), synergy-RGD peptide + tethered EGF surfaces (CoTethered), serum-adsorptive surfaces (unmodified comb), and serum-adsorptive surfaces + tethered EGF (tEGF) as measured with quantitative image analysis for 8 donors with an average age of 65. b) Table of statistical comparisons between the different surfaces. No significant differences were observed between any surfaces ($p > .05$).

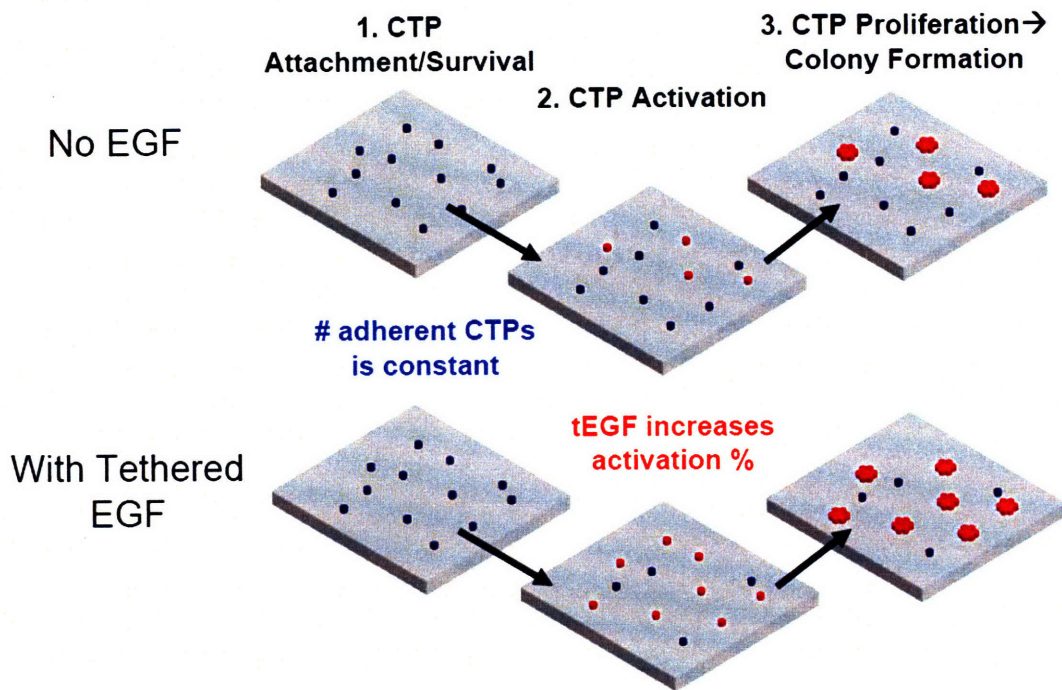


Figure 3.17 Schematic of mechanism in which tethered EGF increases colony formation by enhancing the activation percentage of CTPs.

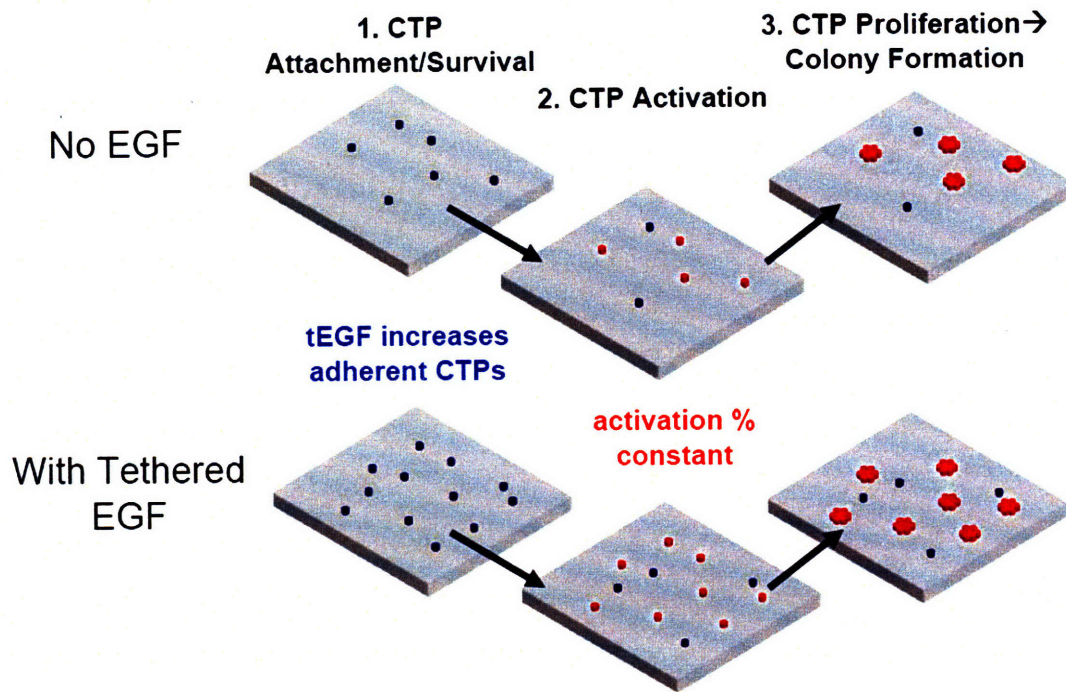


Figure 3.18 Schematic of mechanism in which tethered EGF increases colony formation by enhancing CTP adhesion and survival.

Chapter 4. Conclusions and future directions

The overall goal of this thesis was to contribute to the development of tissue engineering strategies that could be used in the design of synthetic bone grafting materials that promote the selective retention of connective tissue progenitors (CTPs) from freshly aspirated autologous bone marrow. As discussed earlier, CTPs are uniquely capable of osteogenic differentiation, and retention of CTPs on a biomaterial *in vivo* could contribute to faster bone healing and bone graft incorporation. Specifically, we tested the hypothesis that tethered epidermal growth factor (EGF) could promote CTP osteogenic colony formation using a poly(methyl methacrylate)-graft-poly(ethylene oxide) (PMMA-g-PEO) amphiphilic comb copolymer system that allows tethered ligands to be presented in a manner that allows natural signaling through integrin clustering and EGF receptor dimerization. Because of the interplay between a cell's adhesion state and growth factor induced cell behavior, we investigated the effect of tethered EGF under multiple adhesion environments including adsorbed serum, pre-adsorbed fibronectin, and covalently tethered synergy-RGD peptides.

The use of RGD-peptides as cell adhesion ligands has the benefit of allowing quantification of binding sites, in comparison to adsorbed serum, with multiple matrix proteins, or fibronectin, which can contain multiple binding sites of differing specificities. The synergy-RGD peptide has been used previously in our lab to promote integrin-mediated binding, although integrin specificity has been inconsistent between cell types. In Chapter 2, we characterized the specific binding interactions promoted by the synergy-RGD peptide using cells with a well-defined expression profile of RGD-binding integrins. This information could be used to inform any differences that we observed

between adhesive conditions in the course of our examination of tethered EGF on CTP colony formation. While, with this cell system, we did not observe a synergistic effect on cell adhesion and spreading resulting from the inclusion of the PHSRN synergy sequence, we were able to show that the synergy-RGD peptide was capable of promoting cell adhesion through both the $\alpha 5\beta 1$ and the $\alpha v\beta 3$ integrin. Because both serum and fibronectin can support both $\alpha 5\beta 1$ and $\alpha v\beta 3$ binding, the synergy-RGD peptide would allow us to study CTP colony formation on a surface that could provide a minimally adhesive environment, but was also capable of mediating cell attachment through the same set of integrins.

In Chapter 3, we investigated the effect of tethered EGF on osteogenic colony formation in comparison to soluble EGF. Using the colony forming unit assay, we found that tethered EGF enhanced osteogenic colony formation on surfaces seeded with freshly aspirated bone marrow, suggesting that tethered EGF enhanced the retention of CTPs. We observed a robust enhancement in colony formation across three different adhesive conditions. Interestingly, in the absence of tethered EGF, colony formation was increased on native ECM proteins; however, in the presence of tethered EGF, all surfaces promoted a similar degree of colony formation, suggesting that increases in colony formation were due to the tethered EGF-induced adhesion and survival of CTPs. Unlike tethered EGF, soluble EGF failed to enhance colony formation, suggesting that the mode of EGF presentation is an important factor. Additionally, we observed that tethered EGF was able to enhance colony formation in distinct patient populations which is an important consideration for future clinical application. Quantitative image analysis also suggested that tethered EGF did not increase the number of cells undergoing osteogenic

differentiation, but may promote proliferation and migration under specific adhesion conditions.

The results of this work suggest that tethered EGF is a potential candidate for inclusion in biomaterials for use bone grafting procedures with autologous bone marrow. In addition to the clinical implications, this work has also contributed to the body of research investigating the effect of EGF on CTP behavior and has also served to highlight the importance of the mode of ligand presentation in tissue engineering applications and associated cell behavior.

To further study the potential use of tethered EGF in clinical applications, an obvious next step is to incorporate tethered EGF as a surface-modification to a synthetic bone graft that can be tested *in vivo*, such as in a canine model. Ideally, tethered EGF could be incorporated onto the surface of a polymer that has appropriate mechanical, degradation, and geometric properties. Because the current work showed an enhancement in colony formation on multiple surfaces, tethered EGF could be incorporated onto a material that is resistant to non-specific adsorption and functionalized with RGD peptides similar to the synergy-RGD included here, or alternatively, it could be incorporated into a material that allows serum adsorption. The fact that tethered EGF showed a positive effect on selective CTP retention in multiple adhesive conditions makes it easier to identify a bulk material with ideal mechanical and degradation properties that can also be functionalized with tethered EGF, making it more conducive to *in vivo* testing.

Our results clearly support our initial hypothesis that tethered EGF could be used to enhance CTP osteogenic colony formation from primary human bone marrow

aspirates. The mechanism behind this enhancement appears to be a tethered EGF induced increase in the initial attachment and survival of CTPs, which is supported by previous results with culture expanded CTPs (Fan, Tamama et al. 2007). However, this mechanism, as well as the signaling cascade responsible for our observations, requires additional studies to be fully elucidated.

Previous studies have shown that tethered EGF induced cultured CTPs cell spreading in an ERK-dependent manner, suggesting a possible mechanism for CTPs from freshly aspirated marrow. Additionally, image analysis of individual colonies suggested that tethered EGF might also affect migration and proliferation under certain conditions. Although we did not observe increased osteogenesis, it is conceivable that tethered EGF could affect the differentiation process at later time points. Due to the inherent differences that can arise by culturing primary cells, ideally, signaling studies would be performed using freshly aspirated CTPs to examine all of these mechanisms. However, the time and difficulty in acquiring human marrow necessitates such studies, which require many experimental conditions and large quantities of cells, to first be performed on culture expanded cells, to narrow down signaling pathways to be studied with primary cells. These studies are ongoing in our laboratory. Just as in this thesis, these studies are being carried out in the context of different adhesion environments, which, together with the above study of the adhesive interactions resulting from synergy-RGD peptide, can also help to elucidate the interplay between integrin and growth factor mediated signaling.

The work in this thesis has not only provided clear evidence that tethered EGF can be used to promote CTP colony formation, but has motivated additional scientific

questions that are important for tissue engineering in general, and bone grafting applications in particular. Together with future studies examining tethered EGF in vivo, this work can provide an important contribution towards orthopedic tissue engineering therapies that can address a clear clinical need.

4.1 References

Fan, V. H., K. Tamama, et al. (2007). "Tethered epidermal growth factor provides a survival advantage to mesenchymal stem cells." Stem Cells **25**(5): 1241-51.